DIELECTRIC AND OTHER PROPERTIES

OF THIN FILMS

A Thesis
Submitted to the
UNIVERSITY OF POONA
for the degree of
DOCTOR OF PHILOSOPHY
(IN PHYSICS)

By
R. RAMESH VARMA
M. Sc.

THIN FILM DIVISION
NATIONAL CHEMICAL LABORATORY
POONA - 411 008 (India)
JUNE 1975

C O N T E N T S

CHAPTER-I   :   GENERAL INTRODUCTION

CHAPTER I

GENERAL INTRODUCTION

A. THIN FILMS

It has been recognised for many years that vacuum deposition can play an important part in the manufacture of electronic components. Vacuum metallised paper and plastic foils have been used for several years in the production of rolled foil capacitors and evaporated selenium films are commonly used in the manufacture of selenium rectifiers. Vacuum deposition has also been used extensively for making ultra-clean metallic coatings to a wide range of components, including cathode ray tube screens, quartz crystal oscillators, transistors and diodes. High quality thin film dielectrics are also required by the electronic industry for use in capacitors and in field effect devices. Electrical, mechanical, optical, ferromagnetic, superconducting and other properties of solids achieved new dimensions as a result of their investigations in thin film forms. Intensive researches in these fields have been rewarded in the form of useful inventions such as a variety of active and passive microminiaturised components and devices, solar cells,

magnetic memory devices, bolometers, interference filters, reflection and antireflection coatings and many others.

An ideal thin film is generally regarded as bounded by two parallel planes extended infinitely in two directions, but restricted along the third direction (i.e. thickness) which is perpendicular to the other two. The thickness may vary from one atomic layer to several thousand angstroms. A multitude of techniques have been developed to prepare polycrystalline and nearly single-crystalline films of all types of materials. The various deposition techniques are primarily (i) thermal evaporation by resistive, electron bombardment and laser heating, (ii) sputtering by means of glow discharge, r.f. and ion beams and (iii) vapor deposition by a variety of chemical reactions. It is desirable to control the growth and thickness of thin films by directly monitoring the properties for which they are being deposited. The different techniques of monitoring are microbalance techniques, quartz crystal monitors, optical and electrical methods and ionization monitors.

The growth of a vapor-deposited film consists of a statistical process of nucleation of the vapor atoms, adsorption and sticking of nuclei to the substrate,

surface migration, surface diffusion, controlled growth

of the three dimensional nuclei and the formation of a

network structure and its subsequent filling. The most

characteristic stage is the liquid-like coalescence of the

nuclei to form the network structure. The growth of thin

films are influenced by the deposition parameters such as,

rate of deposition and substrate temperature. According to

Pashley et al. (1964), the growth of a thin film may be

visualised by the following stages: (i) nucleation and

island structure, (ii) coalescence of the islands, (iii) growth

of the islands to form a continuous network structure in which

the deposited material is separated by long, irregular and

narrow channels and (iv) a continuous film formed by the

bridging of these channels.

Several micro-analytical techniques have been used

to determine the composition and microstructure of thin

films. Electron diffraction and electron microscopy are

now responsible for much of the understanding of the structure

of thin films. Pashley (1959), Mathews (1959), Philips (1960)

and many other workers have already shown the presence of

many defects viz., dislocations, stacking faults, voids,

impurities, etc. in the deposited films. These defects play

a dominant role in the electrical (Mayer, 1959), dielectric

(Weaver, 1962; Harrop and Wanklyn, 1965), optical (Heavens,1955)

and other properties of thin films. Besides, the physical

properties of thin films are sensitive to their structure
and deposition parameters. Eventhough extensive works have
been carried out on the above properties for the bulk
materials (Shockley, 1950; Smyth, 1955; Frohlich, 1958;
Moss, 1959; Kittel, 1966) it is only recently that special
interests have been taken for the study of thin films
properties. (Heavens, 1955; Holland, 1958; Axelrod, 1968;
Chopra, 1969; Vratny, 1959; Maissel and Glang, 1970). Our
interest in the present investigations would be mostly on
dielectric, electrical and optical properties of vacuum
deposited films. In the following sections, the general
theories for these have briefly been accounted.

B. DIELECTRIC PROPERTIES

Interest in the study of dielectric materials arose
from the practical need of insulators and with the advent of
microelectronics in recent years. The properties of these
materials have been studied more closely for their increasing
practical demands in both active and passive circuits.
Dielectric properties, such as storage of electrical and
magnetic energy, are observed for solids as well as for liquids
and gases. However, in the present investigations we shall
restrict the work mainly to solids having resistivity ranging
from $10^4 - 10^{13}$ ohm cm or greater, particularly in the form
of thin films.

(1) General theory of dielectrics

A capacitor is a device capable of storing electric charge and consists of two conducting electrodes separated by a dielectric. If two parallel plates of area A, separated by a distance d apart in vacuuo are charged by a surface density q, one plate being positive and other negative, then the homogeneous electric field between the plates E is equal to

$$E = 4\pi q = D \qquad esu \qquad \ldots \quad (I-1)$$

where D is the electric displacement or flux density. The potential difference between the plates is given by

$$V = E.d \qquad \ldots \quad (I-2)$$

From the well known Maxwell's equation,

$$D = \epsilon E \qquad \ldots \quad (I-3)$$

where ϵ is the permittivity of the medium. Then

$$\epsilon = D/E = \frac{Q/A}{V/d} = Cd/A \qquad farads/metre$$

where Q is the total charge and C is the capacitance. The magnitude of C is given by

$$C = \epsilon\epsilon_0 A/d \qquad farads \qquad \ldots \quad (I-4)$$

where ϵ is the relative permittivity or dielectric constant of the medium and ϵ_0 (8.85×10^{-12} farads/metre) is the permittivity of vacuum.

When a dielectric is subjected to an alternating field $E = E_0 \cos\omega t$, the polarisation P and also the displacement D varies periodically with time, but D lags behind in phase relative to E so that the eqn. (I-3) becomes,

$$D = D_0 \cos(\omega t-\delta) = D_1 \cos\omega t + D_2 \sin\omega t$$

where δ is the phase angle. Then,

$$D_1 = D_0 \cos\delta \text{ and } D_2 = D_0 \sin\delta \qquad \ldots \text{ (I-5)}$$

For most dielectrics D_0 is proportional to E_0, but the ratio D_0/E_0 is generally frequency dependent. Hence, we introduce two frequency dependent dielectric constants viz.,

$$\epsilon'(\omega) = D_1/D_0 = (D_0/E_0) \cos\delta \qquad \ldots \text{ (I-6a)}$$

$$\epsilon''(\omega) = D_2/E_0 = (D_0/E_0) \sin\delta \qquad \ldots \text{ (I-6b)}$$

These two can be conveniently expressed by a single complex dielectric constant ϵ^* where

$$\epsilon^* = \epsilon' - j\epsilon'' \qquad \ldots \text{ (I-7)}$$

From I-6a and I-6b,

$$\tan\delta = \epsilon''/\epsilon' \qquad \ldots \text{ (I-8)}$$

where $\tan\delta$ is the loss tangent or dissipation factor. If I_1 is the loss current due to the resistance R of the medium and I_c is the charging current of the capacitor, then $\tan\delta$ is also given by

$$\tan\delta = I_1/I_c \qquad \ldots \text{ (I-9)}$$

(ii) <u>Polarisation</u>

A dielectric material increases the storage capacity of a capacitor by neutralising some of the free charges at the electrodes which would otherwise contribute to the external field. This phenomenon is known as dielectric polarisation. Polarisation can be written in vector form as

$$\bar{D} = \epsilon_0 \bar{E} + \bar{P} \quad \text{(for vacuum)}$$

where P is the dipole moment per unit volume of the material. For a material of relative dielectric constant ϵ,

$$\bar{P} = \epsilon_0 (\epsilon-1) \bar{E} \qquad \qquad \ldots \text{(I-10)}$$

Also $\bar{P} = N \bar{\mu}$ ... (I-11)

where $\bar{\mu}$ is the average displacement of the elementary particles, which is assumed to be proportional to the local electric field strength E' that acts on the particle. Then,

$$\bar{\mu} = \alpha \bar{E}' \qquad \qquad \ldots \text{(I-12)}$$

where α is the polarisability of the dipole. Thus the relation

$$\bar{P} = \epsilon_0 (\epsilon-1) \bar{E} = N\alpha \bar{E}' \qquad \ldots \text{(I-13)}$$

known as the Clausius equation, links the macroscopically measured permittivity to three molecular parameters, viz., N, α and $\bar{E}'$.

The total polarisability α of a dielectric material is the sum of four polarisabilities viz., electronic (α_e), atomic (α_a), orientational or dipolar (α_d) and space charge or interfacial (α_s). Thus,

$$\alpha = \alpha_e + \alpha_a + \alpha_d + \alpha_s$$

The polarisability α is defined in terms of dipole moment and its magnitude is a measure of the extend to which electric dipoles are formed by the atoms or molecules.

The electronic polarisation arises from the displacement of the negative electron clouds with respect to the positive atomic nuclei. At optical frequencies, the high frequency dielectric constant is equal to the square of the refractive index (n^2). When atoms of different types form molecules, a pair of atoms form a dipole and if a field is applied, the atoms are displaced with respect to each other, thus giving rise to atomic polarisation. In ionic crystals, displacement of ions take place giving rise to ionic polarisation. In general, solids containing more than one type of atoms, but having no permanent dipoles exhibit ionic polarisation. The atoms form a dipole and the asymmetric charge distribution between the opposite atoms give rise to permanent dipole moments which exist also in the absence of the applied field. Such dipoles experience a torque (rotation of the pair about an axis through the line joining them) in the applied field

that tends to orient them in the field direction, thus
giving rise to <u>orientational polarisation</u>. In real crystals
and more so in thin films (Sutton, 1964; Argall and
Jonscher, 1968) there exists a large number of defects. Under
the influence of an applied field the charges (ions or electrons
migrate through the material and get trapped or accumulated
at such defects or at the electrode-dielectric interface.
This localised accumulation of charges induces an image
charge on the electrode and give rise to a dipole moment.
This mechanism is known as <u>interfacial polarisation</u>.

(iii) <u>Frequency behaviour of tan δ in thin films</u>

The dependence of tan δ with frequency is much
significant. Peaks in tan δ have been observed at various
frequency regions depending on the polarisation present.
Several models have been put forward to explain these behaviour;
Initially it was assumed that such a loss in dielectric arises
due to pinholes in the deposited films. But this assumption
has been rejected by Harrop and Campbell (1968) on the ground
that tan δ shows some correlation with forbidden energy gap
of the dielectric. Young (1961) suggested that the losses
are due to an exponential variation of conductivity through
the thickness of the film. Simmons and co-workers (1970)
have been able to explain the ac behaviour of vacuum deposited
highly doped MoO_3 films. In their model they assumed the

presence of an addition$_\wedge^{al}$capacitance due to Schottky

barriers at the electrode - dielectric interfaces which

is in series with the interior capacitance.

Recent investigations on ac properties of thin

film capacitors of oxides (Siddal, 1959-60; Gaffee, 1962;

Maddocks and Thun, 1962; Hirosa and Wada, 1964; McLean, 1961;

Harrop and Wanklyn, 1964) halides (Weaver, 1962; MacFarlane

and Weaver, 1966), sulphides (Chopra, 1965) etc. showed

pronounced loss peaks or loss minima in the frequency

dependent loss factor curves. Goswami and Goswami (1973)

suggested a model for the general ac behaviour of vacuum

deposited thin film capacitors which accounts for the tan δ

minima in the frequency spectra. In the above model, a

capacitor system has been assumed to comprise (i) an inherent

capacity element C unaffected by frequency f and temperature,

(ii) a discrete resistance element R due to the dielectric

film in parallel with C and (iii) a series resistance r

due to the leads. The variation of R with temperature

is given by

$$R = R_0 \exp (\Delta E/kT) \qquad \cdots \quad (I\text{-}14)$$

where ΔE is the activation energy. The series capacitance

and tan δ are given by

$$C_s = 1+\omega^2 R^2 C^2/ \omega^2 R^2 C \qquad \cdots \quad (I\text{-}15)$$

$$\tan \delta = 1 / \omega R C + r/\omega R^2 C + \omega r C \cdots (I\text{-}16)$$

A loss minimum will be observed at frequency given by

$$\omega_{min} = (I/rRC^2)^{1/2} \qquad \dots \quad (I-17)$$

The increase of tan δ at higher frequencies is due to the lead resistance. It is seen from eqn. (I-17) that when temperature is lowered, R will increase and ω_{min} will also be lowered at lower temperatures. Thus ω_{min} will shift to lower frequencies at lower temperatures and vice versa

It is also possible to calculate the activation energy from capacitance and resistance measurements. According to Simmons et al. (1970), capacitance vs log ω curves at different temperatures have exactly the same functional form. Hence,

$$C_s = \text{function of} \quad (\omega R)$$

$$= \text{function of} \quad (\omega R_0 \ \exp \ \Delta E/kT)$$

Also for any constant capacitance,

$$\omega R = A \qquad \dots \quad (I-18)$$

where A is a constant whose magnitude depends on the particular value of capacitance. From eqns. (I-14) and (I-18) we have,

$$\omega = A \ R_0^{-1} \ \exp \ (- \Delta E/kT) \qquad \dots \quad (I-19)$$

Thus plotting log ω or log f ($\omega = 2\pi f$) vs 1/T for any constant capacitance, results in a linear plot

of slope - $\Delta E/k$. Hence from this plot ΔE can be evaluated.
The same can also be estimated from the slope of the graph
log R vs 1/T (eqn. I-14).

(iv) <u>Breakdown voltage and dielectric field strength</u>

The application of a capacitor in a circuit mainly
depends on its breakdown voltage (V_b) and breakdown field
strength (F_b). In dielectric breakdown, a capacitor discharges
initially with a strong current pulse of short duration,
emission of light and localized destruction of the dielectric.
Extensive works have been reported on dielectric breakdown
in thin films (Frohlich, 1937; Von Hippel, 1949; Callen, 1949;
Seitz, 1949; O'Dwyer, 1967; Klein 1966; 1967). Some of the
mechanisms which may cause such a breakdown are (i) electron
avalanching by impact ionisation of the lattice, (ii) collectiv
breakdown by electron - electron interaction, (iii) breakdown
from ionic transport (iv) Joule heating breakdown etc.
Theoretical predictions are more easily compared with
experiments by the breakdown mechanism suggested by Forlani
and Minnaja (1964). They used an avalanche approach along
with the explicit assumption of tunnel emission at the
cathode. This model leads to a thickness dependence of
breakdown field for thin film dielectrics as $F_b \propto d^{-1/2}$.

C. ELECTRICAL CONDUCTION IN INSULATING FILMS

According to the band structure of solids, an insulator is characterised by a full valance band separated from an empty conduction band by a forbidden energy gap, known as the band gap. Conduction cannot take place in either the filled or empty band unless additional carriers are introduced. Carriers may be generated or modulated inside the insulator (bulk - limited process), or injected from the metal electrode (injection-limited process). The metal-insulator contact is of much importance in the conduction process. There can be three types of contacts, viz., ohmic, neutral and blocking (Shottky) contacts.

There are several conduction mechanisms observed in thin films. If the barrier is very thin, according to quantum mechanics, the electron has a finite penetration probability, which cannot be explained classically. This is observed generally in very thin films of thicknesses less than 50 A^{o} and the process is known as tunneling. Just like thermionic emission in vacuum tubes, electrons can be emitted in to the conduction band of a dielectric from the contact metal electrode by thermal activation over the interface barrier and under an applied electric field, which is called Schottky emission (Simmons, 1964; Gundlach, 1964 and Mann, 196(

Conduction through sandwich layer of an insulator under high field can be quite complex because of the possibility of several mechanisms involved and it is often difficult to distinguish them. These mechanisms are generally governed by a number of factors inter alia work function of the electrodes and the sandwich layer, applied field, structural defects of the film such as stacking faults, impurities, dislocation etc, which act as potential trapping centers for current carriers. Under the application of high field, the conduction can be either electrode limited or bulk limited, depending on the field strength, the former prevails at lower fields and the latter at higher fields. The abrupt changes in potential at the metal-insulator interface imply infinite electric field. But in practice the potential step changes smoothly as a result of image force. (Shottky, 1914). The bulk analog of the Schottky effect at an interfacial barrier is the Poole-Frenkel effect (field assisted thermal ionisation) which is due to the lowering of a coulombic potential barrier when it interacts with an electric field. In electrode limited process the I-V characteristics can be represented by

$$J \propto \exp (\beta V^{1/2})$$

such that a plot of log J or log I vs $V^{1/2}$ will show

a steep slope depending on β, which is a constant.

D. SPACE-CHARGE LIMITED CONDUCTION

If the insulator is sufficiently thick, tunneling will not normally be the conduction process. However, if an ohmic contact is made to the insulator, at low fields if the injected carrier density is lower than the thermally generated free carrier density, Ohms law is obeyed. But when the injected carrier density is greater than the free carrier density, a space charge is built up at the electrodes and the current is known as space charge limited current (SCLC). For the simple case of one carrier trap free SCLC, the wellknown Mott-Gurney relation (1948) is given by

$$J = \frac{9}{8} \mu \epsilon \frac{V^2}{d^3} \qquad \qquad \dots \quad (I-20)$$

where J is the current density and μ is the drift mobility of charge carriers. The above relation is independent of temperature. However, in actual cases J is little lower than the theoretical value and also temperature sensitive. These deviations are due to the presence of traps in the insulator. If the insulator contains traps, a large fraction of the injection space charge will condense therein, thus the free carrier density will be much lower in a perfect insulator. Furthermore, the occupancy of traps is a function of temperature. The SCL current for an insulator with shallow traps is given by (Rose, 1955; Lampert, 1956; 1964).

$$J = \frac{9\,\mu\,\epsilon\,\Theta}{8}\,\frac{V^2}{d^3} \qquad \cdots \quad (I\text{-}21)$$

where $\Theta = N_c/N_t \; \exp \; (-\Delta E/kT)$ ... (

N_t is the number of traps positioned at an energy ΔE below the conduction band and N_c is the density of states approximately equal to 10^{19} cm^{-3} at room temperature. When the injected carrier density n_i exceeds the free carrier density n_o, SCL conduction predominates. Lampert calculated the voltage V_x at which the transition from ohmic to SCL conduction occurs to be

$$V_x = en_o d^2 / \Theta \epsilon \qquad \cdots \quad (I\text{-}22)$$

If charges are further injected into the insulator, the traps will become filled (trap filled limited TFL). Beyond TFL, the I-V characteristics will be governed by eqn. (I-20) for trap free insulator. The voltage V_{TFL} at which TFL occurs is given by

$$V_{TFL} = eN_t d/2\epsilon \qquad \cdots \quad (I\text{-}23)$$

For a trap distribution whose density decreases exponentially as the energy from the band edge increases (exponential trap distribution), the current density is given by

$$J \propto V^{1+1} / d^{21+1} \qquad \cdots \quad (I\text{-}24)$$

where 1 is a parameter characteristic of the distribution of traps. A relation $J \propto V^n$ is also observed for uniform

trap distribution. After the traps are filled, J will follow the square law with voltage.

E. OPTICAL PROPERTIES

Because of the extensive applications of thin solid films in various optical and electro-optical devices, considerable interest has arised in the optical properties of these films. Since the optical behaviour of a material is generally determined from its optical constants, viz., refractive index (n) and absorption index (k), it is of much importance to determine them accurately. There are several methods available for the determination of n and k, viz., Abeles method (1950), Polarimetric and Ellipsometric methods (Heavens, 1955) and spectrophotometric method.

The spectrophotometric method is one of the simplest methods for determining n and k. The reflectance (R) and transmittance (T) of films at normal angle of incidence are measured using an unpolarised light. Hadley (1955) greatly simplified this process by preparing a set of curves by calculating R and T as a function of d/λ for a range of values of n, producing one set of curves for each of a range of values of k and a given substrate index. The refractive index of a fairly transparent film on a transparent substrate can be calculated much easily from the transmittance data and by assuming k = o using the relation (Heavens, 1955).

$$T = \frac{8 n_0 n_1^2 n_2}{[(n_0^2+n_1^2) (n_1^2+n_2^2) + 4 n_0 n_1^2 n_2 + (n_0^2-n_1^2) (n_1^2-n_2^2) \cos 2\delta]} \qquad \dots \text{(I-25)}$$

where n_0, n_1, n_2 are the refractive indices of glass, film and air respectively and $\delta = (2\pi/\lambda) n_1 d \cos\phi$ is the phase thickness of the films, ϕ ($=90^\circ$) is the angle of incidence and λ is the wavelength of light used.

If the transmittance curve in the visible region has interference fringes associated with maxima and minima, refractive index n of the film can be calculated from the following relations.

For maxima, $n = m\lambda/2d$ $\qquad \dots$ (I-26a)

For minima, $n = (m+1/2)\lambda/2d$ $\qquad \dots$ (I-26b)

where m is the order of the fringe maxima or minima as the case may be and λ is the wavelength associated with the mth order. The order of the fringe may be calculated from the relation

$$m = \lambda_2/\lambda_1-\lambda_2 \qquad \text{or} \qquad m = \bar{\nu}_1/\bar{\nu}_2-\bar{\nu}_1 \qquad \dots \text{(I-27)}$$

where λ_1 and λ_2 are the wavelengths and $\bar{\nu}_1$ and $\bar{\nu}_2$ are the wave numbers associated with m^{th} and $(m+1)^{th}$ fringe.

The absorption coefficient α can be calculated at any wavelength from the slope of the log T vs d curves assuming the relation.

$$\alpha = \left(\log T_1 - \log T_2\right)/\left(d_2 - d_1\right) \qquad \ldots \text{(I-28)}$$

From α, the absorption index k also can be estimated at different wavelengths from the relation

$$\alpha = 4 \pi k / \lambda \qquad \ldots \text{(I-29)}$$

F. PRESENT WORK

It is seen from the above survey that the studies on dielectric, electrical and optical properties give an insight into the structure of matter viz., the nature of charges and species constituting the matter, the state of polarisation, type of conduction and band structure, band gap etc. Besides the increasing applications of thin films in electronic components like capacitors and resistors and also in micro-electronic circuits, as well as in optical devices, detailed studies on the basic properties of thin films are much essential. Eventhough extensive investigations have been made for the dielectric and other properties of bulk materials, very few studies have so far been carried out on thin films, and also systematic studies of the dielectric, electrical and optical behaviour of thin films are much less. It is wellknown that many of the physical properties of thin films are dependent

on their structure and methods of preparation as well as
on thickness, A correlation of the dielectric, electrical
and optical features is essential for the understanding of
the basic phenomena in dielectric films. Hence detailed
investigation on the above properties supported by electron
diffraction studies was undertaken in the present work.

CHAPTER-II : EXPERIMENTAL TECHNIQUES

CHAPTER II

EXPERIMENTAL TECHNIQUES

For studying the dielectric properties, d.c. electrical conduction and optical properties of thin films, several experimental techniques were adopted and these are described in detail in the subsequent paragraphs. It is well known that the properties of thin films are affected by so many factors and for any useful meaning of the measurements and consequent results, the deposition parameters have to be kept as non-variant as possible. To achieve this, necessary precautions were taken for their prepafation, especially as far as possible under the same experimental conditions. Special care was taken so that these films were homogeneous, uniform in thickness etc. The reproducibility of the measurements for different physical parameters was found to be very much facilitated by maintaining the above conditions. All the measurements were carried out when the films were completely stabilised.

A. DIELECTRIC PROPERTIES

(i) Preparation of films

The various films were generally prepared by the thermal evaporation of the bulk material in vacuo (better than 10^{-5} Torr). A conventional coating unit, which

consisted of an oil diffusion pump backed by a rotary

pump was used. The deposition was carried out by the

evaporation of the bulk material directly from tungsten

or molybdenum boats or from a silica boat heated externally

by a tungsten filament. All the boats were flashed in vacuo

prior to the deposition to remove the surface impurities.

Aluminium electrodes were deposited from preflashed tungsten

spiral boats. High purity aluminium wires were used. The

boat was heated slowly till aluminium melted and then flashed

immediately.

(ii) Substrates and substrate heating

Microscopic glass slides (Blue Star deluxe) were

generally used as substrates. These substrates were cleaned

with chromic acid and then washed thoroughly in distilled

water followed by a washing in isopropyl alcohol. They were

then dried in an oven. Sometimes these substrates were heated

in vacuo for degassing and then cooled down to room temperature.

The substrates were heated by resistance heating filaments

called the substrate heater which was in contact with the

substrates and the temperature was monitored by a cromel-p-

alumal thermocouple.

(iii) Fabrication of capacitors

The shape of a typical capacitor fabricated is shown

in fig. II-1. Generally aluminium deposits ($2000 \text{ A}^{\text{o}}$) were

used both as the base and counter electrodes. Aluminium

GLASS
SUBSTRATE

COUNTER
ELECTRODE

EDGE-A

DIELECTRIC
LAYER

BASE
ELECTRODE

Fig. II-1

microscope

beam
splitter

source

a
b

fringes as
seen through
microscope

(not to scale)
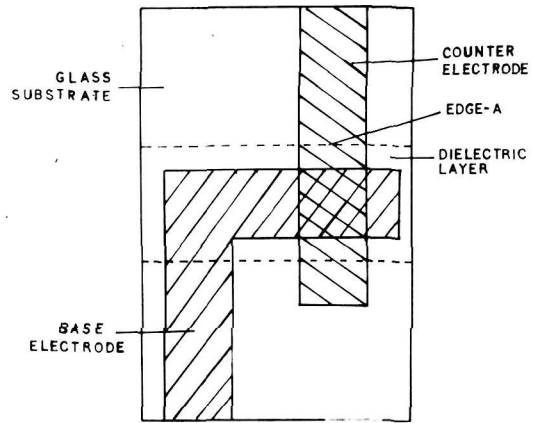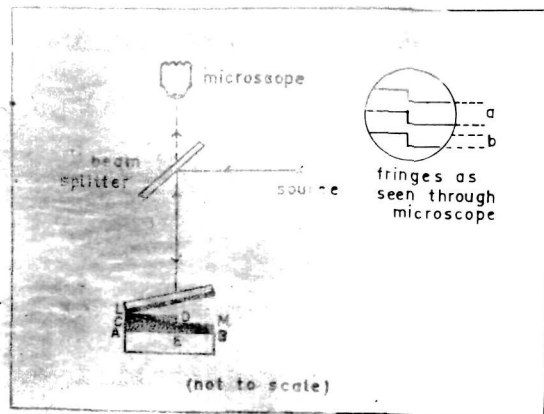
Fig. II-2

(99.9% purity) in the form of a wire, was deposited from
a multistrand tungsten boat on glass substrates. Different
metal masks were used to get the required shape of the
capacitor. The Al/dielectric/Al system was fabricated by
successive deposition after breaking the vacuum. The
capacitors had an effective geometrical area of about 0.16 sq.cm.
For uniform deposition and also to avoid spitting, the
dielectric material was initially degassed by slow heating in
vacuo prior to their deposition at temperatures much lower
than their melting points for about 30 minutes. The rate of
deposition was controlled by adjusting the current passing
through the boats and the time of deposition. Arrangements
were such that six capacitors of varying thickness could be
simultaneously prepared. The thickness of the dielectric
film was measured at the edge A (fig. II-1) of the capacitor
by multiple beam interferometry method.

(iv) <u>Ageing</u>

All the capacitors were aged in air by keeping them in
a desiccator. They were further stabilised by heating and
cooling cycles in vacuo at temperatures depending on the
nature of the material.

(v) <u>Measurement of film thickness</u>

Since many physical properties of thin films are
thickness dependent, a precise knowledge of its thickness
is essential for computing many dielectric and optical

parameters. One of the simplest method is gravimetric method. In this method, the mass (m) of the film was determined by weighing the substrates on a micro-balance (Mettler) before and after deposition. Assuming that the density (g) of the film is same as that of the bulk material, thickness may be calculated using the relation

$$d = m / gA \quad cm$$

where A is the surface area of the film. This method, though approximate, was useful for thicker films. A better and more precise one is the Tolansky's multiple beam interferometry method (Tolansky, 1948).

A substrate AB (fig. II-2) supports a film ACDE whose thickness is to be measured. Over this an opaque layer of aluminium is evaporated, thus forming a step DE. An optically flat glass slide coated with a semi-transparent layer of aluminium is placed in contact with this so that the two plates form a small wedge. A monochromatic light (sodium, 5893 A$^{\circ}$) is reflected by a beam splitting glass slide on to the plates and the back reflected rays are observed by a low power microscope. Straight line fringes called Fizeau fringes of equal thickness are observed. At the edge, these fringes are shifted showing a step as in fig. II-2. This fringe shift and the fringe width can be measured by the travelling microscope and the film
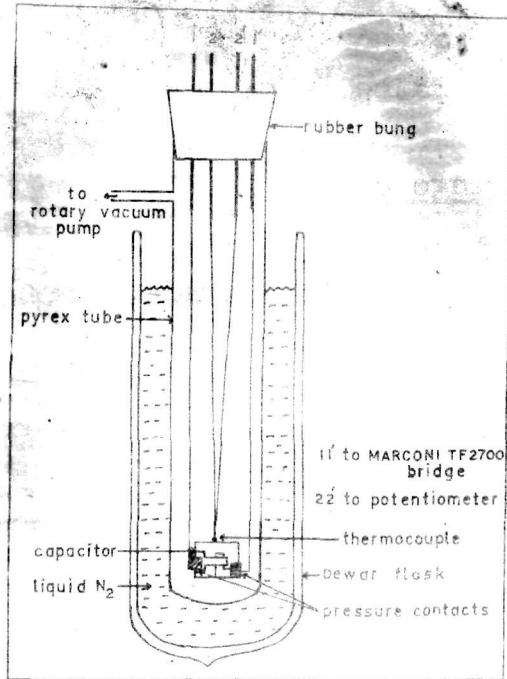
to
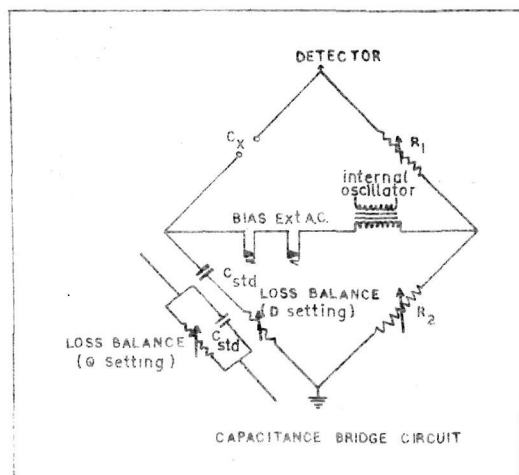rotary vacuum
pump

rubber bung

pyrex tube

1' to MARCONI TF2700
bridge
2' to potentiometer

thermocouple

capacitor

Dewar flask

liquid N$_2$

pressure contacts

Fig. II-3

DETECTOR

C_x

R_1

internal
oscillator

BIAS Ext.A.C.

C_{std}

LOSS BALANCE
(D setting)

C_{std}

R_2

LOSS BALANCE
(Q setting)

CAPACITANCE BRIDGE CIRCUIT

Fig. II-4

thickness (d) is calculated by the relation

$$d = \frac{\lambda}{2} \frac{fringe\ shift}{fringe\ width}$$

where λ is the wavelength of the monochromatic light used (5893 A^o).

(vi) <u>Cryostat</u>

All dielectric measurements were carried out in a cryostat (fig. II-3) where the temperature could be varied from 87 to 400° K. It consists of a pyrex tube closed at one end and stoppered with a rubber bung at the other end, through which the leads for the capacitor, thermocouple etc. were taken out. The system was continuously evacuated by a rotary vacuum pump. Short length r.f. cables were used as leads for capacitance bridge. The thermocouple was connected to a potentiometer or a microvoltmeter (Philips PP 9004). The cryostat was kept inside a Dewar flask containing liquid air for low temperature measurements, whereas an external heater was used for measurements above room temperature.

(vii) <u>Measurements of C and tan δ</u>

The important parameters viz., capacitance (C) and loss factor (tan δ) were directly measured by a Marconi TF2700 Universal Bridge. The basic capacitance bridge net work is shown in fig. II-4. This is a modified form of a Wheatstone bridge circuit where the two resistive arms of the bridge are replaced by the unknown capacitance C_x and a standard

capacitance C_{std} (0.1 μF). R_1 and R_2 are two standard resistances. The bridge is excited by an internal oscillator of 170 mV and 1 KH_z. and the balancing point (null point) is read on a sensitive micro-ammeter. To increase the sensitivity of the null point, the out put of the signal is amplified by a three stage transisterised amplifier and is fed to the meter after rectifying so that the needle of the meter always deflects to one side of the zero for all ac measurements. When the bridge is balanced,

$$C_x / C_{std} = R_2/R_1$$

In this instrument, when R_1 and R_2 are properly adjusted, the unknown capacitance can be read directly from the dial readings.

The bridge has a small variable resistance (0 to 175 ohms) known as the loss balance resistor connected in series with C_{std} (Fig. II-4) which helps to measure the loss factor tan δ directly. It has two positions D and Q for measuring loss factor. In the D position, the series capacitance (C_s) and tan δ are measured whereas in Q position C_{std} becomes parallel to a larger variable resistance and hence the parallel capacitance (C_p) and quality factor Q are measured.

$$C_s / C_p = 1 + Q^2 \quad \text{where} \quad Q = 1/\tan \delta.$$

In all the experimental results, the capacitance has been expressed in terms of C_s only.

The above bridge has a provision for measuring C and tan δ at variable frequencies (1 H_z to 10^5 H_z) by using an external oscillator (Philips PM 5100) which is connected to the bridge through an isolating transformer (Marconi TM 7120). The loss factor is then given by

$$tan\ \delta\ =\ tan\ \delta_f\ \ f/1000$$

where tan δ_f is the loss factor measured at any frequency f. The bridge sensitivity at 100 pf range is 0.5 pf and can measure tan δ down upto 0.001.

(viii) Dielectric constant

The capacitance C of a parallel plate condenser with a dielectric thickness d (metre) and effective electrode area A (sq.metre) is given by

$$C\ =\ 8.85\ x\ 10^{-12}\ \varepsilon A/d\ \ farads$$

where ε is the permittivity of the dielectric, which has the dimensions of farads/metre and $8.85\ x\ 10^{-12}$ is the permittivity of free space in farads/metre. For all practical purposes, a dimensionless quantity viz., the relative permittivity or dielectric constant is used in the present work, which is the ratio of permittivity of a medium to that of free space.

B. I-V CHARACTERISTICS

The dc conduction in the dielectric films was studied in vacuo at different temperatures by keeping the sample in the cryostat used for dielectric measurements. The experimental arrangements were similar to that of Fisher and Giaever (1961). The voltage (V) across the sample was measured by a VTVM (Heathkit Model V-7A) and the current (I) by a FET nano-ammeter (Aplab. TFM.13) which was in series with the sample.

In some cases, the resistance of the samples (not in sandwiched samples) were measured directly by a million megohm meter (Elico. RM.70).

C. BREAKDOWN VOLTAGE (V_b) AND DIELECTRIC FIELD STRENGTH (F_b)

There are numerous methods available for measuring the breakdown voltage accurately (Budenstein et al. 1967; Klein et al. 1966; 1967). A simple circuit was adopted to measure V_b in which a variable dc (0-100 V) was applied across the capacitor. A FET nano-ammeter (Aplab. TFM 13) in series with the test capacitor and a VTVM parallel to it were used to measure the current and voltage. At the breakdown region, a steep rise in current was observed and sparking took place many times at the capacitor junction of the top electrode. The dielectric field strength F_b is given by

$$F_b = V_b / d \quad \text{volts} / \text{cm}$$

where d is the thickness of the dielectric layer (in cm).

It may be pointed out that both the electrodes were aluminium and no change in I-V characteristics were observed when the polarity of the electrodes were reversed.

D. OPTICAL PROPERTIES

(i) Film preparation

Microscopic glass slides (3.5 cm x 1 cm) of refractive index 1.52 were used as substrates for studying optical properties in the visible spectrum. These substrates were also cleaned properly as described in Section A (ii). In some cases quartz plates of the same dimensions were also used as substrates for studying the optical properties in the UV region. Films were prepared by vacuum evaporation and different film thicknesses could be obtained by keeping the substrates spaced apart so that the distances between each substrate and the source were different. The thickness of these films were estimated by interferometric method by depositing aluminium films on its edges after all optical measurements.

(ii) Optical measurements

Optical properties of these films in the visible region were studied by transmission and reflection measurements by normal angle of incidence method and the optical constants such as refractive index (n_f), absorption index (k_f) and absorption coefficient (α) were estimated. The optical band gap (E_g) was also calculated in many cases.

(iii) Spectrophotometer

A double beam Beckmann DK2 spectrophotometer with
automatic recording was used to measure the transmittance of
these films in the UV and visible region. (The maximum error
of the instrument was $\pm$ 5 A$^{\circ}$ in the wavelength calibration
and $\pm$ 1% for the recorded transmittance measurements).

Since the above instrument had no provision for
transmittance and reflectance measurements, a special
spectrophotometer was designed and fabricated in this
laboratory (fig.II-5) in which the reflectance could be
measured between 5 to 10° of incidence. It consists of
mainly a light source 1, a condensing lens 2, a filter 3, a
collimator 4, a prism 5, fixed on a rotating table moving
on a graduated scale 6, a telescope 7, a focussing lens 8,
a sample holder 9, a photocell 10, and a graduated disc 11.
A tungsten lamp with straight filament and with a stabilised
power supply was used as the source. The graduated scale 6 was
calibrated for different wavelength using different filters
by adjusting the scale for maximum intensity in the photocell.
The sample holder 9 placed at the focus of the lens 8 could
be rotated freely on the graduated base 6 and the angle of
rotation could be identified. The photocell (Philips 90 CV
or 92 AV) placed very near to the sample holder also could
be rotated around the same axis of the sample holder. The
photocell current was measured by measuring the voltage across
a 470 K ohm resistance by a dc microvoltmeter (Philips PP 9004)

The whole instrument was kept in a light-proof case.

E. STRUCTURAL ANALYSIS

The structure of the bulk powder was analysed by x-ray powder diffraction (Cu K_α radiation) whereas the vacuum deposited films were studied by both transmission and reflection electron diffraction techniques. The samples were deposited on polycrystalline NaCl tablets as well as on (100) face of NaCl crystals at room temperature and at higher substrate temperatures under the same experimental conditions in which the capacitor samples were fabricated. The reflection studies were also carried out with the deposited films on glass substrates and on well cleaved mica sheets. In some cases the structure was studied also by selected area diffraction method in an electron microscope.

CHAPTER-III : STUDIES ON DYSPROSIUM OXIDE FILMS

CHAPTER III

STUDIES ON DYSPROSIUM OXIDE FILMS

A. INTRODUCTION

Rare earth oxides have extensively been used as important constituents in dielectric materials to control their dielectric properties. Templeton et al. (1954) studied the structure of Dysprosium oxide (Dy_2O_3) for the first time and reported that it has a cubic structure with lattice parameter a = 10.667 A^o. Staritzky (1956) also reported the same structure for Dy_2O_3 and the lattice parameter was in agreement with the above result. A new high temperature stable crystalline variety of Dysprosium sesquioxide namely, Dy_2O_5 was examined by Foex et al. (1965) and the lattice parameters were given as a = 3.82 A^o and c = 6.11 A^o. The structural properties of intermediate phases of systems formed from CaO and Dy_2O_3 were reviewed by Queyroux (1965) and found that Dy_2O_3 presents two allotropic varieties, cubic and monoclinic reversible at 2000°C. Rudenko et al. (1971) also reported the stoichiometry and phase transformation of Dy_2O_3. Hare (1963) used neutron diffraction for studying the crystal structure. Powder pattern measurements of Dy_2O_3 were made with neutrons of wavelength 1.197 A^o. The structure parameters were thus obtained and the variation of metal-oxygen distance in the series was discussed. The melting point of Dy_2O_3 was found

to be 2625° K (Mordovin et al. 1967) which was determined
by heating the oxide in an atmosphere of argon or hydrogen
and observing the temperature by an optical pyrometer.
Bondarenko et al. (1964) studied the thermionic emission
using Dy_2O_3 as cathode.

New dielectric bodies, particularly those with low
TCC over a wide range of temperature are being sought for
electronic equipments designed for operating at a high
ambient temperature. Marzullo et al. (1958) studied the
dielectric properties of titania and tin oxide containing
varying proportions of rare earth oxides in the range
-40 to $+ 200^{\circ}$C. A ceramic dielectric with high ϵ $(1-3 \times 10^4)$
was prepared by firing $BaTiO_3$, Dy_2O_3 and SiO_2 system at
$1250-1400^{\circ}$C. (Shigeru Waku et al. 1968). Tare et al. (1964)
measured the emf. of Dy_2O_3 to yield the electronic portion
of the conductivity in the temperature range $650-900^{\circ}$C and
with different oxygen pressures. Depending on the temperature
and oxygen pressure, the oxides showed either ionic or
electron-hole conductivity. The electrical conductivity of
powdered rare earth oxides compressed at 2500 Kg/sq.cm was
determined by Bogoroditski et al. (1965) from room temperature
to 900°C and of specimens sintered at 1300°C from $240-1300^{\circ}$C.
The study showed that dielectric constant of Dy_2O_3 was a
function of temperature.

Staritzky (1956) studied the refractive indices of
rare earth oxides using Na 5893 A° light and Dy_2O_3 had a

bulk refractive index equal to 1.97. Baun et al. (1963) reported that the oxides of rare earths gave individualistic IR absorption spectra in the region 800-240 cm^{-1}. The diffuse refluctance spectra of the oxides were reported by White (1967) and the electronic spectra of Dy_2O_3 single crystals in the region 0.26 -40 μ was studied by Henderson et al. (1967). Batsanov et al. (1962) investigated the optical properties of powdered lanthanide oxides at $800^{\circ}C$ and the refractive index of Dy_2O_3 was reported to be 1.92.

Winkler (1969) prepared thin films of rare earth oxides for specific activity measurements by sedimentation method on thin Mylar backing and the films were particularly suited for activation measurements on K-radiation emitters. Hacskaylo (1968) studied the properties of capacitors of the system $Dy_2O_{3_{80}}B_2O_{3_{10}}SiO_{2_{10}}$ evaporated below $1900^{\circ}C$ from tungsten or tantalum boats. The films were amorphous with $n = 1.54$, tan $\delta = 0.0025$ and $F_b = 4 - 1.7 \times 10^6$ V/cm. Further, the dielectric properties of thin films of rare earth oxides were studied as a function of frequency and temperature by Kadzhoyan et al. (1968). Mirowski et al. (1970) reported the results on thin film transistors using CdSe semiconductor and a single insulating layer of SiO_2 or a double layer of SiO_2 and Dy_2O_3. Chernobrovkin et al. (1971) vaporised rare earth oxides by an electron beam to get dielectric films whereas Tsutsumi et al. (1970) deposited Dy_2O_3 films by high frequency bombardment technique.

From the above survey it is seen that only very little work has been carried out on the dielectric and optical properties of Dy_2O_3, especially in thin films. The conduction in Dy_2O_3 thin films has not yet been studied. It is well known that various properties of thin films are influenced very much by the film thickness, deposition conditions, annealing, substrate temperature etc. In view of the above, an extensive study has been carried out on the ac behaviour, the dc conduction mechanism and the optical properties of vacuum deposited Dy_2O_3 films.

B. EXPERIMENTAL

Bulk dysprosium oxide powder (99.9% purity, supplied by M/s. Koch-Light Laboratories Ltd.) white in colour was vacuum deposited (10^{-5} mm.Hg) at room temperature from tungsten boats on thoroughly cleaned glass substrates. The substrates were heated at $100^{o}C$ prior to the deposition of the dielectric and cooled down to room temperature. The powder was heated slowly and no appreciable degassing was observed. Then the temperature of the boat was increased till deposition started on the glass substrates, which were kept about 12 cms away from the source. Aluminium deposits were used both as the base and counter electrodes. The rate of deposition on substrates just above the source was about 50 A^{o}/min. The detailed methods for electrode deposition, fabrication of $Al/Dy_2O_3/Al$ system etc. are given in Chapter II.

The effective area of a capacitor was 0.16 cm^2.

These capacitors were then aged in a desiccator for a few days and then further stabilised by annealing in vacuo at about $100^{\circ}C$ by repeated heating and cooling cycles. The capacitance (C) and loss factor (tan δ) were measured at different frequencies ($10^2 - 10^4$ H_z) and temperatures ($78 - 373^{\circ}K$) in a cryostat as described in Chapter II. The dielectric constant (ε) was evaluated from the relation (I-4) given in Chapter I.

For I-V characteristics studies of these capacitors, a dc voltage was applied in steps of 0.5 V and corresponding current was measured. This was repeated by changing the polarity of electrodes. The measurements were taken at differen temperatures and for different film thicknesses also. The variation of current at a fixed voltage was also measured at different temperatures. All the above measurements were carried out in vacuo (10^{-2} mm Hg). The dc breakdown voltage of these capacitors were tested in air after all measurements and the film thickness was measured by multiple beam interferometry method.

Films were deposited on glass substrates for optical measurements and they were annealed in vacuo at about $100^{\circ}C$ prior to measurements. Optical constants n and k of these films in the visible region (4000-7000 A°) were evaluated from the transmittance data obtained by normal incidence

Fig. III-1
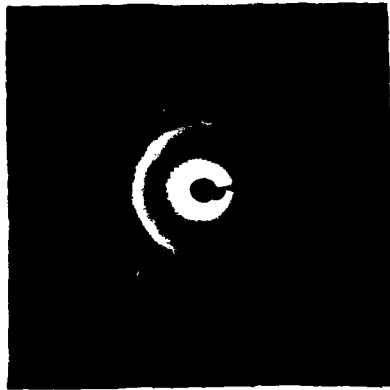
Fig. III-2

Fig. III-3

measurements from a Beckmann DK2 spectrophotometer using the formula (I-25) given in Chapter I.

The natures of the deposited films were studied by electron diffraction and electron microscopy methods. For these studies, films were deposited on smooth surfaces of polycrystalline NaCl tablets under the same experimental conditions described above and these were transferred to grids with collodion by dipping the tablets in distilled water. The structure of the bulk powder was analysed by X-ray powder method.

C. RESULTS

1) Structure

X-ray studies of the bulk oxide showed that the material was crystalline having a bcc structure (a = 10.66 A^{o}) conforming to Dy_2O_3 structure. The X-ray powder pattern is shown in fig. III-1 and the measured d values are given in table III-1. But vacuum deposited films, on the other hand, did not yield any sharp pattern (fig. III-2) at all when analysed by electron diffraction, thus suggesting that they were either fine-grained or amorphous in nature. Electron micrographs also showed that these were featurless (fig.III-3). These films even after repeated heating and cooling in vacuo as carried out in annealing process did not show any significal grain growth or crystallinity when observed by transmission electron microscopy or selected area electron diffraction

TABLE III-1

I/Io	d A$^{\circ}$	hkl
s	3.070	222
ms	2.685	400
f	2.520	411
f	2.270	322
f	2.107	422
s	1.880	440
f	1.84	$\begin{cases} 530 \\ 433 \end{cases}$
f	1.71	532
vf	1.67	620
s	1.61	622
f	1.57	631
f	1.54	444
f	1.51	550
vf	1.41	642

s - strong

f - faint

m - medium

v - very

a = 10.66 A$^{\circ}$

Fig.

Fig.

Fig.
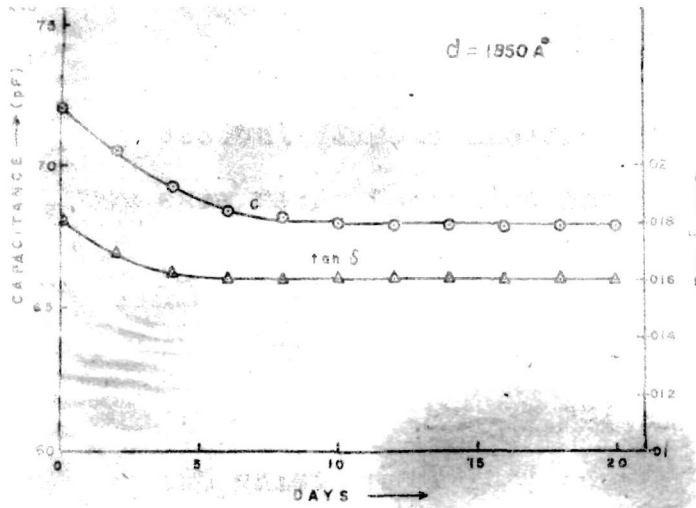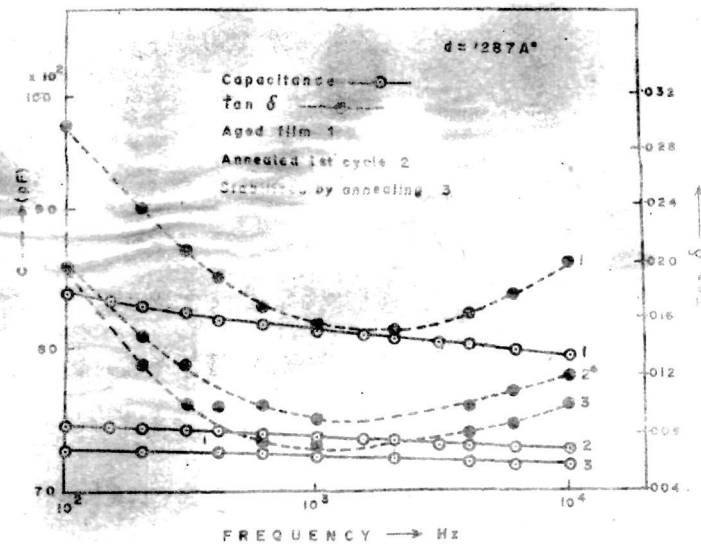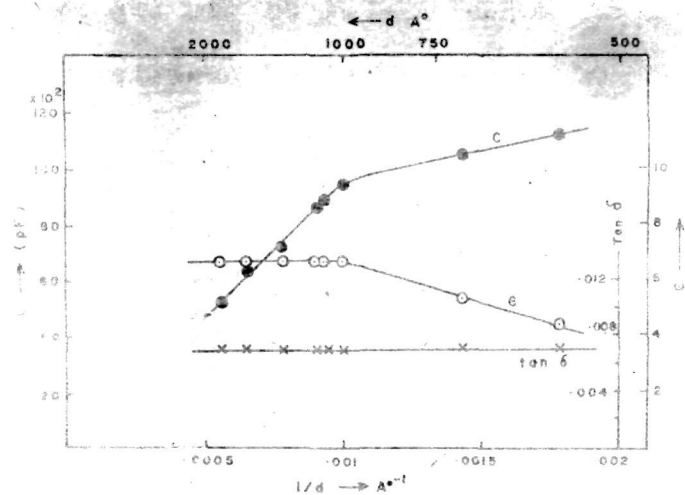
methods. These observations clearly indicated that films
used for electrical and optical studies were mostly amorphous
in nature.

ii) Dielectric properties

a) Ageing and annealing effect

It has been found that both ageing and annealing have
considerable effect on capacitance and tan δ. Fig. III-4
shows typical variations of C and tan δ for a film thickness
d = 1850 A$^\text{o}$. It is seen that C and tan δ showed a continuous
decrease with increase of time and eventually became more or
less constant. It was however noticed that even after long
ageing or self-annealing process, these capacitors did not
attain stability unless they were annealed in vacuo. Fig.III-5
shows the variations C and tan δ with frequency for different
annealing cycles of an aged capacitor. It was found that
these capacitors attained stability generally after the
second annealing cycle at about 100$^\text{o}$C. Capacitance and tan δ
of these stabilised samples did not vary much when measured
even after a few months. It was also noticed that when a
SiO protective layer was deposited on the top of these
capacitors, both C and tan δ remained practically same even
after six months.

b) Thickness effect on ϵ, C and tan δ

Unlike bulk materials, film thickness also affect
both ϵ and tan δ. C decreased continuously with increasing
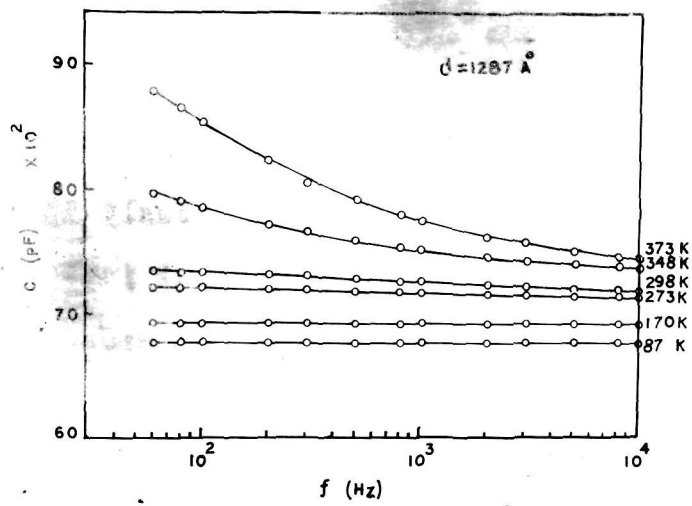film thickness. This variation showed some important feature
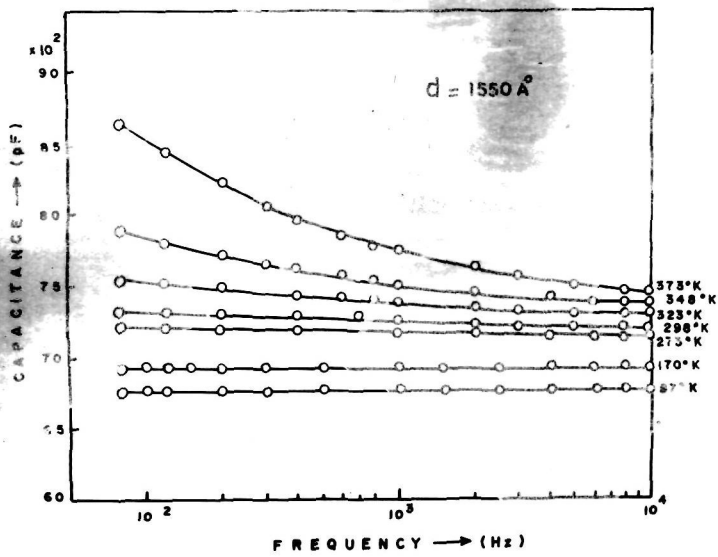
Fig. III-7

Fig III-8

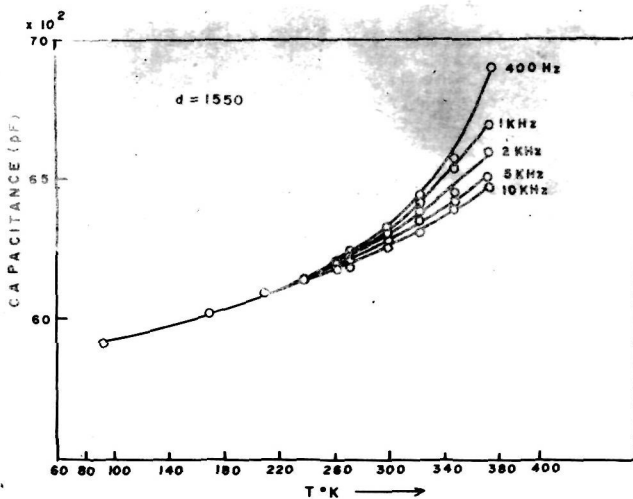Fig. III-9

when C and ϵ were plotted against 1/d instead of d (fig.III-6).
It is seen that though C decreased continuously for thicknesses
between 600-2000 $\overset{o}{A}$, the fall was gradual at initial stage,
but at higher thickness (d > 1000 A^o) C decreased linearly
with 1/d, thus suggesting that C $\propto$ 1/d in the higher thickness
region. ϵ increased gradually for film thicknesses less than
1000 $\overset{o}{A}$, but became constant for thicker films (d > 1000 A^o).
It thus suggests that C $\propto$ 1/d and ϵ is constant are valid
only for thicker films (d > 1000 A^o). It is also interesting
to note that tan δ remained constant (0.007) for all film
thicknesses.

c) <u>Frequency and temperature effects on C and tan δ</u>

Fig. (III-7) shows the typical variations of C with
frequency (10^2-10^4 Hz) at different temperatures for a film
thickness d = 1287 $\overset{o}{A}$. It is seen that C decreased with
increase in frequency and decrease in temperature. The change
of C with frequency was less sensitive as the temperature
decreased and eventually C became invariant with frequency
at low temperatures generally below the room temperature.
Similar results were also obtained for other film thicknesses
also (Fig. III-8).

However when C was plotted against temperature at
different frequencies, some interesting features were observed
(fig. III-9). At higher temperature, separate curves were
formed characteristic of the frequencies. But on lowering the
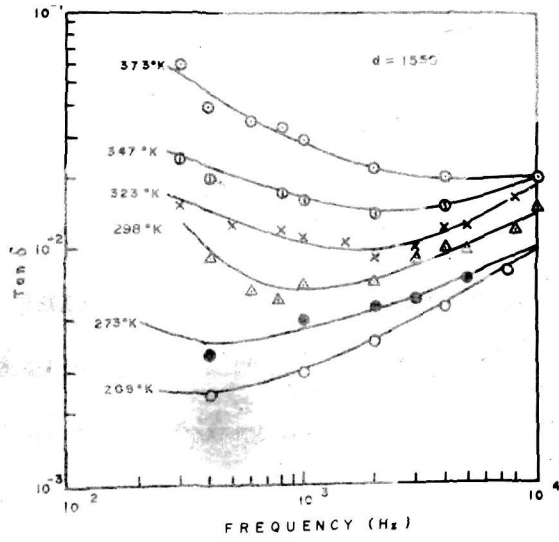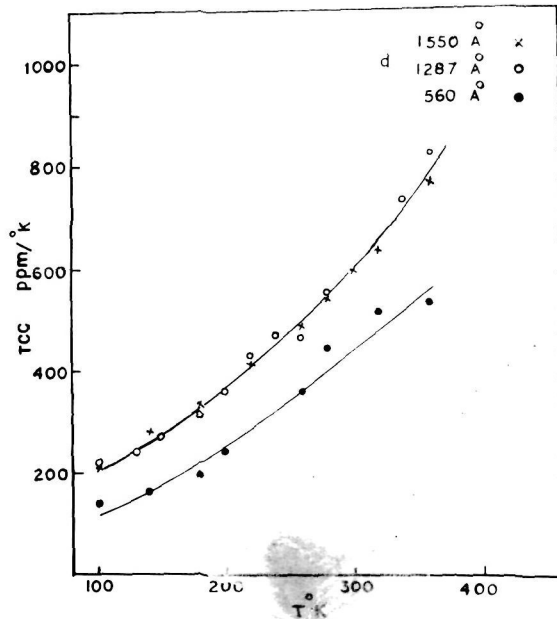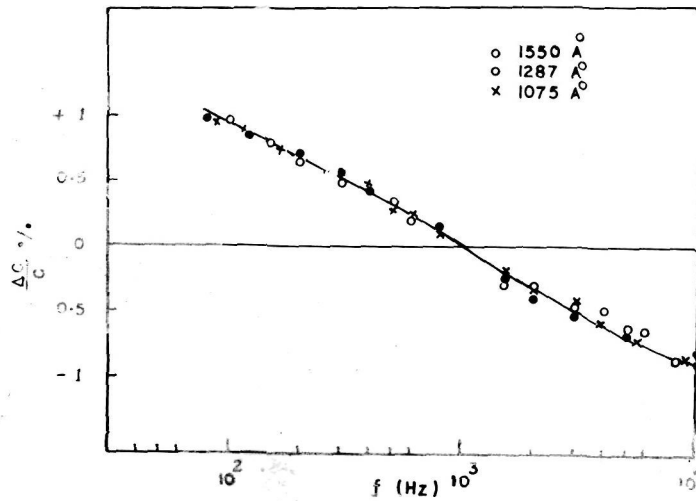temperature, these curves became closer and finally merged to

Fig. III - 10

Fig. III - 11

Fig. III - 12

a single one at about 240° K, below which C varied very slowly with temperature. On extrapolating C to 0°K, the dielectric constant at 0°K could be evaluated and it was found to be about 6.3. This appears to be the static dielectric constant which is a slow function of temperature at least in the low temperature region.

The variations of tan δ with frequency at different temperatures are shown in fig. III-10 for d = 1550 A°. These curves show several features. Tan δ decreased with frequency, attained a minimum and then increased for higher frequencies. Thus a tan $δ_{min}$ was observed which however shifted to higher frequencies for higher temperatures. Such variations were first reported by Goswami and Goswami (1973, 1974) and later by Goswami and Varma (1974). However, tan δ increased with increasing temperature. Similar behaviour was also observed for other film thicknesses also.

d) Temperature coefficient of capacitance (TCC) and percentage variation of capacitance (ΔC/C).

The TCC of the capacitors were measured and found to be very small. It varied from 200-800 ppm/$^{\circ}$K in the temperature range 100 - 370° K (fig. III-11). This parameter was generally independent of film thickness (d > 1000 A°) and increased with temperature. However for film thicknesses < 1000 A°, TCC was found to be slightly lower.
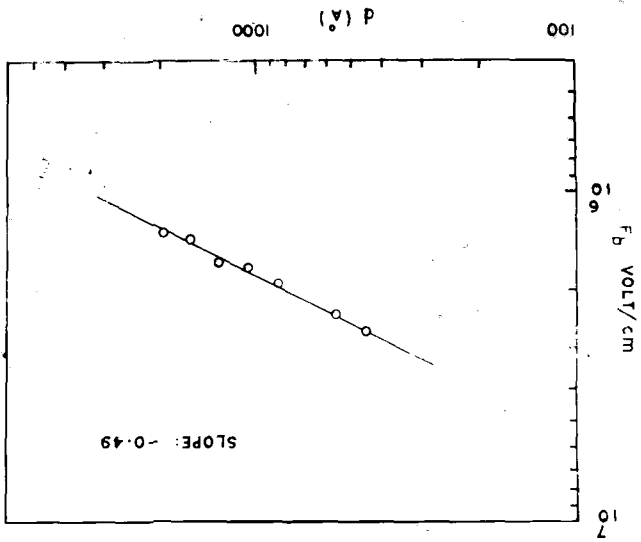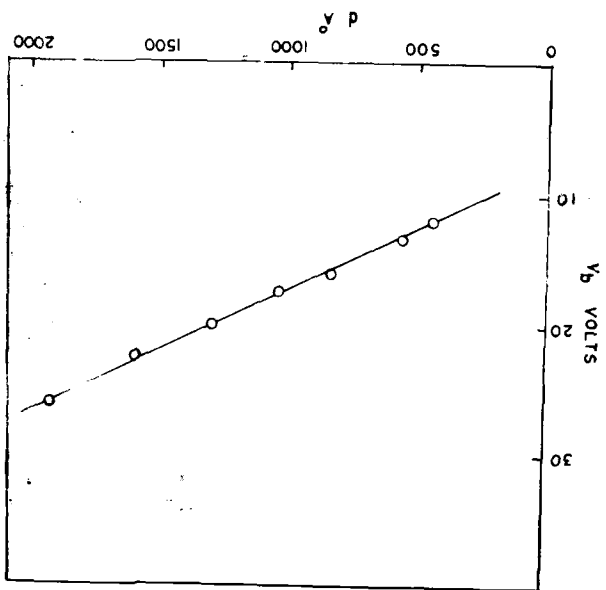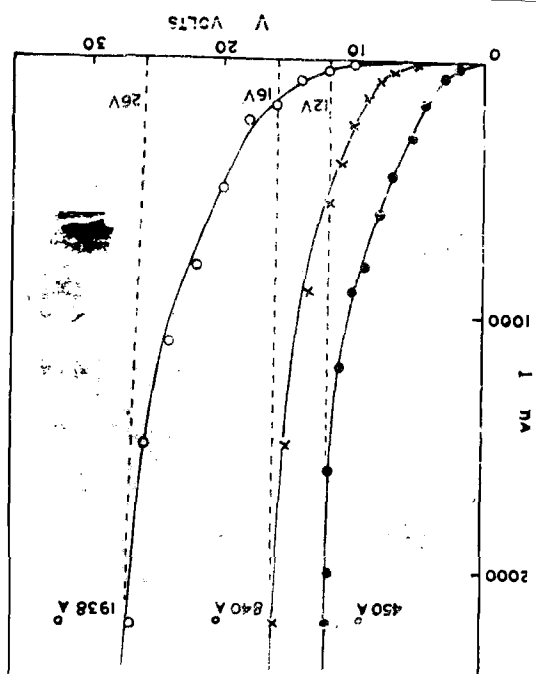
Another parameter of importance is the percentage
variation of capacitance with frequency. This is defined as
the percentage change of C at any frequency (C_f) from the
value of C at any arbitrary frequency, say at 1 kH_z (C_{1kHz}).
This can be expressed as

$$\Delta C \,/\, C \,\% \;=\; (C_f - C_{1kHz}) \quad x \;\frac{100}{C_{1kHz}}.$$

Fig. (III-12) shows $\Delta C/C$ % for three capacitors of different
film thicknesses. It is seen that this variation is less
than $\pm$ 1% for the frequency range studied.

e) **Breakdown voltage and dielectric field strength**

The breakdown voltage (V_b) was measured in air at
room temperature by applying a dc voltage across the capacitor
and measuring the current. The voltage was increased in
steps till the current shot up thus causing a destruction of
the capacitor. Fig. III-13 shows the variation of current
with applied voltage for three film thicknesses. The current
increased rapidly at higher voltages and the straight lines
extrapolated to the voltage axis gave V_b. V_b increased
with increasing film thickness (fig. III-14). However, it
is interesting to note that the breakdown field ($F_b = V_b/d$)
decreased with increasing film thickness. In fig. III-15,
F_b is plotted against d in log-log scale. The graph is a
straight line with a negative slope = 0.49, thus following
the Forlani-Minnaja relation $F_b \propto d^{-1/2}$. F_b was high and
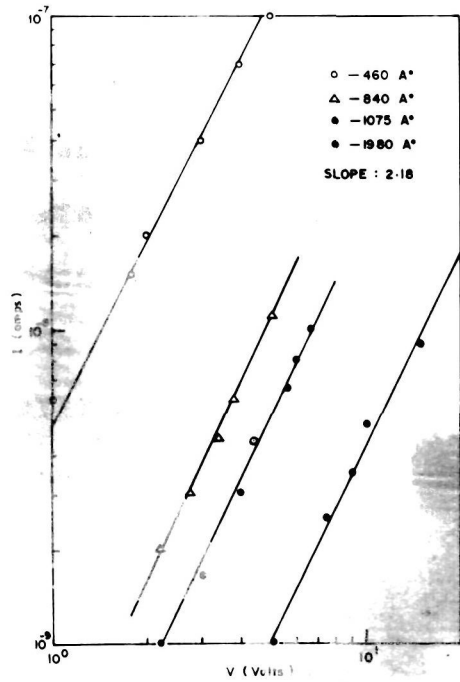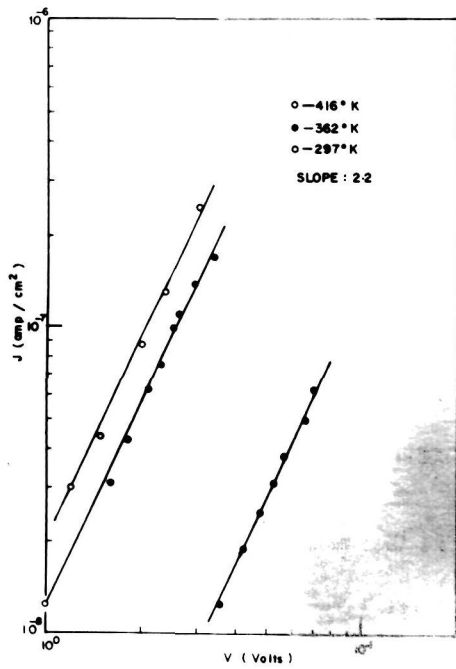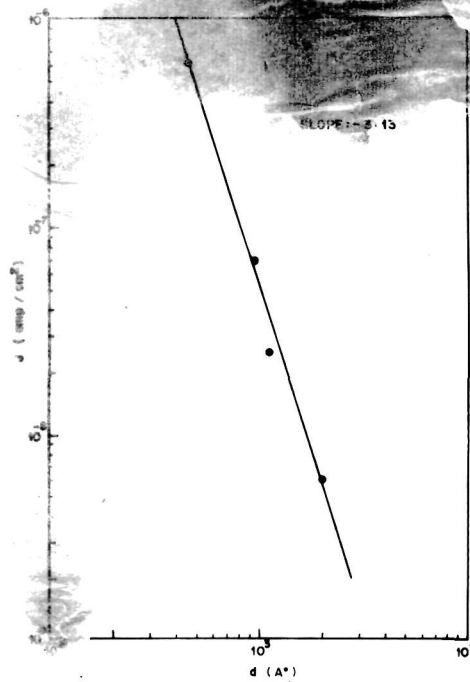of the order of 10^6 V/cm.

Fig. III – 16

Fig. III – 17

Fig. III – 18

iii) I-V Characteristics

The dc conduction in Dy_2O_3 films was also investigated for the same capacitor systems used for studying dielectric properties. Current was measured with increasing applied voltage. The experiment was repeated by changing the polarity of the electrodes. But no appreciable difference was observed and the I-V curves were symmetrical irrespective of the polarity of the electrodes. Fig. III-16 shows the I-V characteristics of four film thicknesses plotted in log-log scale. It is seen that the slopes of all these graphs are the same (2.18) and do not change even when the voltage is increased to about 15 V for the thickest film, thus suggesting that current varied approximately with voltage as $I \propto V^2$.

Fig. III-17 shows the variation of current density with voltage at different temperatures in log-log scale for a film thickness of 1075 A^O. The positive slope of the graph is about 2.2 and remained the same for all temperatures showing that current is increasing with voltage approximately following the square law J or $I \propto V^2$ which is found to be true for all the ranges of temperature studied (297 - 410° K).

Since J or I is dependent on film thickness, it is plotted against d (fig. III-18) in log-log scale. All the above readings were however from the room temperature measurements. The straight line graph shows a negative slope of 3.13, thereby indicating that $J \propto 1/d^3$. From the above
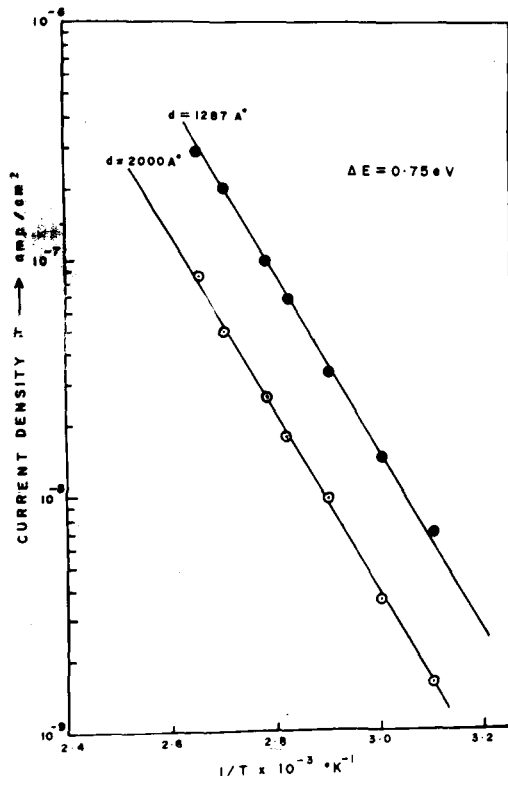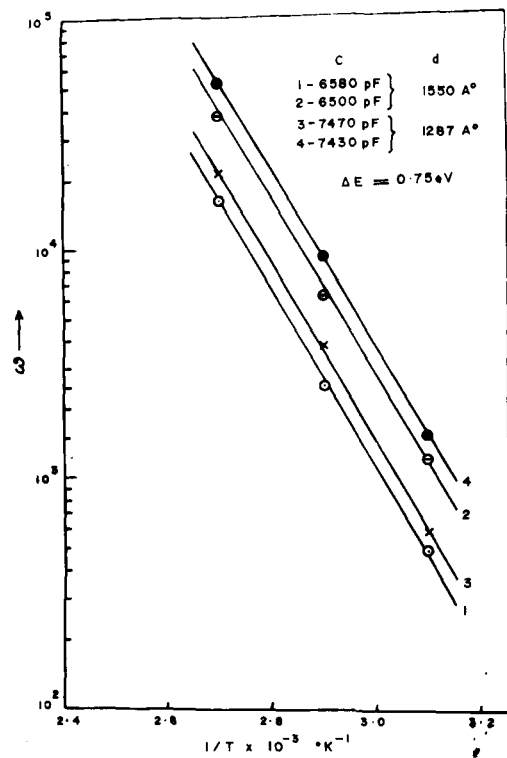
Fig. III-19

Fig. III-20

results it can be concluded that the variation of current follows the relation $J \propto V^2/d^3$ and the conduction process is space charge limited.

iv) <u>Activation energy (ΔE)</u>

It is also possible to estimate ΔE from the variation of current density J with temperature at a fixed applied voltage, assuming the relation

$$J = A \exp (- \Delta E/kT) \qquad \dots \quad (III-1)$$

where A is a constant (Dekker, 1957). Fig. III-19 shows the variation of J at a constant applied voltage (4 V) for two film thicknesses (1287 and 2000 A^o). The slopes are the same for the two thicknesses. ΔE calculated from the slopes of these curves was found to be about 0.75 eV.

It has recently been suggested by Simmons et al. (1970) that ΔE can be calculated from capacitance measurements (eqn. I-19 of Chapter I). Fig. III-20 shows the variation of ω with 1/T (semi log scale) for two film thicknesses at different capacitances. ΔE (0.75 eV) thus estimated was found to be in good agreement with that obtained by using the relation (III-1).

v) <u>Optical properties</u>

The Dy_2O_3 films deposited on glass substrates (n = 1.52) were annealed in vacuo at about $100^o C$ for about three hours and cooled to room temperature. The transmittance of these

films in the visible region (4000-7000 A^o) was measured by normal angle of incidence method in a Beckmann DK2 spectrophotometer. The transmittance was high (T > 90%) and this was true for all film thicknesses studied (800-3000 A^o). Absorptic index (k) evaluated from the transmittance data for different film thicknesses was found to be negligibly small. Refractive index (n) was estimated from the transmittance data using the relation (I-25) of Chapter I, assuming k = 0. n thus evaluated was found to be 1.85 which was practically independent of wavelength (4000-7000 A^o) as well as film thickness (800 - 3000 A^o) studied.

D. DISCUSSION

Even though the bulk Dy_2O_3 had a bcc structure, the vacuum deposited films were amorphous in nature as shown by electron diffraction. It is generally an observed fact that many of the vacuum deposited oxide films formed at room temperature are amorphous or have fine-grained structure as in the case of praseodymium oxide films (Goswami et al. 1974).

The general features of thickness effect on dielectric parameters, variation of tan δ with frequency giving a tan $δ_{mi}$ and other results could not be explained by the general theories on dielectrics. But recently Goswami et al. (1971, 1 proposed a theory assuming a simple model for their similar results observed in the case of vacuum deposited ZnS films. Such behaviour was also observed by Maddocks et al. (1962) for ZnS films and Sealy et al. (1972) for MgF_2 films.

The general features of thickness effect on dielectric parameters for films of thicknesses greater than 1000 A^o are as expected. C varied linearly with $1/d$ where ϵ and tan δ were independent of film thickness. But the dependence of ϵ on thickness for thinner films ($d < 1000\ A^o$) was similar to those observed for ZnS, praseodymium oxide films (Goswami 1973; 1974) etc. This is mainly because of defects such as voids and dislocations present in vacuum deposited films. In such cases total capacitance can be considered as consisting of two types of dielectric media, viz., (i) Dy_2O_3 films and (ii) air or vacuo ($\epsilon = 1$) in voids and discontinuity region. The effective capacitance can be written as

$$C \text{ effective} = C_{voids} + C_{Dy_2O_3}$$

When the thickness increases, the void concentration decreases and the films tend to become continuous. When the films thus become continuous, ϵ becomes characteristic of the material and hence independent of film thickness.

Ageing and annealing of capacitors invariably showed that C and tan δ decreased with time and annealing. Freshly deposited films always have many defects and imperfections such as voids, grain boundaries, dislocations, stress, inhomogenity etc. But with ageing, a self-annealing process takes place whereby many of the above defects, especially stress, will be reduced or removed from the films. Annealing

in vacuo results in the removal of other defects which are not removed early by self-annealing process. Such a reduction of defects will however lower the concentration of charge carriers, thereby increasing the resistance of the dielectric films. The decrease of capacitance with ageing and annealing can now be explained from the equation for C_s (I-15) of Chapter I. C_s decreases with increase in R. In the same way the lowering of tan δ can also be explained by the increase of R in equation (I-16) of Chapter I. Similarly, the increase of R in equation (I-17) reduces the value of ω_{min}, hence by ageing and annealing, tan δ_{min} shifts towards lower frequency region.

The most important feature is the observation of tan δ_{min} and its shifting towards higher frequencies at higher temperatures. The relations I-16 and I-17 explain the behaviour of tan δ with frequency and temperature. As the resistance of the dielectric decreases with temperature, it is clear from the relation $R = R_0 \exp (\Delta E/kT)$, that tan δ increases with temperature and ω_{min} shifts towards higher frequency at higher temperatures (eqn. I-17). The increase of tan δ at higher frequencies is due to the lead resistance.

Similarly as ω increases (eqn. I-15), C_s decreases with frequency and at higher frequencies $1/\omega^2 R^2 C$ of eqn. I-15 is much less than 1, as a result C_s becomes invariant with frequency at higher frequency region. As the temperature

decreases, the dielectric resistance R increases, thus increas[i]
the denominator of eqn. I-15, resulting once again $C_s = C$
(constant) at low temperatures, even at low frequencies. Henc[e]
C_s is independent of frequency and temperature at lower
temperatures. Since R decreases at higher temperatures, C_s is
much pronounced at higher temperatures. As C_s increases with
temperature, TCC is positive and its magnitude (200-800 ppm)
is comparable with that of any of the other dielectric films
successfully used as capacitor elements. At low temperatures,
capacitance is independent of frequency, and the extrapolation
of the capacitance temperature curve to 0° K will no doubt
give a measure of the static dielectric constant. The
temperature has an influence on the crystal expansion, electron
and ionic polarisability and crystal defects. At room temperat
the dielectric constant is practically independent of frequency
($\varepsilon = 6.7$). The optical dielectric constant is $n^2 = 3.42$ which
is the electronic contribution and the rest is that of atomic
contribution to the dielectric constant.

The principal theories of electronic breakdown in
solids have concentrated mainly on the inception of breakdown,
leaving the actual destructive phase relatively unexplored.
But a new experimental approach is possible in thin film
capacitors. In dielectric breakdown, a capacitor discharges
internally with a strong current pulse of short duration with
many times emission of light and localised destruction of
dielectric. Frohlich (1937) in his original theory for

electronic breakdown in ionic crystals assumed that at a
sufficiently high field, there occurs a rise in electron
current due to impact ionization from the valence to the
conduction band. The breakdown studies on Dy_2O_3 films give
the variation of breakdown field with thickness $F_b \propto d^{-1/2}$
which is in close agreement with Forlani-Minnaja relation
(1964) in which an avelanche mechanism is assumed to be
initiated by the injection of electrons from the electrodes
by a tunneling process. Here the film thickness is much lower
than the recombination length of the electrons, hence,
following the above relation.

The activation energy measured from the capacitance
measurements with frequency at different temperatures and
that from the dc current measurements with temperature at
fixed voltage agreed well ($\Delta E = 0.75$ eV). But this is much
lower than the expected band gap of Dy_2O_3 films. This may be
because of the presence of traps in the insulator which owe
their existence to the structural imperfections of the films.
Moreover, the presence of traps are established during the
I-V characteristics studies. However it shows that this
measured activation energy may be the trap depths from the
conduction band.

The dc I-V characteristics studies have given a much
clear insight to the Dy_2O_3 insulator system. Experimental
results for electrical conduction in amorphous films show

common trends which have been categorized by various
authors (Harrop et al. 1968; Jonscher, 1968; Jonscher et al.
1969). The band theory of conduction was first developed to
describe the behaviour of metals and semiconductors and it is
not necessarily applicable to insulators, particularly those
which are amorphous (Heikes et al. 1957; Ioffe et al. 1960;
Regel, 1960). If the insulator is sufficiently thick,
tunneling will not normally conduct significant current.
However, if an ohmic contact is made to the insulator, the
space charge injected into the conduction band of the insulator
is capable of carrying current and this process is termed
as space charge limited (SCL) conduction. The aluminium
electrodes were found to give good ohmic contact with Dy_2O_3
films since the I-V characteristics were symmetrical
irrespective of the polarity of electrodes.

According to Mott and Gurney (1948), when a conduction
mechanism is limited by space charge, current density J is
given by

$$J \propto V^2 / d^3$$

But the above relation holds only for a trap-free insulator,
in which J is independent of temperature. It is observed in
the case of Dy_2O_3 films that the current density J follows
the above relation, but J increases with temperature (fig. III-
This is due to the presence of traps, which is generally
observed in vacuum deposited films. If there are shallow

traps, the above relation for trap-free insulator holds good, except the fact that J is also dependent on temperature (Rose, 1955) and hence $J \propto \theta \, V^2/d^3$ where θ is a function of temperature, which is given by

$$\theta = \frac{N_c}{N_t} \exp \, (-\Delta E/kT)$$

where N_t is the number of traps positioned at an energy ΔE below the conduction band and N_c is the density of states. This is exactly what is observed in the case of Dy_2O_3 films and hence the conduction process in Dy_2O_3 films is space charge limited modified by shallow traps. There was no change in the square law even when the voltage was further increased and finally dielectric breakdown was observed at very high fields.

The optical transmittance of Dy_2O_3 films in the visible regions is greater than 90% which shows that these films are practically nonabsorbing, i.e. k is negligible. It is generally observed for rare earth oxide films whose band gaps are high ($E_g > 3$ eV) and hence the absorption will be in the UV region. The refractive index (n = 1.85) was practically independent of wavelength (4000 - 7000 A^o). But n is slightly less than that observed in bulk powder, which was 1.92 (Batsanov et al. 1962). This difference is not unusual since vacuum deposited films generally have

lesser density than their bulk materials. Also film thickness
(800 - 3000 A$^{\circ}$) did not have much effect on n. The high
transmittance and wavelength independent refractive index
of Dy_2O_3 films will have much advantages in using it in
optical coatings for many practical purposes.

CHAPTER-IV : STUDIES ON LANTHANUM OXIDE FILMS

CHAPTER IV

STUDIES ON LANTHANUM OXIDE FILMS

A. INTRODUCTION

High quality thin film dielectrics are required by the electronic industry for use in capacitors as well as in field effect devices. Because of the presence of intergrain boundarie in polycrystalline solids which give rise to leakage and ac losses, it is generally agreed that the best dielectric would be a single crystal having low concentration of defects and impurities. With the increasing use of multilayer coatings in antireflection and interference filters, high index dielectrics suitable for producing durable nonabsorbing films are gaining in practical importance. Because of the excellent mechanical and chemical stability, rare earth oxides are promising materials for the above purposes. In the following a brief survey on the dielectric, electrical, optical and structural studies of lanthanum oxide is given.

The X-ray crystal structure of La_2O_3 was first reported by Zachariasen (1926) and the lattice parameters were $a = 3.93 \, A^O$ and $c = 6.12 \, A^O$. But Pauling (1929) modified the above structure with the same lattice dimensions, but using a different arrangement of O atoms. Swanson et al. (1953 also studied lanthanum oxide (La_2O_3) by X-ray powder pattern

method and reported it to be hexagonal with lattice parameters a = 3.937 A^o, c = 6.13 A^o. Bondarenko et al. (1959) investigated the thermionic properties of La_2O_3 on a tungsten ribbon over a wide range of temperature. During the determination of the dissociation energy of the lanthanum molecule by Smoes et al. (1965), the oxide impurities in the sample led to the observation of the gaseous oxide and sub-oxide. Buschbaum et al. (1965) studied the high temperature form (2200^oC) of La_2O_3 (type A) by X-ray diffraction and showed that it could be considered to belong to the space group P6 3/mmm- $D6_h^4$. A structural change was observed near the fusion temperature for La_2O_3.

Janker et al. (1958) prepared resistors having a specific resistance in the range of 0.2 - 5750 ohm-cm and a TCR between 0.5 and -4.3% /^oC from a mixture of oxides containing La_2O_3. Trombe and Foex (1951) studied the nature of increased electrical conduction of mixtures of ZrO_2 and La_2O_3. La_2O_3 was mainly used as an additive to ceramic dielectrics to increase the dielectric strength. Day and Calis (1954) prepared a ceramic dielectric from a mixture containing equimolecular amounts of TiO_2 and $BaCO_3$, 0.5% of CeO_2 and 0.1 - 2% of La_2O_3 by firing at 1200 - 1400^oC. This dielectric had a loss angle below 50 x 10^{-4} and a specific inductive capacity of about 6000 that varied < ± 15% between -15 and $+60^oC$. The effects of adding La_2O_3 to $BaTiO_3$ on

the dielectric properties of the latter were studied by
Lapluye et al. (1960). MacChesney et al. (1963) found that
small amounts of La_2O_3 in $BaTiO_3$ markedly increased the
life-time of the material subjected to high dc fields even
at $200^{o}C$. Yoshioka et al. (1970) succeeded in making high
ϵ (188), high Q (7000) and low TCC ceramic dielectric suitable
for temperature compensating capacitors by an appropriate
mixture of $CaTiO_3$, $PbO.TiO_2$ and $La_2O_3.TiO_2$. Rudolph (1959)
and Rao et al. (1970) reported the mechanism of conduction
in rare earth oxides.

Chernobrovkin (1971) used a mixture of La and Pr oxides
for thin layer capacitors of high dielectric strength.
Chernobrovkin et al. (1971) reported that thermally evaporated
La_2O_3 film capacitors with Al electrodes had ϵ = 18.24 and
tan δ varied from 0.005 to 0.02 and the breakdown field was
about 2-5 x 10^6 V/cm, which was dependent on film thickness.
Thun and Maddocks (1966) described a process for making
capacitors of high dielectric constant using La_2O_3. Hass
et al. (1959) studied the optical properties of various
vacuum deposited rare earth oxides in the spectral region
0.22 - 2 micron. The optical constants were dependent on
deposition rate, substrate temperature, film thickness etc.
and in the visible region the absorption index was zero.
Socha (1960) used La_2O_3 for multilayer low reflectance
coatings for optical elements. Batsanov et al..(1962) reported

that La_2O_3 had n = 1.88 at $800^{\circ}C$. The IR spectrum of La_2O_3 was studied by Goldsmith and Ross (1967) and Rao and Rao (1970)

From the above survey, it is clear that even though much work has been done in bulk La_2O_3, very little work has been reported in La_2O_3 films. Moreover, no systematic study has been carried out on the dielectric properties and conduction mechanism. In view of the above, an elaborate study has been carried out to gain a better outline on the ac behaviour, dc conduction and other properties of La_2O_3 films

B. EXPERIMENTAL

Lanthanum oxide (La_2O_3) powder (AR grade supplied by Bhabha Atomic Research Centre, Bombay, India) was vacuum deposited from initially flashed tungsten boats. The bulk powder was heated to about $400^{\circ}C$ in vacuo for one hour prior to deposition for degassing and also to avoid spurtting of the powder. The deposition was carried out for 30 minutes at a rate of about 50 A°/min. The glass substrates were cleaned as described previously and the films were deposited at room temperature as well as at $200^{\circ}C$. Aluminium deposits ($3000\ A^{\circ}$) were used both as base and counter electrodes and the fabrication of capacitors was carried out in the manner as described in Chapter II. The capacitors were aged in air after deposition. All the samples were stabilised by annealing in vacuo by heating ($150^{\circ}C$) and cooling cycles.
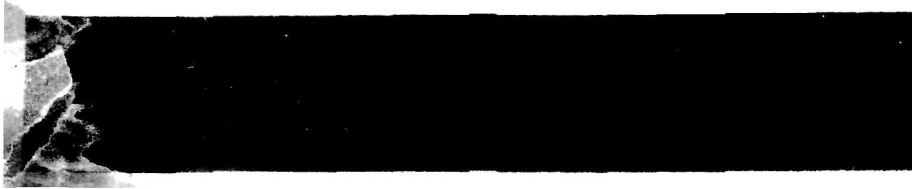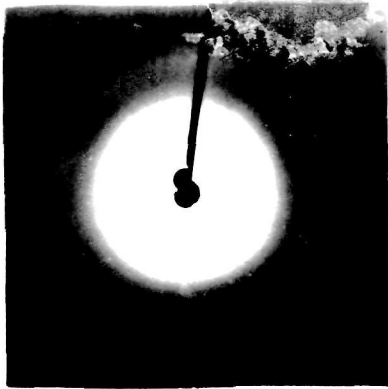
Fig. IV - 1

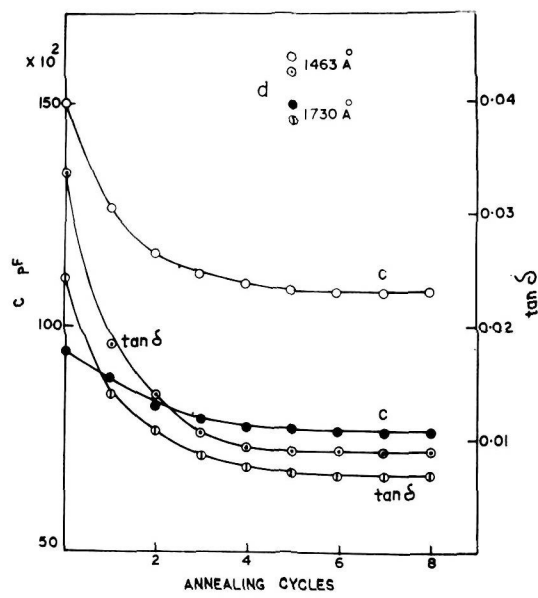Fig. IV - 2

Fig. IV - 3

Fig. IV - 4

The dielectric and I-V measurements were carried out in vacuo unless otherwise stated. La_2O_3 was also deposited on glass and quartz substrates and optical transmittance in UV and visible regions were measured in a Beckmann DK2 spectrophotometer. For structural studies by electron diffraction, films were deposited on polished NaCl polycrystal tablets.

C. RESULTS

i) Structure

X-ray study of bulk La_2O_3 powder confirmed the hexagonal structure with a = 3.94 A^o and c = 6.13 A^o. The X-ray powder pattern is shown in fig. IV-1. On the other hand, vacuum deposited films appeared to be amorphous or had fine grained structure as shown by electron diffraction (fig. IV-2). The electron micrograph (fig. IV-3) shows that the films had fine grained structure. No crystallinity was observed even when the deposition was carried out at 200° C.

ii) Dielectric properties

a) Ageing and annealing effect

Both C and tan δ decreased continuously by ageing in air and finally became more or less constant after 10 days. C and tan δ further decreased on annealing in vacuo by heating and cooling cycles (125^oC). The effect of annealing is shown in fig. IV-4. After three cycles of annealing,
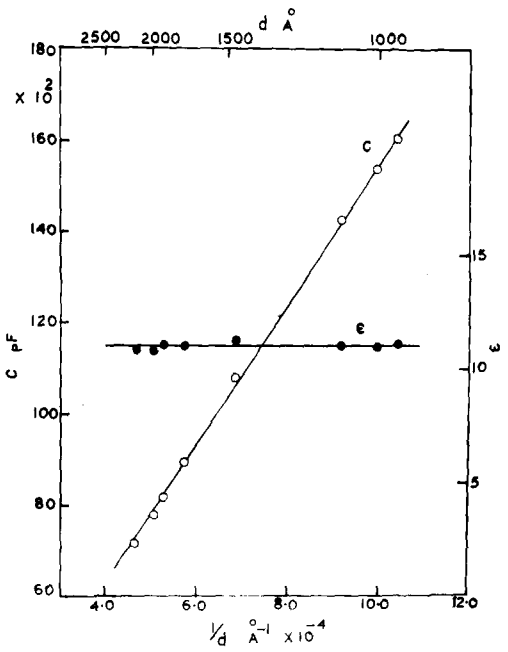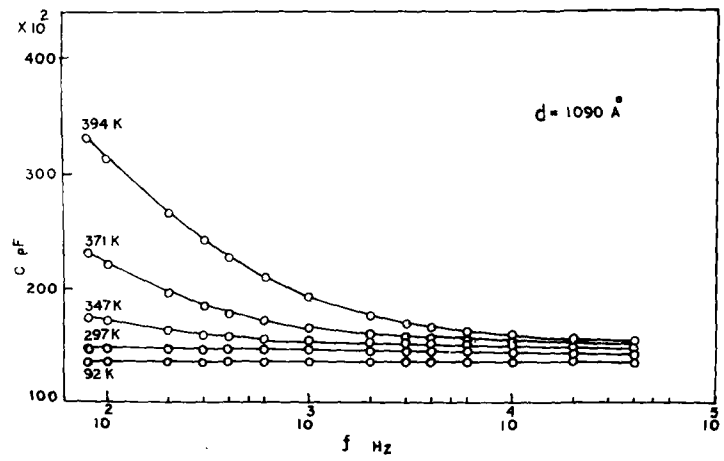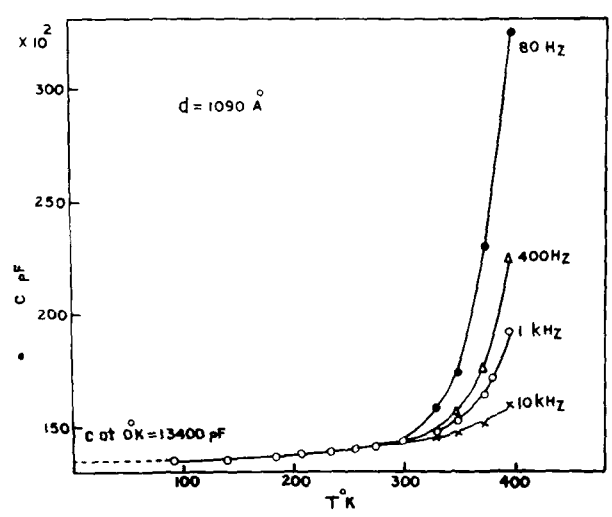
Fig. IV-5

Fig. IV-6

Fig. IV-7

C and tan δ became steady indicating that the capacitors were stabilised in the same way.

b) <u>Effect of film thickness</u>

The variations of C, ε and tan δ with 1/d for samples deposited at room temperature are shown in fig. IV-5. It is seen that C varied linearly with 1/d, whereas both ε (11.0) and tan δ (0.007) were independent of the film thickness (960-2150 A^o) used in the present experiments.

c) <u>Frequency and temperature effect on C and tan δ etc.</u>

Capacitance decreased continuously with increase in frequency and became constant at higher frequencies (fig.IV-6). C was practically invariant with frequency for all temperatures below the room temperature (297^oK) and the variations of C were larger at higher temperatures and lower frequencies. This variation was similar to that of Dy_2O_3 films. Fig. IV-7 and IV-8 show the variations of C and ε respectively with temperature at different frequencies. It is interesting to note that both C and ε tend to become constant at low temperature for all frequencies.

The capacitance at 0^oK was obtained by extrapolating the curve to 0^oK (fig. IV-7) and ε was then evaluated and was found to be 10.31 at 0^oK. This is, no doubt, the static dielectric constant of La_2O_3 film. The dielectric behaviours of capacitors deposited at 200^oC were similar to

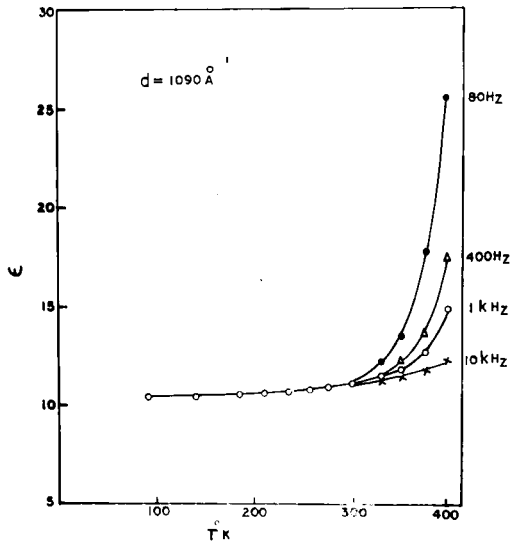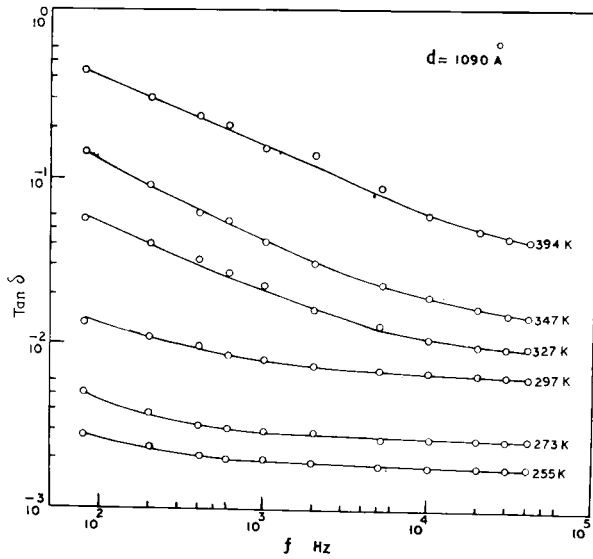Fig. IV- 8

Fig. IV- 9
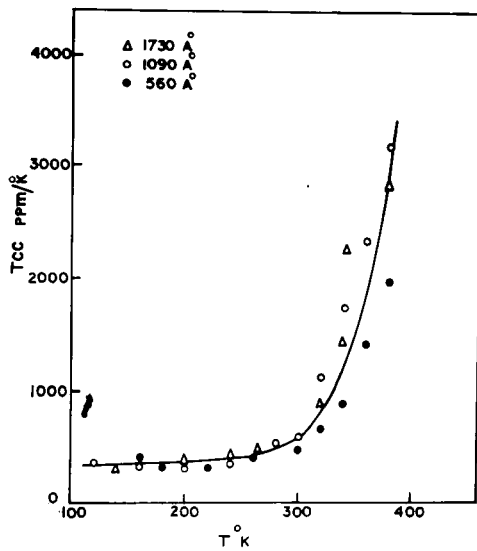

Fig. IV-10

the room temperature deposits.

Fig. IV-9 shows the typical variations of tan δ with frequency at different temperatures. It is seen that tan δ continuously falls with frequency, but there was no tan δ_{min} in the frequency region studied, unlike in the case of Dy_2O_3 films. Tan δ however increased with temperature as was observed for Dy_2O_3 films (fig. IV-9).

d) TCC

The TCC of the capacitors varied from 300 ppm to 3000 ppm for a temperature range of 100° to $380^{\circ}K$. The variation was small upto $300^{\circ}K$, but increased rapidly by further increase of temperature. This parameter was practicall: independent of film thickness (fig. IV-10).

e) Breakdown voltage and breakdown field

The breakdown voltage was measured by increasing the dc voltage across the capacitor step by step and measuring the current. At the breakdown voltage region a number of sparks were observed on the top electrode with a simultaneous sharp rise in current. This was taken as the onset of breakdown voltage. The breakdown voltage was found to increase with film thickness. However the breakdown field F_b (of the order of 10^6 V/cm) of La_2O_3 films decreased with increasing thickness. Fig. IV-11 shows the variation of F_b with d (log-log scale) which is a straight line with a negative
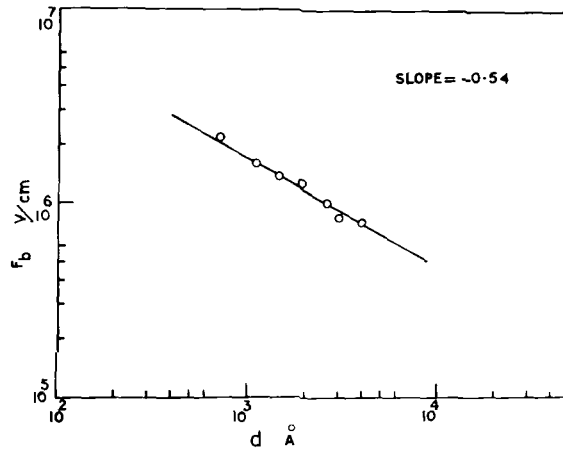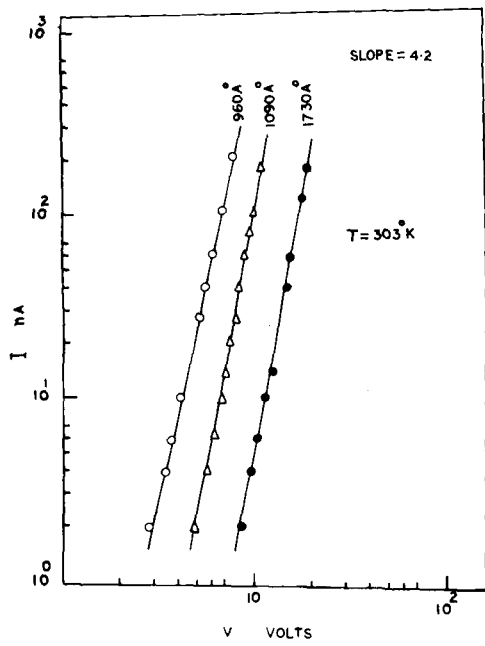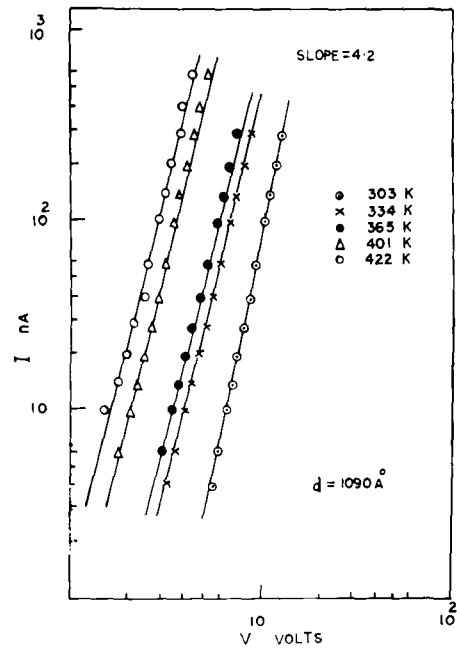
Fig. IV-11

Fig. IV-12

Fig. IV-13

slope = 0.54, thus following approximately the relation $F_b \propto d^{-1/2}$.

iii) I-V Characteristics

The same capacitor system used for studying dielectric properties were also used to investigate the dc conduction mechanism. Fig. IV-12 shows the I-V characteristics (log-log scale) of samples measured at room temperature. It was also found that these curves were symmetrical irrespective of the polarity of the top and bottom electrodes. These I-V curves showed a positive slope of about 4.2 for the three film thicknesses, thus following the relation $I \propto V^4$.

Fig. IV-13 shows the I-V characteristics measured at five different temperatures (303-$422^{\circ}K$) for a film thickness of 1090 A°. The positive slope (4.2) of these lines remained the same for all the temperatures. The effect of film thickness on current at a fixed voltage (5 V) is shown in fig. IV-14 (log-log scale). It is seen that the graph is a straight line with a negative slope equal to 6.8. Thus the variation of current with film thickness approximately follows the relation $I \propto 1/d^7$.

iv) Activation energy (ΔE)

The activation energy was evaluated from the variations of current with temperature at a fixed applied voltage (refer Chapter I). In fig. IV-15, I is plotted against $1/T$

SLOPE-6.8
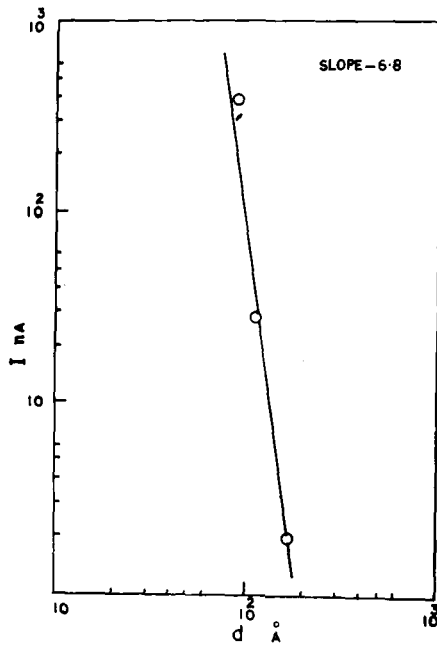
I nA

10^3 10^2 10^1

d Å

Fig. IV-14

d
1730 Å V= 5 V
1090 Å V= 5 V
960 Å V=2.8 V

$\Delta E = 0.8$ eV

I nA

$1/T$ °K^{-1} x10^{-3}

Fig. IV-15

d = 1090 Å

$\Delta E = 0.8$ eV

ω rad/sec

$1/T$ °K^{-1} x10^{-3}
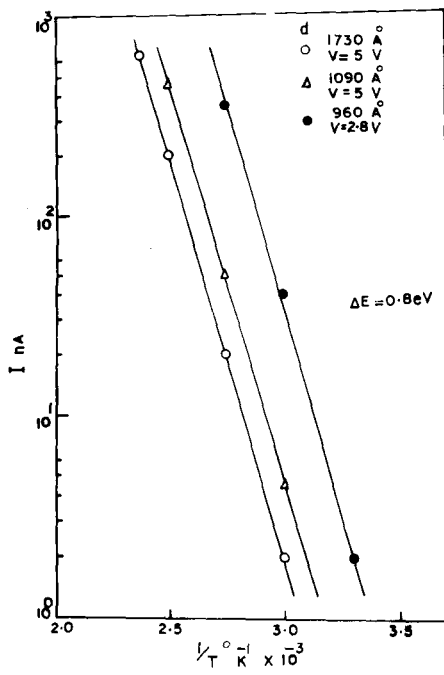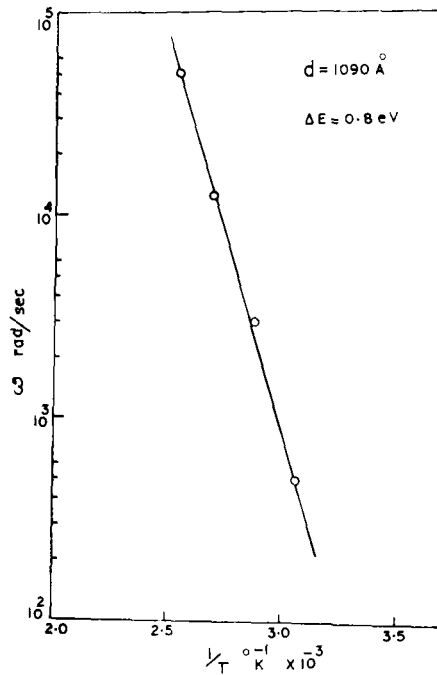
Fig. IV-16

(semi-log scale) for three film thicknesses at different applied voltages. The variation of I is a straight line and the slopes of the three lines remained practically unchanged for the three film thicknesses. Activation energy (ΔE) calculated from the above slope was found to be 0.8 eV (using kT in the exponential factor).

ΔE was also calculated from the variations of C with frequency at a constant capacitance for a film thickness d = 1090 A^o. A plot of log ω vs 1/T is shown in fig. IV-16. The activation energy (ΔE = 0.8 eV) obtained from the above plot agreed quite well with that obtained by the method described previously.

v) <u>Optical properties</u>

La_2O_3 deposited on quartz plates were used for transmittance measurements by a Beckmann DK2 spectrophotometer in the UV as well as in the visible region. The transmittance curves for two film thicknesses formed on quartz plates are shown in fig. IV-17. It is seen that in the visible spectrum the films are practically non-absorbing. Absorption coefficient $\propto$ was calculated from the slope of the plot of log T vs d assuming the relation $\propto = \dfrac{\log T_1 - \log T_2}{d_2 - d_1}$.

From $\propto$ the absorption index k was estimated at different wavelengths using the relation $\propto = 4\pi k/\lambda$. k was found to be negligible in the visible region but increased considerably by decrease of λ in the UV region (table IV-1). In order to find out optical band gap, $\propto^2$ was plotted against photon

TABLE IV-1

Transmittance (%) for film thicknesses d (A°)			Wavelength λ (A°)	Absorption coefficient $(\alpha) \times 10^4$	Absorption index k
1630	1473	1178			
29	32	38	2300	5.83	0.10
36	39	44	2400	4.07	0.09
46	48	54	2500 .	4.0	0.076
56	59	64	2600	2.76	0.055
72	76	82	2800	2.57	0.055
82	85	90	3000	1.93	0.048
88	90	93	3200	0.74	0.028
91	93	95	4000	0.71	0.028
91	93	95	5000	0.71	0.028
90	92	94	7000	0.71	0.028

TABLE IV-2

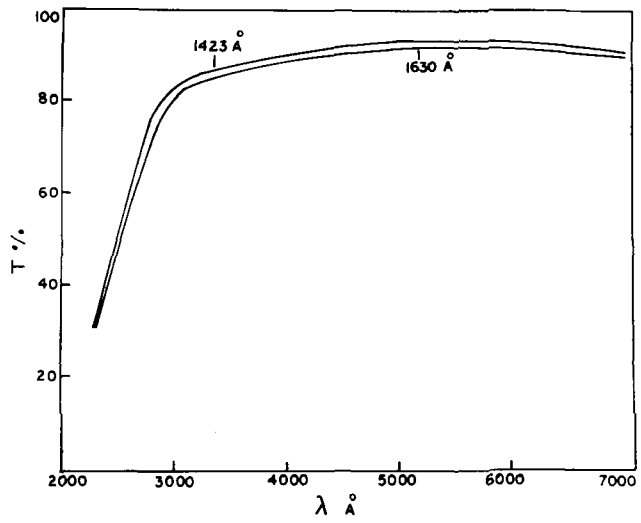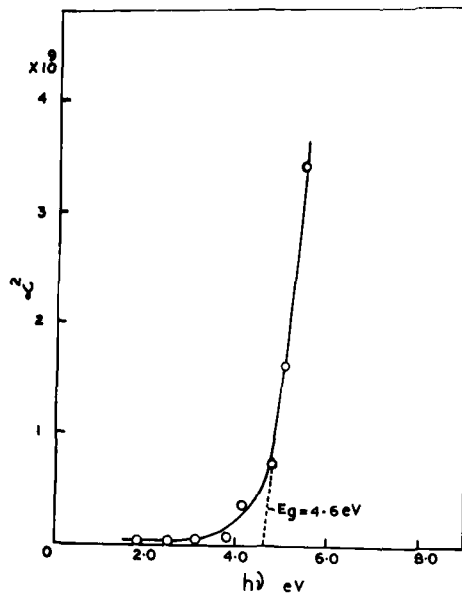| Wavelength λ (A°)	Refractive index (n)
7000	1.80
6000	1.82
5000	1.84
4000	1.89

Fig. IV- 17

Fig. IV- 18

energy (fig. IV-18). It is seen that α^2 was negligible at lower photon energy and then increased rapidly and the straight line extrapolated to $\alpha = 0$ gave the optical band gap (E_g) of the La_2O_3 films which was found to be 4.6 eV. It is in good agreement with the reflectance spectra measurements on polycrystalline La_2O_3 (Derbeneva et al. 1967).

La_2O_3 films in the visible region were highly transparent $(T > 90\%)$ and the absorption index k was negligibly small (k < 0.03). The refractive index (n) was calculated from the transmittance using the relation I-25 of Chapter I. n varied from 1.89 to 1.8 in the region 4000 to 7000 A^o, which is in agreement with that observed by Hass et al. (1959). The variation of n with λ for a typical film thickness of 1423 A^o is given in table IV-2. However, n was found to be independent of film thickness for the thickness region studied (990 to 1800 A^o).

D. DISCUSSION

Electron diffraction and microscopy studies of La_2O_3 films formed at room temperature and at 200^oC showed that they had a fine-grained structure. The dielectric behaviour of these films showed similar behaviour. The capacitance of all these films were inversely proportional to film thickness and ϵ was independent of film thickness and it was equal to 11.0 at $1kH_z$ measured at room temperature. The above thickness

independent ϵ is at variance with the results of Chernobrvkin et al. (1971) who observed a variation of ϵ from 18 - 24. This variation appears to be due to nonstabilisation of samples, which will indeed show variation of ϵ. This is confirmed from the results of the effects of ageing and annealing, where C is found to decrease with time and hence also ϵ.

The variations of C and tan δ with frequency and temperature are similar to that observed in the case of Dy_2O_3 films, except that tan δ did not attain a minima in the frequency region studied. It is likely that at higher frequencies, tan δ may increase, thus showing the general behaviour.

It is well-known that the dielectric behaviour arises primarily from the contributions viz., electronic, atomic, dipolar and interfacial polarisations. Since no tan δ maxima was observed at lower frequency region, especially at low temperatures, the contributions from the last two can be negligible. The contribution from the electronic polarisation is about 3.84 ($=n^2$). Hence, the major contribution ($=7.16$) to the dielectric constant is from atomic polarisation. From the extrapolation of C to $0^\circ K$, the static dielectric constant is obtained (10.3) and its variation with temperature is very slow. TCC of the La_2O_3 film capacitors (300 -3000 ppm/ is comparable with that generally observed for rare earth oxide

The present study also gives some idea regarding the breakdown of La_2O_3 films. A number of breakdown mechanisms have been suggested by various workers (Frohlich, 1937; Kleni et al. 1966; 1967; Forlani and Minnaja, 1964). The variation of breakdown field with thickness agrees well with the Forlani-Minnaja relation viz., $F_b \propto d^{-1/2}$, in which an avalanche approach with tunnel emission at the cathode is assumed. The breakdown field was high (10^6 V/cm) and agreed with the results of the study of Chernobrovkin et al. (1971).

The I-V characteristics studies yield better information regarding the type of conduction in La_2O_3 films. When the injection of carriers into the conduction band, or tunneling is not the rate-limiting process for conduction in an insulator, a space-charge build up of the electrons in the conduction band or at trapping centers may occur which will oppose the applied voltage and impede the electron flow. In the previous study of conduction in Dy_2O_3 films (Goswami and Varma, 1974), a space-charge limited current was observed, following the relation $I \propto V^2/d^3$, but depending on temperature suggesting thereby that the conduction is SCL modified by shallow traps. For an exponential trap distribution, the current-voltage relationship is governed by the relation

$$I \propto \frac{V^{l+1}}{d^{2l+1}}$$

where l is a parameter characteristic of the distribution
of traps (Lampert, 1964). However, it is to be noted that
a relation $I \propto V^1/d^3$ was also observed by Chopra (1965) for
niobium oxide films. Hickmott (1966) reported that the
conduction in $N_b/N_{b_2}O_5/Au$ systems followed the relation
$I \propto V^1/d_z$ as previously observed by Chopra (1965) for
niobium oxide films. Hickmott (1966) reported the conduction
in $N_b/N_{b_2}O_5/Au$ systems also followed the relation $I \propto V^4$
for film thickness between 3000 - 3600 $\overset{o}{A}$.

The mechanisms of conduction are generally governed
by a number of factors inter alia workfunctions of electrodes
and the sandwiched layer, applied field, structural defects
of the deposited films such as stacking faults, impurities,
dislocations, grain boundaries, etc. which act as potential
trapping centers for current carriers. The conduction process
can be either electrode or bulk-limited depending on the
field strength, the former however prevailing at lower fields
and the latter at higher fields. I-V characteristics in the
former case can be represented in the form

$$J \propto exp \; (\beta \; V^{1/2})$$

such that a plot of log J or log I vs $V^{1/2}$ will show a
steep slope depending on β which is a constant. Any deviation
from the straight line slope generally observed at higher
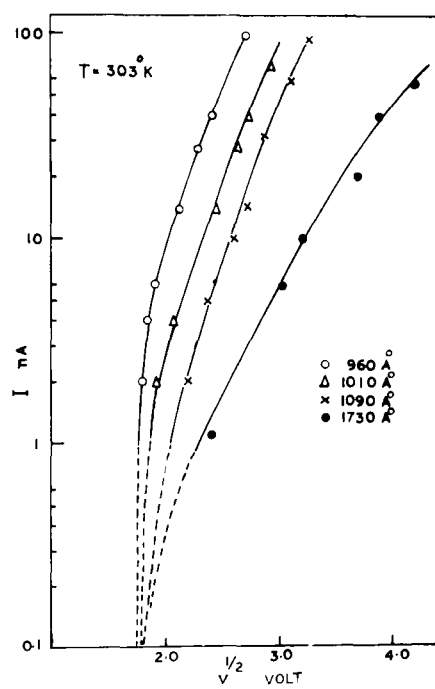fields or with increasing film thickness will indicate the

Fig. IV-19

onset of the bulk-limited process. Simmons (1970) and Stuart (1967) and others already observed these features and also reported that the curves for bulk-limited cases had a tendency to saturate at higher fields.

Taking the above into consideration, the I-V characteristics at 303°K of four different film thicknesses have been replotted as log I vs $V^{1/2}$ (fig. IV-19). The curves clearly delineate electrode and bulk effects, the transition stage occurring at about 3.6 volts. At higher fields the current tends to show a saturation, thinner films having higher slopes. This is more distinct in the case of thicker films (d = 1730 A^{o}) in which the saturation is more pronounced, whereas for the thinner films the curves get close However, at about 3.6 volts, all the curves merge together to form approximately a single line with considerably higher slope, which is characteristic of the electrode-limited process Hence, at fields < 3.6 volts, the conduction process was mainly electrode limited whereas at fields > 3.6 volts, the conduction was primarily bulk-limited.

In the present study of dc conduction in La_2O_3 films, the variation of current obeyed approximately the relation $I \propto V^4/d^7$, thus agreeing with the relation $I \propto V^{1+1}/d^{21+1}$ where l = 3. Further, the current was temperature dependent unlike trap-free insulators. It can be thus concluded that the conduction process in La_2O_3 films is space-charge limited

with an exponential trap distribution.

The activation energy evaluated from the current-temperature as well as capacitance measurements agreed well giving a value of 0.8 eV. The above value of ΔE appears to be an indication of trap depth.

The optical transmittance studies of La_2O_3 films showed that the absorption was in the U V region. The optical bandgap (E_g = 4.6 eV) estimated from the plot of α^2 vs photon energy was in good agreement with the reported bandgap by reflectance measurements (Derbeneva and Batsanov, 1967) which was about 4.4 - 5.6 eV. La_2O_3 films in the visible region showed high transmittance and absorption index k was negligible. However refractive index was dependent on wavelength of light and it decreased from 1.89 to 1.8 for λ varying from 4000 - 7000 Å This is in agreement with the studies of Hass et al. (1959). The high transmittance of La_2O_3 films suggests that it can be used for multilayer coatings, interference filters etc.

CHAPTER-V : STUDIES ON LANTHANUM FLUORIDE FILMS

CHAPTER V

STUDIES ON LANTHANUM FLUORIDE FILMS

A. INTRODUCTION

The design of multilayer film combinations such as antireflection coatings or interference filters depends to a large degree on the variety and the qualities of the materials available. Unfortunately the number of suitable film materials are still quite restricted. Rare earth fluorides, just like their oxides, give promising results because of their excellent mechanical and chemical durability as thin films. These fluorides have an advantage over the oxides because of their comparatively low melting point. The dissociation probability is also very less. The following is a survey on the dielectric, optical and other properties of lanthanum fluoride.

By X-ray diffraction, Oftedal (1929) showed that lanthanum fluoride (LaF_3) had a hexagonal structure with lattice parameters $a = 7.177$ A^o and $c = 7.344$ A^o. Swanson et al. (1957) and Staritzky (1957) also reported the same structure for LaF_3. On the other hand, Mansmann (1964) suggested that LaF_3 belonged to the trigonal system with $a = 7.19$ A^o, $c = 7.367$ A^o and $z = 6$. Zalkin et al. (1966)

recently studied the structure of LaF_3 in more detail and confirmed that its structure is trigonal rather than hexagonal. Oftedal (1929) suggested the hexagonal structure with the assumption that the space group was P 63/mcm, but the atomic coordinates corresponded almost to the symmetry P63/mcm with a smaller unit cell. The evidence for large cell was the presence of weak reflections which might have easily escaped detection in power diagrams. Zalkin et al. (1966) concluded that Oftedal's cell was correct and that his coordinates for La were quite accurate, but that the crystals were trigonal.

Soloman et al. (1964; 1966) reported the low frequency dielectric behaviour of LaF_3. It exhibited an unusually large dc polarisation and low frequency capacity. The effect in LaF_3 and other rare earth fluorides were at least two orders of magnitude larger than that in any other crystal. The capacitance at 100 cps was typically about 10^4 times larger than the geometrical capacitance. Their measurements on single crystals of LaF_3 distinguished at least two components of polarisation. The component with a time constan of the order of milliseconds was linear in the applied voltage, but the long term polarisation was proportional to its square. These phenomena were associated with the surface effects. The thermal variation of dielectric constant

had been studied for LaF$_3$ at 1 kH$_z$ by Claveric et al. (1974) and the high value of ε and dielectric losses were attributed to the mobility of the F ion.

Gosh and Gosh (1938) determined the specific conduction of La and some other rare earth fluorides at temperatures between 260 and 310° and the data were used to calculate the splitting of the 4f bands in the crystals, which was approximate 0.6 eV in agreement with the theoretical value. Sher et al. (1966) reported the measurements of lattice and bulk thermal expansion, fluorine NMR and electrical conductivity of single crystals of LaF$_3$ in the temperature range 300-1000°C. In the lower temperature range, the activation energy for the formation of Schottky defects was 0.07 eV and for F ion diffusion was 0.45 eV. Fielder (1969) studied the ionic conductivity of LaF$_3$ at temperatures 25-740°C and stated that the conduction was due to thermal formation of La and F ion vacancies by Schottky mechanism with ΔE = 192 kj/mole and migration of F$^-$ with energy = 32 kj/mole. Collins et al. (1971) observed electroforming process even at low voltage in air at room temperature.

Bourg et al. (1964, 1965) studied the X-ray diffraction of thin layers of LaF$_3$ (2000 A^o) prepared by thermal evaporation in vacuum on an amorphous silica substrate. The results showed that the layers were crystalline and the

structure depended on the substrate temperature. Their
results on the electron diffraction showed that depending
on the substrate temperature as well as film thickness,
three separate zones of deposits were observed viz.,
(i) amorphous zone for film thickness < 1000 A^o at substrate
temperatures 100, 200 and 300°C, (ii) disordered crystalline
zone for thickness between 1000-5000 A^o at 200°C and 300°C
and (iii) ordered crystalline zone for thickness > 10,000 A^o
at 100°C. Films deposited at low temperature were
microcrystalline and formed in random directions.

Thun et al. (1962) reported typical vacuum deposited
capacitors of high dielectric constant from fluorides or
oxides of Ce and La with Al as electrodes. While studying
the dielectric properties of various thin films of rare
earth fluorides evaporated from tantalum and alumina crucibles
Maddocks and Thun (1962) found that the deposits from tantalum
boat yielded a thickness dependent dielectric constant whereas
those from alumina crucibles had thickness independent
dielectric constant. Decomposition of the deposit leading
to the formation of metallic grains embedded in the dielectric
could yield a high dielectric constant.

La Roy et al. (1973) studied the electrical properties
of solid state electrochemical cells using thin films of
LaF$_3$ electrolyte. The conductivity of the cell was found
to be a function of the concentration of reducible gases

like O_2, CO_2, SO_2 etc. Lilly et al. (1973) studied the transport properties of LaF_3 thin films from the pulsed I-V measurements and the data fitted a relationship of the form I = Io Sin bαV. The ionic conduction in LaF_3 films was studied by Tiller et al. (1973) and found that the activation energy for F^- diffusion through the film was about 0.4 ± 0.08 eV at < $500^{\circ}K$ except in the vicinity of Debye temperature ($360^{\circ}K$). Above $500^{\circ}K$, ΔE increased to 0.8 ± 0.1 eV.

Hass et al. (1959) investigated the optical properties of vacuum deposited films of rare earth oxides and fluorides. LaF_3 deposited at $300^{\circ}C$ was practically absorption-free down to 0.22 μ. The refractive index was found to be 1.6, in agreement with bulk value (Batsanava, 1962). Bourg et al. (1965) showed that the films of thickness < 7000 A° deposited on silica at $30^{\circ}C$ were homogeneous. Kagaku (1965) evaporated a mixture of Ce, La and Nd fluorides from W or Mo boats for antireflection coatings, interference filters etc. The refractive index of the mixture was $n \geq 1$. The extreme UV reflectance spectra (7-40 eV) measurements of LaF_3 films by Stephan et al. (1972) showed a complex permittivity and loss function.

From the above survey it is clear that a detailed study of dielectric and optical properties of LaF_3 films is still lacking. In view of the above an effort had been

made to study the ac behaviour, optical properties etc.
of vacuum deposited thin films of LaF_3 and the results
were compared with other results observed previously.

B. EXPERIMENTAL

Lanthanum fluoride powder (supplied by V.O. Sojuzehimexport,
Moscow, USSR) was vacuum deposited from tungsten boat and
from alumina crucible. In the former case, a flat tungsten
boat which was flashed previously in vacuo was used. In
the latter case, recrystallised alumina crucible which
was heated externally by a tungsten spiral was used.
In both cases the bulk powder was heated slowly and degassed
for about 30 minutes in vacuo and then the temperature
was increased to the melting point of LaF_3 to get a slow
and steady deposition at a rate of about 100 $A^o/$ minute.
The glass substrates were kept at about 12 cm above the
source and were at room temperature ($30^o C$). The deposited
films were transparent and often showed interference
colours. For structural studies by electron diffraction
films were deposited on polycrystalline NaCl tablets,
glass plates, freshly cleaved mica etc. and examined in
the usual way. The capacitor $Al/LaF_3/Al$ systems were
fabricated and the dielectric measurements were carried
out as described in Chapter II.

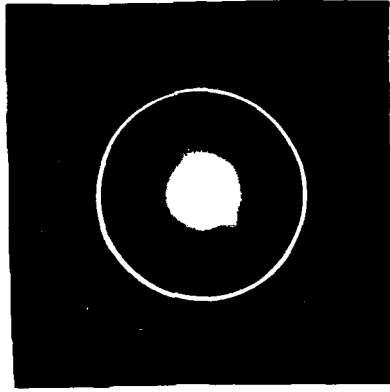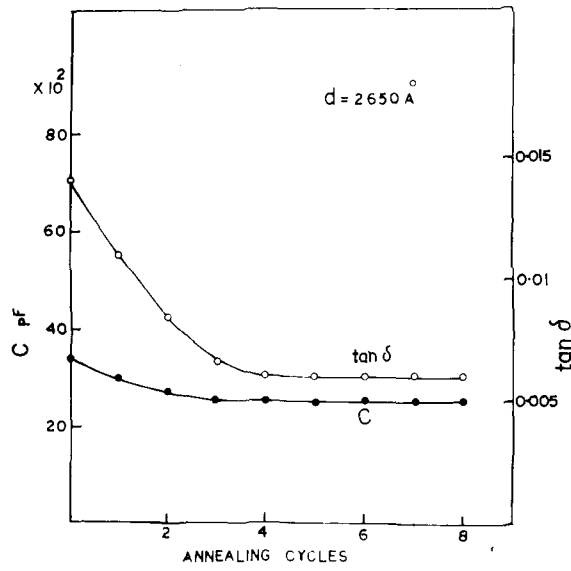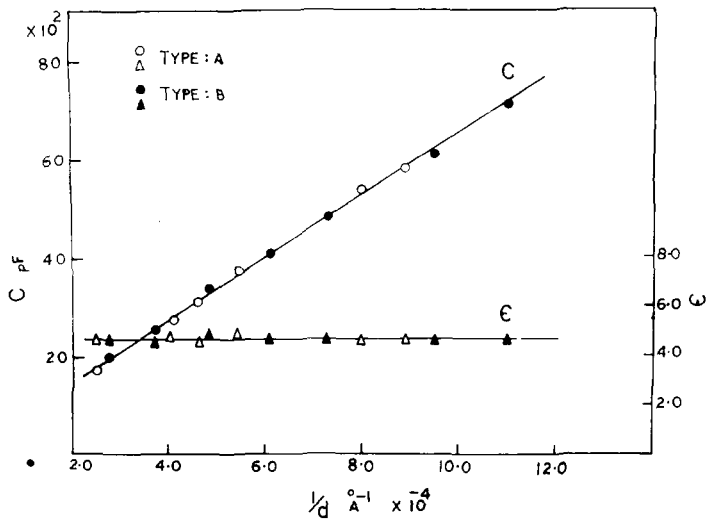LaF_3 films were deposited on glass substrates and

Fig. V-1

Fig. V-2

Fig. V 3

the resistances of the samples were measured by a
million meg-ohm meter. Platinum foils were used for
contacts and necessary leads were taken. Before measurements,
the samples were annealed in vacuo at about 150°C. Resistance
measurements were carried out at different temperatures
in vacuo for different film thicknesses. Films were
deposited on glass as well as on quartz plates for optical
measurements.

C. RESULTS

i) Structure

The X-ray diffraction studies of the bulk lanthanum
fluoride powder showed that LaF_3 has a trigonal structure.
But the powder pattern contained some other lines which
were due to some oxide impurities in the bulk powder.
The vacuum deposited films of LaF_3 on substrates at room
temperature were poly-crystalline and they had structures
exactly similar to that of the bulk powder. The electron
diffraction pattern is shown in fig. V-1.

ii) Dielectric properties

The dielectric behaviour of LaF_3 capacitors with the
dielectric deposited from W boats (here-after called
type A) and alumina crucibles (hereafter called type B)
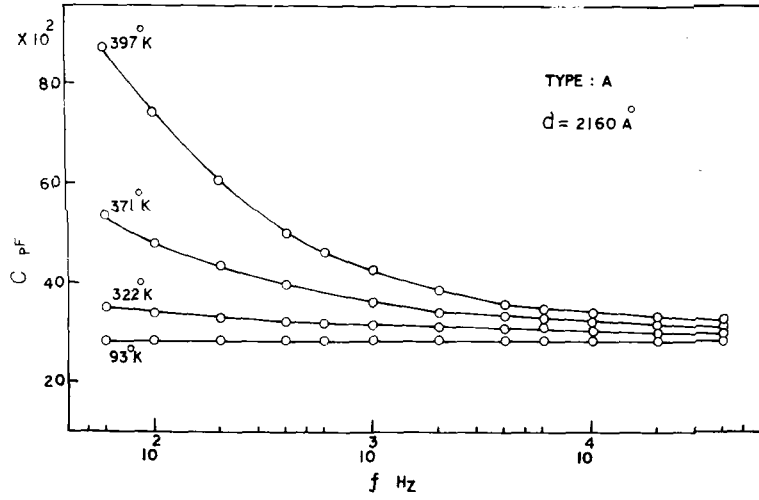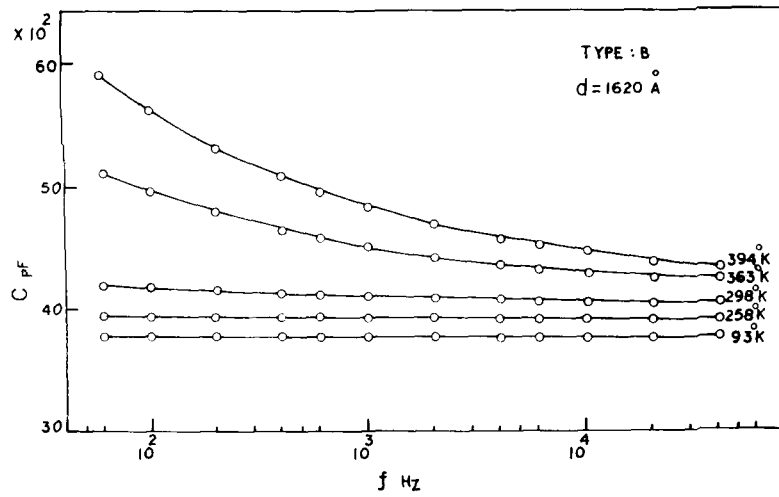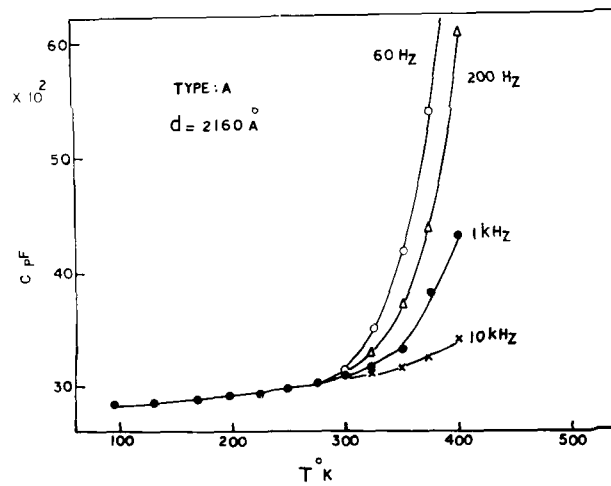were almost similar in nature.

Fig. V-4

Fig. V-5

a)   Ageing and annealing effect

All the capacitors when aged in air for a few days showed a decrease in C and tan δ and became more or less steady. However, on stabilising them in vacuo by heating and cooling cycles (150°C), both C and tan δ further decreased. C and tan δ (at 1kH$_z$) became steady after four annealing cycles as shown in fig. V-2.

b)   Effect of film thickness

Fig. V-3 shows the variations of C and ε with 1/d for the two types of capacitors A and B. It is seen that C varied linearly with 1/d and ε (4.7) was independent of film thickness. Results were the same for both type A and type B capacitors. Tan δ was also low (0.01) and independent of film thickness (table V-1).

c)   Effect of frequency and temperature on C and tan δ

The variations of C with frequency at different temperatures are given for type A (d = 2160 $\overset{o}{A}$) in fig. V-4 and type B (d = 1620 $\overset{o}{A}$) in fig. V-5 respectively. It is seen that C decreases continuously with frequency for both types and become more or less constant at higher frequencies. But below room temperature, (297°K) C is independent of frequency for the regions studied. The variations of C is much pronounced at higher temperatures and lower frequencies. This is similar to that observed for Dy$_2$O$_3$ and La$_2$O$_3$ films. Fig. V-6 shows the variations of C with

TABLE V-1

LaF$_3$ deposited from alumina boat

Film thickness d (A$^\circ$)	1/d x 10^4 cm^{-1}	C (pF) at 1 kHz	ϵ at 1 kHz	tan δ
2880	3.47	2280	4.64	0.011
2650	3.77	2520	4.7	0.006
2455	4.07	2860	4.9	0.011
2120	4.71	3140	4.7	0.01
2062	4.85	3380	4.9	0.017
1620	6.17	4110	4.7	0.011
1370	3.3	4820	4.67	0.019
910	11.0	7120	4.62	0.013

LaF$_3$ deposited from tungsten boat

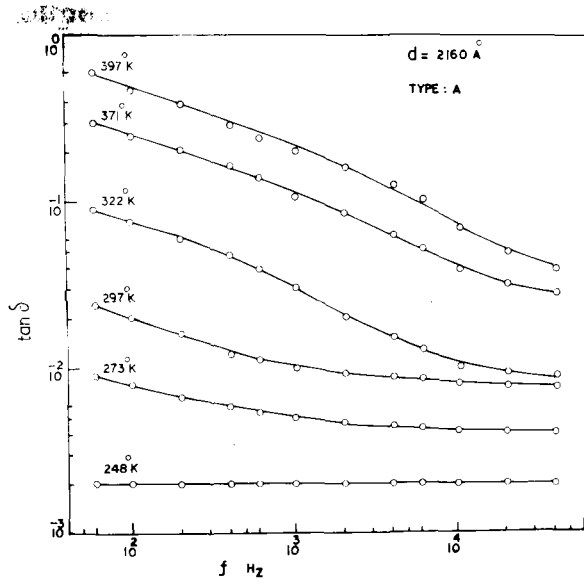| 3985	2.51	1671	4.70	0.030
3800	2.63	1757	4.70	0.010
3240	3.09	2104	4.80	0.010
2423	4.13	2730	4.67	0.030
2160	4.63	3090	4.71	0.013
1124	8.93	5800	4.71	0.015

Fig. V. 7
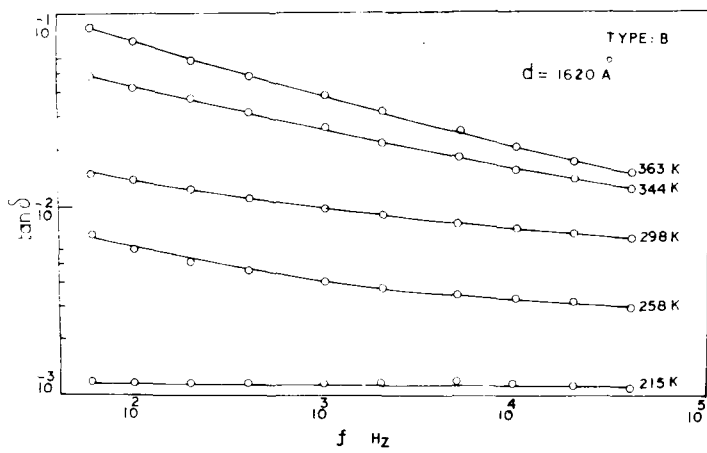
Fig. V. 8

temperature (90-400°K) at different frequencies for type A (d = 2160 A°). It is seen that the frequency branches of the curve merged together to a single one (around 280°C) and C tend to attain a constant minimum value at lower temperature region.

Figs. V-7 and V-8 show the typical variations of tan δ with frequency at different temperatures for type A and type B. Tan δ decreased continuously with frequency, but increased with temperature at a fixed frequency. It is to be specified here that unlike in the case of Dy_2O_3 films, no tan δ_{min} was observed, and the behaviour was more or less similar to La_2O_3 films. It appears that tan δ_{min} is likely to appear at higher frequencies.

d) Percentage variation of C and TCC

Fig. V-9 shows the percentage variation of C normalized at 1 kH$_z$ measured at room temperature (297°K) for different film thicknesses. $\Delta C/C$ varied about 4% in the frequency region 60 - 10^4 H$_z$, which was practically independent of film thickness. In fig. V-10 TCC is plotted with temperature for type A and B for different film thicknesses. TCC varied from 100 to 6000 ppm/°k for a temperature range 100-400°K. TCC variation was much low (100 - 1000 ppm/°k) in the temperature range 100-300°K, which was independent of film thickness and the variation
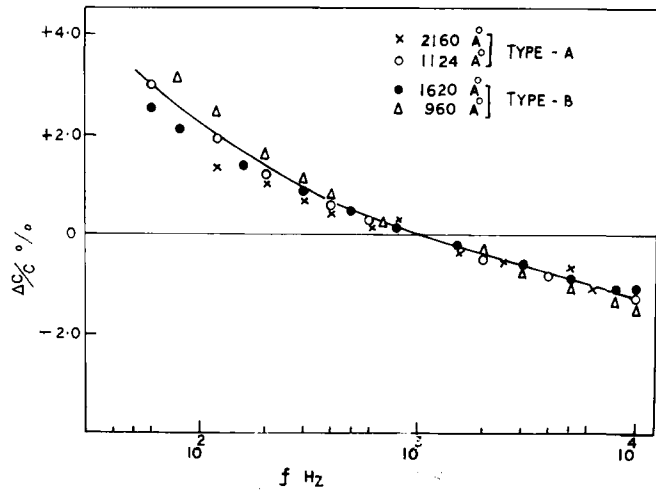
Fig. V. 9

Fig. V-10

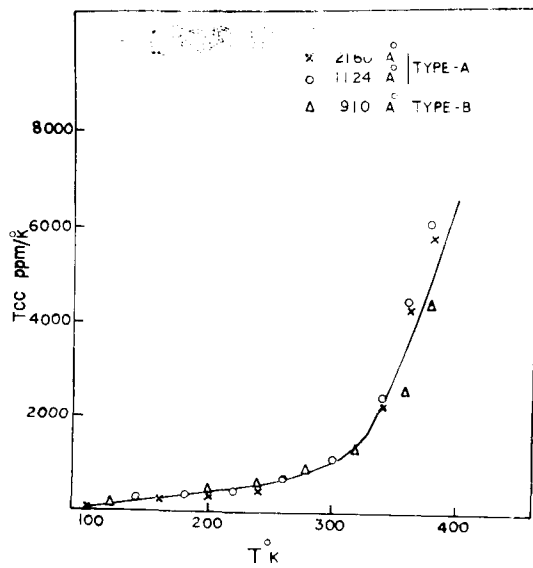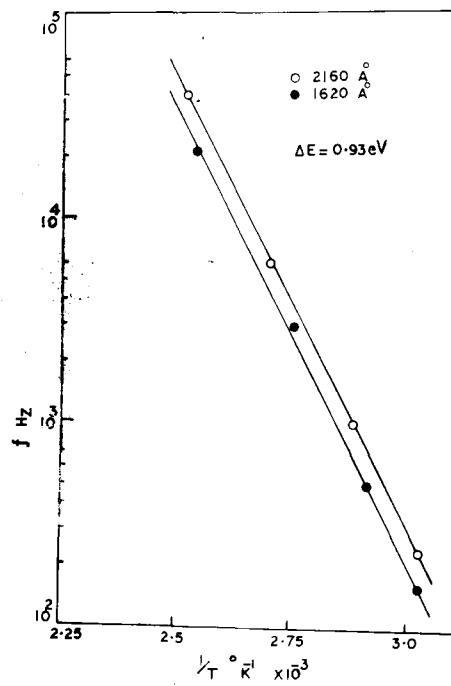Fig. V- 11

was more or less linear. But above $300^{\circ}K$, TCC increased rapidly.

e) Activation energy

ΔE was calculated from the variations of C with frequency at different temperatures as in previous studies. In fig. V-11 log f is plotted against 1/T at constant C. ΔE calculated from the slopes of the lines assuming kT in the exponential was the same (0.93 eV) for both the types.

The resistance (R) of the films were measured at different temperatures. In fig. V-12 log R is plotted against 1/T for four different film thicknesses. The slopes of all the lines were the same and ΔE calculated was about 0.95 eV, in good agreement with the previous measurements.

iii) I-V Characteristics

The I-V characteristics showed much typical behaviour unlike that observed in the previous studies. When the voltage was applied across $Al/LaF_3/Al$ capacitor, the initial current observed was very high. But the current decreased continuously with time to a much smaller value which was about 1/100 of the initial value. Practically no stabilisation was observed. It was also noticed that if the applied voltage was cut off, a discharge current flowing in the opposite direction was also observed. This, however, also decayed with time.
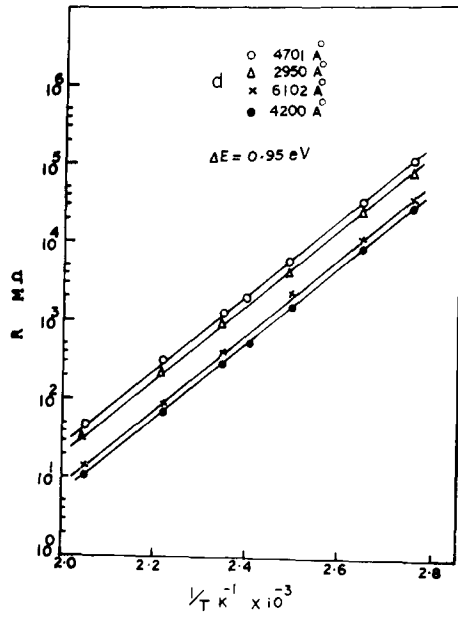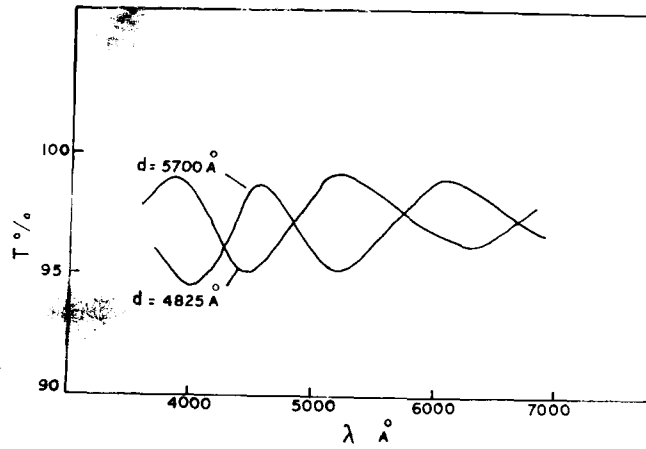
Fig. V. 12

Fig. V. 13

LaF_3 is an ionic conductor even at room temperature.
The peculiar behaviour observed above suggests the presence
of high ionic polarisation. This study also indicates a
space-charge region near the electrodes, which plays a
large role in the transport properties. This was in
conformation with the studies of Solomon et al. (1966)
and Lilly et al. (1973).

Because of the above disadvantages in dc measurements,
the I-V characteristics and the dc breakdown of LaF_3 films
could not be studied properly. However, the breakdown
field was found to be approximately 10^5 V/cm.

iv) <u>Optical properties</u>

Transmittance of LaF_3 films formed on quartz
substrates at room temperature was studied for the UV
and visible region (2200-7000 Å). The transmittance in
the UV region do not show any special feature except that
absorption slowly increased with decrease of λ. No
significant absorption was observed upto 2300 Å suggesting
the absorption in far UV. Interference peaks were observed
in the visible region. A typical transmittance curve is
shown in fig. V-13 for two film thicknesses (4825 and
5700 Å). Transmittance was high (T > 94%) and the
refractive index was calculated from the λ_{min} and λ_{max}
using the relations (eqns. I-26a and 26b) of Chapter I.
The refractive index in the visible region (4000 - 7000 Å)

TABLE V-2

Film thickness d (A°)	For maxima n = mλ/2d				For minima n = (m+1/2)λ/2d			
	λ (A°) max	m	n	k	λ (A°) min	m	n	k
4825	3840	4	1.60	negligible	4450	3	1.61	negligible
	5200	3	1.61	negligible	6300	2	1.62	negligible
5700	4550	4	1.60	negligible	4000	4	1.58	negligible
	6100	3	1.605	negligible	5200	3	1.60	negligible

thus evaluated was about 1.6, which was practically independent of wavelength and thickness of the dielectric films (table V-2).

D. DISCUSSION

The properties, especially the electrical properties of LaF_3 films which were ionic in nature were somewhat different from those observed previously in the case of insulating films such as Dy_2O_3 or La_2O_3. The structural studies of the bulk powder by X-ray diffraction showed that it contained traces of other impurities presumably lanthanum oxide. The electron diffraction studies showed that the deposits contained primarily LaF_3. The presence of faint rings appears to be due to traces of the oxide impurities. The ageing and annealing effect on LaF_3 films showed a decrease of C and tan δ suggesting that after annealing, the defects present in the deposits were much reduced and the films became more or less homogeneous and the dielectric constant was independent of film thickness for both type A and B. Maddocks et al. (1962) reported that when LaF_3 films were deposited from alumina boat, ε was thickness independent (8.2 at 1 kH_z), but when deposited from tantalum boats, a thickness dependent high value of ε was observed. The increase in thickness dependent ε, seems to be due to partial dissociation of LaF_3 leading to the formation of mixed species of metallic and dissociated

products. This will give rise to thickness dependent ϵ, as observed in the case of niobium and indium oxide films (Goswami et al. 1974; 1975). Since in the present study deposition from alumina or tungsten boat did not cause any change in ϵ, which is thickness independent, it may be concluded that the deposited films *consisted mainly of* LaF_3.

C decreased with increasing frequency and increased with increase of temperature as in the previous studies. But unlike Dy_2O_3 films, no tan δ_{min} was observed in the variation of tan δ with frequency. The percentage variation of capacitance $\Delta C/C$ was about 4% in the frequency region $60-10^4$ H_Z which is slightly higher than that for the oxide films studied. TCC varied from $100-6000$ ppm/$^{\circ}$k in the temperature region $100-400^{\circ}$K. It is interesting to note that TCC variation was small ($100-1000$ ppm/$^{\circ}$k) upto 300°K. At higher temperatures it increased rapidly because of the increase of charge carriers by the increase of thermal energy resulting in a reduction of resistance R and a rise in C.

Current-voltage characteristics of LaF_3 films were quite different from the normal dielectric films and the studies indicated the presence of high polarisation as observed previously by Solomon et al. (1966), Lilly et al. (1973) and others. The presence of polarisation

in ionic crystals has been widely discussed for a number of years. Still the phenomenon is not understood fully. The reason for this appears to be the variety of effects which have been invoked as responsible for the phenomenon in different materials and the difficulty of determining the dominant one. The electrical conductivity and NMR measurements showed that the electrical conductivity is due to ionic motion (F^-) with a little electronic contribution. Solomon et al. (1966) suggested the existence of a permanent double layer at the surface of LaF_3 crystals and potential probe measurements confirmed this.

There are two broad categories of effects which have been proposed: center polarisation and space charge polarisation. In the former category Sutter and Nowic (1963) proposed that in pure alkali halides, dielectric relaxation of defect clusters causes low frequency polarisation. A standard theory for space charge polarisation was proposed by Jaffe (1952). The pulsed I-V measurements of Lilly et al. (1973) clearly indicated a space charge region near the electrodes which play a large role in the transport properties. Further, the high current observed by the application of a dc voltage, the decay of it with time and also the depolarisation current in the opposite direction by the removal of the applied voltage clearly

indicate the presence of large polarisation in LaF_3 whose magnitude is unusual compared to other ionic crystals.

The activation energy measured by current measurements as well as by capacitance measurements agreed well ($\Delta E = 0.93$ eV). But Tillar et al. (1973) reported an activation energy of F^- ion diffusion to be about 0.4 eV for < $360^{\circ}K$ and 0.8 ± 1 eV for > $360^{\circ}K$. This difference may be due to structural and morphological defects and also the method of preparation of LaF_3 films which may cause differences in impurities.

It is interesting to mention that LaF_3 films showed high transmittance suggesting that they are practically transparent in the visible region. Also the films showed interference associated with maxima and minima in the visible region and the refractive index (n = 1.6) calculated from the maxima and minima is in good agreement with the value previously reported by Hass et al. (1959). The high transmittance of LaF_3 films in visible region shows that these films can be used in optical coatings. The optical transmittance in the UV region definitely shows that the absorption and hence the optical bandgap lie in the far UV region.

CHAPTER-VI : STUDIES ON CALCIUM FLUORIDE AND STRONTIUM
              FLUORIDE FILMS

CHAPTER VI

STUDIES ON CALCIUM FLUORIDE AND STRONTIUM FLUORIDE FILMS

A. INTRODUCTION

Structural aspects and many of the physical properties of calcium fluoride and strontium fluoride which are ionic in nature have been studied by various workers. Crystal structure of CaF_2 was first analysed by Bragg (1914) by X-ray method and found to have a cubic structure (a = 5.48 A^o). Arkel (1924) found that SrF_2 had also a cubic structure (a = 5.86 A^o). Swanson et al. (1951,1955) from X-ray diffraction analysis later reported that CaF_2 and SrF_2 had lattice parameters a = 5.4626 A^o and 5.8 A^o respectively, both belonging to the space group O^5H - FM3M with Z = 4.

The colour centres produced by X-rays in CaF_2 and BaF_2 crystals were reported for the first time by Smakula (1950) and four absorption bands were observed at wavelengths 5800, 3380, 2200 and 400 A^o. Jacobs (1957) studied the dielectric relaxation in two batches of CaF_2 crystals. The loss curves observed with frequency of the first type were straight lines caused by the ionic conductivity by the free carriers whereas for the second

type it was due to the dipolar relaxation in the
frequency region 10^2 - 10^5 Hz. These crystals in
presence of calcium vapour, however, became coloured
and showed dipolar relaxation in the same frequency range.
Rao et al. (1966) studied the dielectric properties of
various alkali earth fluoride crystals at the temperature
range 193 - 500°K at frequencies 10^2-10^6 Hz. Dielectric
constants of CaF_2 and SrF_2 at 20°C were 6.78 and 6.48
respectively at 1 kHz and were independent of frequency
but increased with temperature. However, ϵ was independent
of temperature below 25°C. Activation energy calculated
for CaF_2 and SrF_2 was 1.4 eV and 1.5 eV respectively.
Johnson et al. (1966) observed that an addition of NaF
to CaF_2 caused a loss peak at higher frequencies due to
the dielectric relaxation. Chen et al. (1969) studied
the dielectric relaxation at different temperatures in
CaF_2 and SrF_2 crystals doped with NaF and YF_3 and determined
the activation and association energies for the dipolar
complexes.

A temperature and pressure dependence of low
frequency dielectric response of CaF_2 and SrF_2 crystals
was reported by Lowndes (1969). The temperature dependence
of dielectric response was found to be principally due to
intrinsic volume changes in the crystals rather than to
intrinsic temperature changes in the anharmonic contribution.

The static dielectric constant for SrF_2 at $300^{\circ}K$ was about 6.5. Andeen et al. (1971) also measured the dielectric constants of alkali earth fluorides at $300^{\circ}K$ by the method of substitution. Dielectric constant, tan δ and conductivity of Mn and Na doped CaF_2 crystals were studied by Agrawal (1974) in the region 10^2-10^7 Hz and at temperatures in the range 30 - $450^{\circ}C$. Both the samples exhibited dipolar relaxation at room temperature. Ure (1957) studied the transference number measurements on pure and doped CaF_2 crystals and showed that the predominant defect was anti-Frenkel disorder type involving equal concentrations of negative ion vacancies and negative ion interstitials and from the electrical conductivity measurements, the mobilities of the F^- vacancy and F^- interstitial have been determined.

Lewowski et al. (1965) studied the I-V characteristics of CaF_2 and found to be applicable for the construction of diodes having a negative resistance region. Further studies on the ionic conductivities of Ca and Sr fluorides were made by Barsis et al. (1966) and Fielder (1967). The Hall mobility measurements in CaF_2 and SrF_2 by Seager (1971) showed that in all cases the sign of the Hall effect was that of electrons. Seetharaman et al. (1973) studied the defect structure of the fluorides of Ca and Sr and discussed their application as solid

electrolytes. Podgorsak (1973) correlated the space
charge electret state in CaF_2 with its bulk ionic conduction.
The high field conduction ($10-10^4$ V/cm) in CaF_2 crystals
was reported by Manfredi et al. (1974) at temperatures
80 - 300°K and the I-V characteristics showed an initial
linear behaviour followed by a non-linear trend, where
the temperature of the sample increased considerably.

While studying the structure of CaF_2 and SrF_2,
Swanson et al. (1951 and 1955) found that the bulk
refractive indices of both were the same. The effect of
temperature on vacuum UV transmittance of CaF_2 was measured
by Laufer et al. (1965). With the aid of a long wavelength
IR spectrometer, Berman et al. (1965) studied the transmission
of CaF_2 in the region 1700-6000 A° at room temperature and
1500-2500 A° at -90°C. Reflectance data in the far UV
region (8-14 eV) showed three absorption bands for SrF_2
(Robin-Kandare et al. 1966). Caffyn et al. (1967) reported
the dielectric and optical absorption measurements on doped
CaF_2. Also the optical, dielectric and lattice properties
of Ca and Sr fluorides were studied by Denham et al. (1970).

The structure of CaF_2 thin films were studied by
Bujor and Vook (1967) and the dependence on substrate
temperature and film thickness of the deposits on (100)
face of NaCl was reported. The complex epitiaxial growth

of vacuum deposited CaF_2 films had been studied by several workers (Vook et al. 1970; Koch et al. 1973 and Reichelt et al. 1973). Thick films were polycrystalline especially when formed at room temperature. The first study of the dielectric properties of CaF_2 films was reported by Laurila (1950) in which case ϵ measured just after the deposition was about 150 - 6000 which decreased considerably to about 7-10 after a few days of ageing. A detailed work on $Al/CaF_2/Al$ capacitor system was reported by Weaver (1962). He observed an increase in C by ageing, whereas tan δ decreased continuously. He found that the optical thickness of CaF_2 films increased with ageing, which was due to the increase in refractive index. By absorption of moisture C increased and also tan δ showed a maxima with frequenoy in the audio frequency region. The dielectric constant was found to be about 3.2.

The prebreakdown and breakdown electrical properties of CaF_2 films using aluminium electrodes were studied by Budenstein et al. (1969). The light emitted during breakdown contained the arc spectra of the dielectric and the electrodes. The breakdown field (10^6 V/cm) varied with film thickness as $d^{-1/2}$. Smith et al. (1969) studied the breakdown conduction and breakdown phenomena in CaF_2 films (700-30000 A°) in more detail. The dielectric relaxation and dc current-temperature measurements in CaF_2

films were reported by Smith (1969) who observed an ϵ
maxima at about 215°K and also a step in the variation of
ϵ with temperature.

The above survey shows that even though considerable
amount of work has been carried out on bulk CaF_2, very
little investigation has been carried out on vacuum deposited
CaF_2 films especially its ac behaviour and optical properties.
For SrF_2 films still less work has been done even though
its properties are much similar to those of CaF_2. Consequently
an effort has been made to study the ac behaviour, optical
properties, moisture effect and other properties of vacuum
deposited films of CaF_2 and SrF_2 and compare these results.

B. **EXPERIMENTAL**

Bulk CaF_2 supplied by M/s Koch Light Laboratories Ltd.
(99.93% purity) was used for preparing films. Pure SrF_2
was prepared from strontium nitrate. Strontium nitrate
(21 g, 0.1 M) was dissolved in distilled water (100 ml)
and added to a solution of sodium fluoride (8.4 g, 0.2 M
in 100 ml) and the contents were boiled for one hour,
cooled to room temperature and filtered. The precipitate
was washed several times with distilled water till free
from soluble impurities, dried at 110°C in oven and finally
at 110° in vacuum (yield 11.3 g, 90% of theory).

Both the powders were then deposited from tungsten boats on glass substrates kept at room temperature. The deposition was carried out for about 20 minutes and the rate of evaporation was about 200 A^o per minute. The deposited films were highly transparent. Al/CaF$_2$ or SrF$_2$/Al capacitors were fabricated in the manner described previously. To study the substrate temperature effect, SrF$_2$ was also deposited at 125°C.

For optical studies in UV and visible regions, films were deposited on quartz substrates. For structural investigations, films were deposited at room temperature and also at 200°C on polycrystalline NaCl tablets, NaCl (100) face, glass and mica.

Effect of moisture on C and tan δ of CaF$_2$ films capacitors was studied at room temperature by keeping the samples in different relative humidity conditions which were obtained by different concentrations of sulphuric acid in water in a closed system. The electrode effect on CaF$_2$ films were also studied and the Al/CaF$_2$/Cu and Al/CaF$_2$/Au samples were fabricated in the same manner as described previously.

C. RESULTS

i) Structure

The structure of the bulk CaF$_2$ and SrF$_2$ powder was analysed by X-ray powder method and found to be cubic

TABLE VI-1

I/Io	d A^{o}	hkl
s	2.152	111
s	1.930	220
ms	1.660	311
f	1.768	400
f	1.257	331
ms	1.111	422
f	1.050	511
f	0.969	440
f	0.922	531
f	0.858	620

s - strong

f - faint

m - medium

a = 5.46 A^{o}

TABLE VI-2

I/Io	d A$^{\circ}$	hkl
s	3.357	111
f	2.970	200
s	2.053	220
ms	1.749	311
f	1.453	400
f	1.335	311
ms	1.183	422
f	0.974	531
f	0.955	600

s   - strong

f   - faint

m   - medium
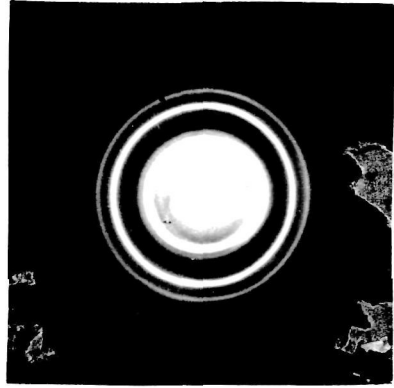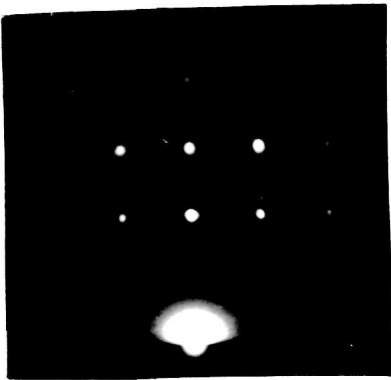
a   = 5.8 A$^{\circ}$
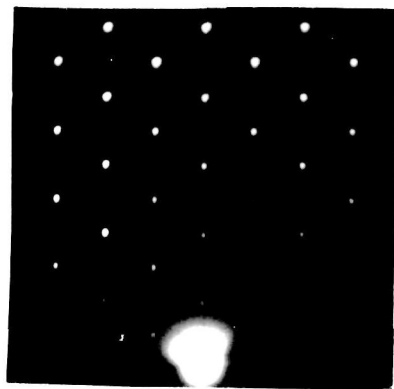
Fig. VI - 1

Fig. VI - 2

Fig. VI - 3

Fig. VI - 4

(a = 5.46 A^o and 5.8 A^o for CaF$_2$ and SrF$_2$ respectively).
The deposits formed on glass or NaCl at room temperature
yielded polycrystalline patterns when studied by electron
diffraction corresponding to normal CaF$_2$ and SrF$_2$ structure.
The electron diffraction patterns for deposits at room
temperature are given in fig. VI-1 and VI-2 for CaF$_2$
and SrF$_2$ respectively. The measured d values are given
in table VI-1 and 2. When the substrate temperature was
high (200°C), these deposits developed epitaxial
orientations on the (100) face of NaCl, but remained
polycrystalline on glass or polycrystalline substrates.
Thicker deposits however developed 1-d 111 orientations.
The reflection studies of the SrF$_2$ films grown on the
NaCl (100) face are shown in figs. VI-3 and VI-4. These
show typical expitaxial growth of SrF$_2$ films developing
2-d {100} orientations.

ii) Dielectric properties

a) Ageing and annealing effects

Ageing and annealing effects on capacitance of CaF$_2$
and SrF$_2$ films showed some peculiarities, different from
those of the other films discussed before. Fig. VI-5 shows
the variations of C and tan δ with time for the two above
films. It is seen that while C of SrF$_2$ films decreased
with ageing, for CaF$_2$ films, on the other hand, it continuously
increased suggesting that some changes are occuring in
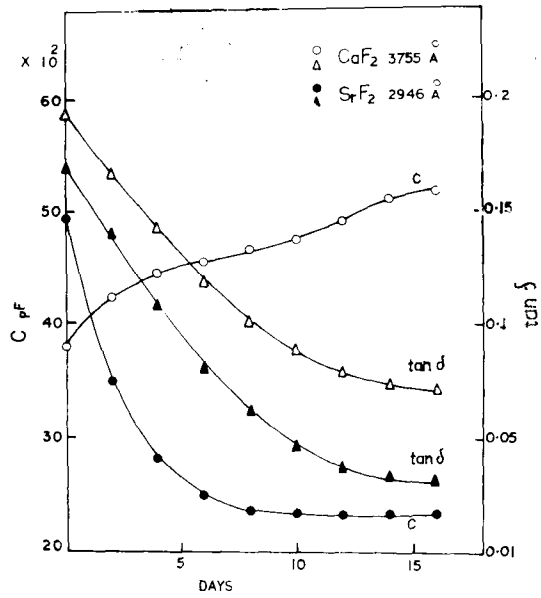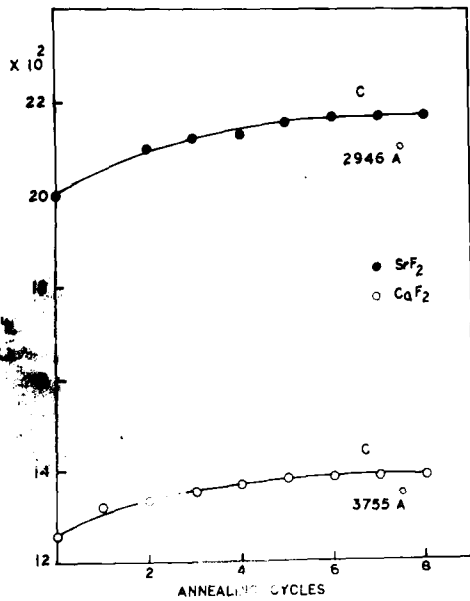CaF$_2$ films possibly due to their exposure to atmosphere.
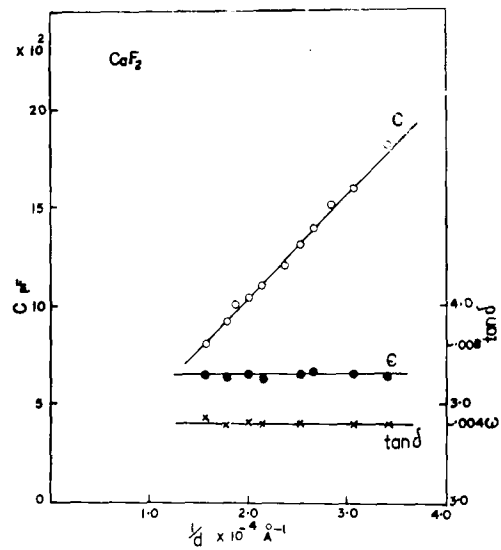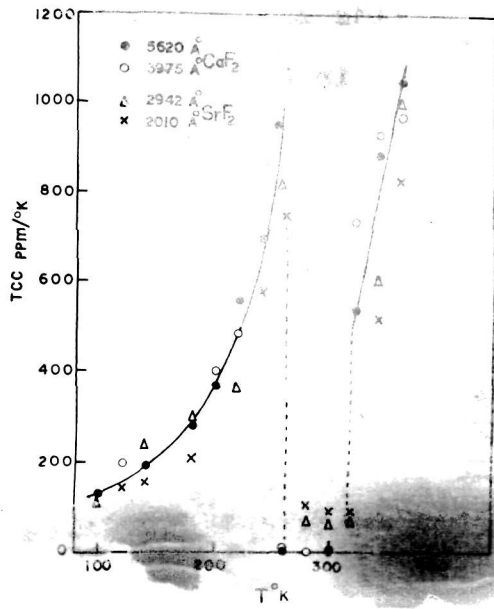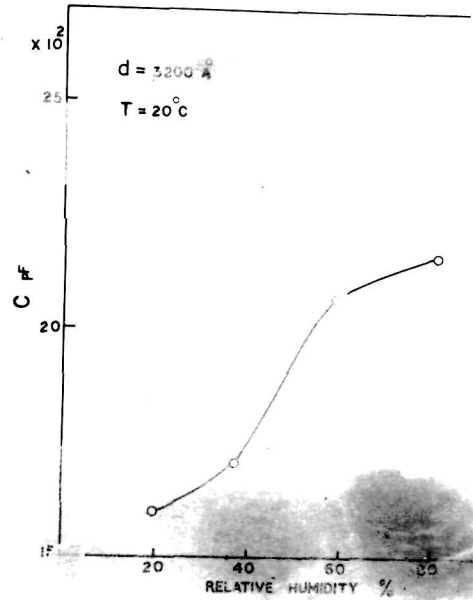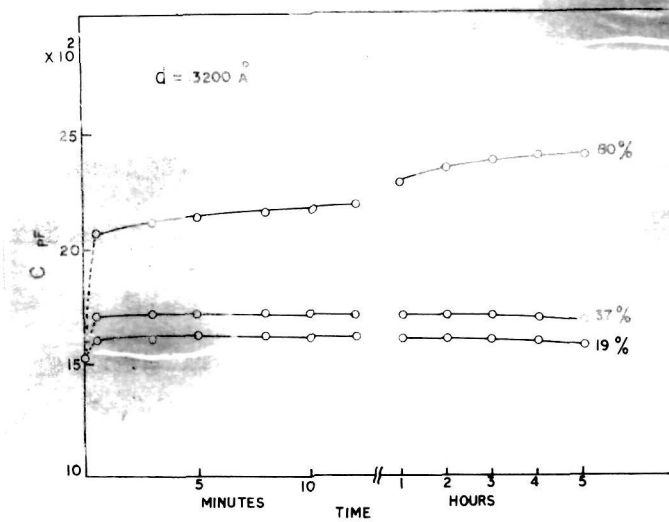
Fig. VI-5

Fig. VI-G

Fig. VI-7

Fig.VI-17

Fig.VI-18

Fig.VI-19
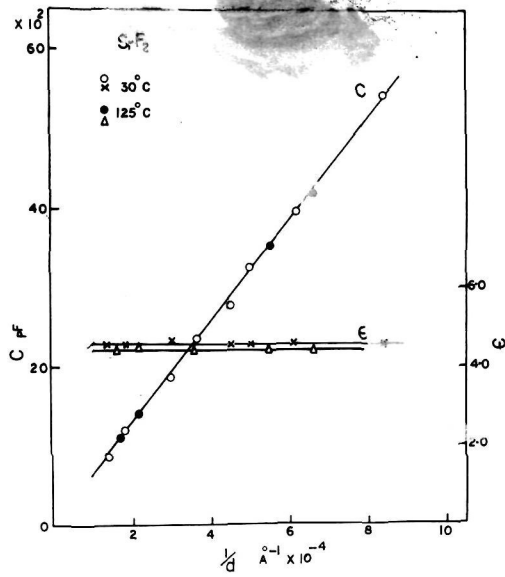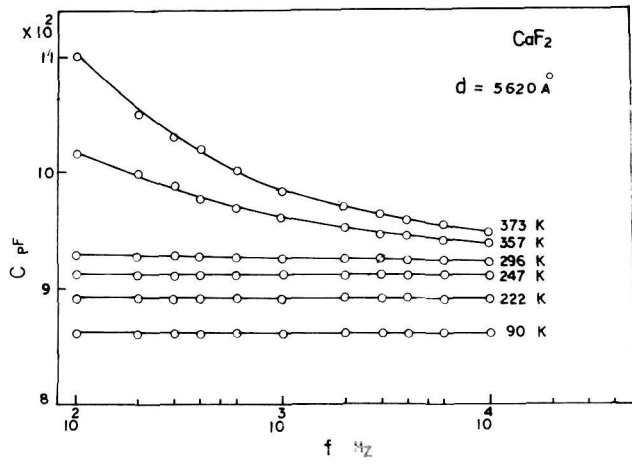
Fig. VI-8

Fig. VI-9

Fig. VI-10

But in both cases, tan δ decreased continuously. The behaviour of these capacitors with annealing is shown in fig. VI-6. It is interesting to note that unlike all previous studies, C of CaF_2 and SrF_2 films gradually increased, ultimately attaining constant values after a few cycles. However, tan δ decreased by annealing. This behaviour was similar to those observed by Weaver (1962) for CaF_2 films during ageing.

b) Effect of film thickness on C, ε and tan δ

Fig. VI-7 shows the variations C, ε and tan δ with 1/d for CaF_2 films. It is seen that C decreased linearly with increasing film thickness, whereas ε (3.65) and tan δ (0.004) were independent of film thickness (2500 - 7500 A^o). Fig. VI-8 shows the similar variations of C, ε and tan δ for SrF_2 films deposited at room temperature as well as at 125°C. At higher substrate temperature, however, ε slightly increased from 4.45 to 4.55. But tan δ (0.004) remained more or less the same.

c) Effect of frequency and temperature on C and tan δ

The typical variations of C with frequency at different temperatures are shown in fig VI-9 and VI-10 for CaF_2 and SrF_2 films. In both cases C became independent of frequency around room temperature and below. However, the variations are much pronounced for lower frequencies at higher temperatures.
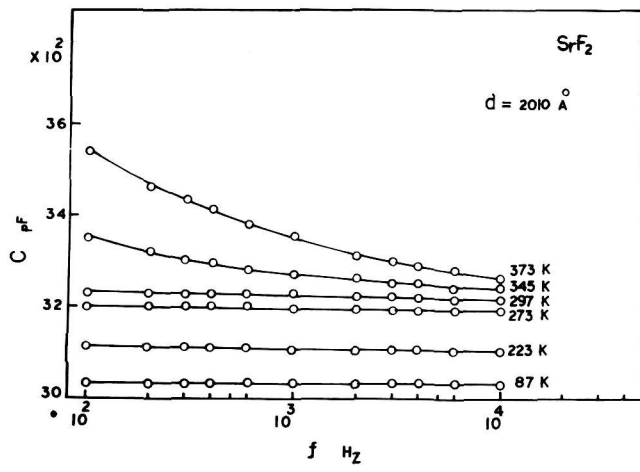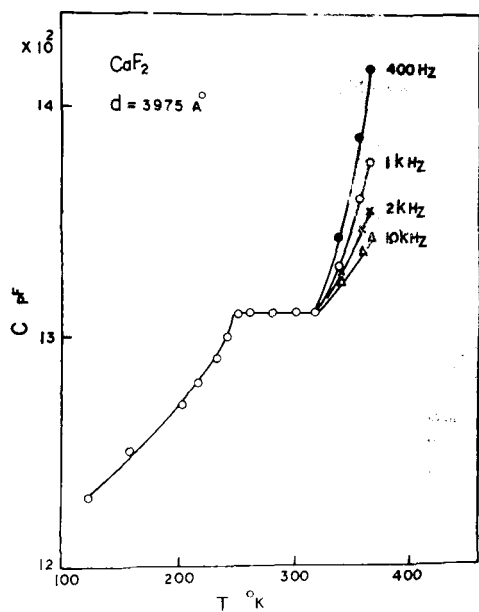
Fig. VI-11
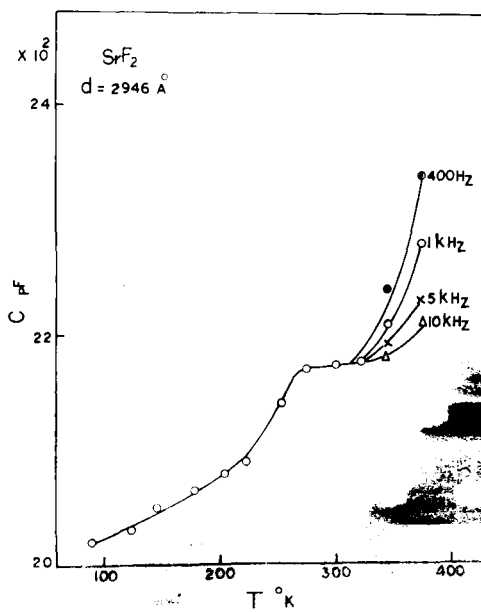
Fig. VI-12
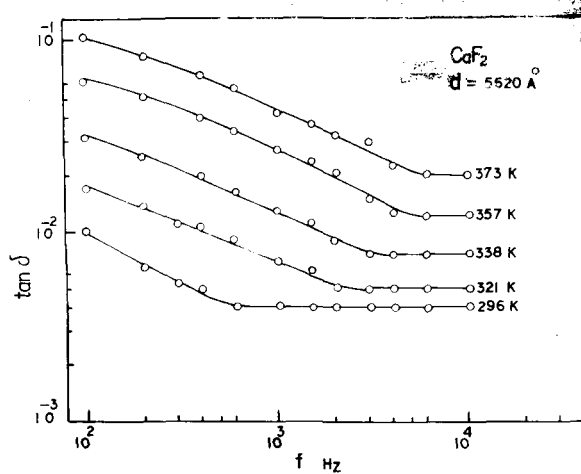
Fig. VI-13

Figs. VI-11 and VI-12 show the variations of C with temperature at different frequencies for CaF_2 and SrF_2 films respectively. It is interesting to see that C at lower temperatures is independent of frequency. However C increases with temperature, but later on it remains more or less constant for a certain temperature range, forming a sort of step in the graph and with further increase in temperature, C increases following the path which is dependent on frequency. The temperature range for constant C was $264-316^{\circ}K$ for SrF_2 films and $250-315^{\circ}K$ for CaF_2 films. This temperature independent behaviour of C suggests a relaxation phenomena to be discussed later.

Figs. VI-13 and VI-14 show the variations of tan δ with frequency at different temperatures for CaF_2 and SrF_2 films respectively ($d = 5620 \text{ A}^{\circ}$ and 2010 A°). For both cases tan δ slowly decreases with frequency and invariably become constant at higher frequencies. Further, tan δ also decreases with decrease of temperature and becomes constant at much lower frequencies in the lower temperature region. These variations are somewhat similar to the previous observations of tan δ_{min} shifting to higher frequency region at higher temperatures for Dy_2O_3 films. However, instead of a sharp minima, it shows a flat one.

The effects of temperature on ϵ and ϵ'' (tan $\delta = \epsilon''/\epsilon$) at 1 kHz are shown in fig. VI-15 and VI-16 for CaF_2

(d = 3975 A^O) and SrF_2 (d = 2946 A^O) films respectively.
It is seen that ϵ slowly increases and attain a steady
value and later on again rise with further increase of
temperature which is similar to the behaviour of C with
temperature. The formation of a step for ϵ is between
250 - 316°K for CaF_2 films and 264-320°K for SrF_2 films.
ϵ'', on the other hand, increases, attain a sharp maxima
at about 254°K, falls and again starts increasing for
CaF_2 films. These ϵ'' maxima and saturation of ϵ clearly
indicate a relaxation process for CaF_2 films. But in the
case of SrF_2 films, even though there was a flat feature
of ϵ curve, ϵ'' maxima was not sharp.

d) <u>Temperature coefficient of capacitance</u>

Since C was practically constant for a particular
range of temperature, the variation of TCC (at 1 kHz) was
somewhat unusual (fig. VI-17). TCC at first increased
from about 200 to 900 ppm/^{O}K for CaF_2 films in the
temperature region 100-260°K and then dropped suddenly
to practically zero. It is seen that TCC is practically
zero in the temperature range 260-300°K and then it
increases upto 1000 ppm/^{O}K for a temperature about 360°K.
This behaviour is observed also for SrF_2 films. TCC
increased from 150-1000 ppm/^{O}K for temperature 100-270°K
which dropped to about zero in the region 270-300°K and
then again increased.
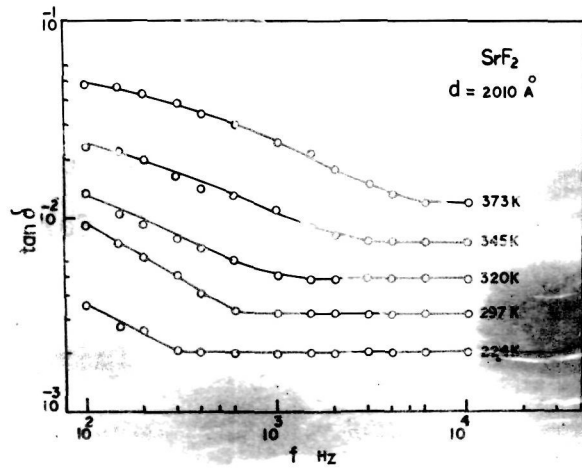
Fig. VI-14
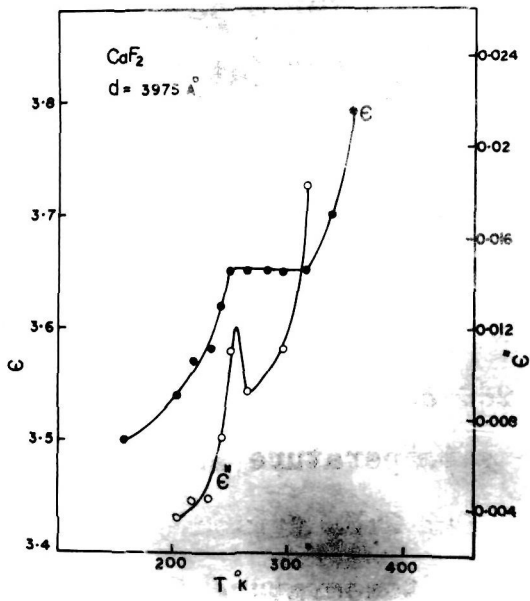
Fig. VI-15
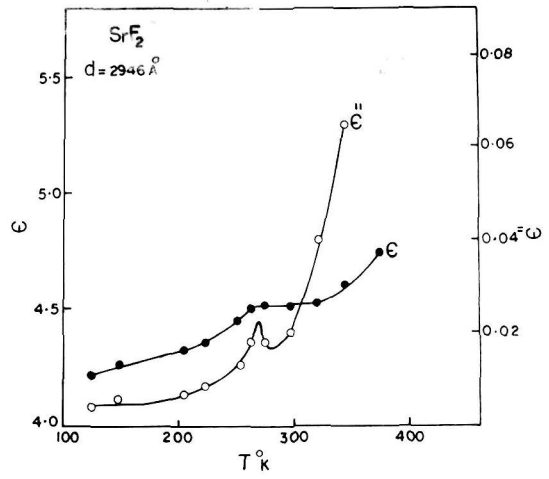
Fig. VI-16

e) Humidity effect

The effect of moisture on CaF_2 films has also been studied because of the observed increase in C with ageing and annealing. The variations of C and tan δ of CaF_2 film capacitors were studied at $20^\circ C$ by exposing them to different humidity conditions. Different humidity was attained by using sulphuric acid solutions of different concentration in water. The acid of suitable concentration was kept in an enclosed container for a few hours to ensure the equilibrium. Capacitors were then quickly transferred from vacuuo to the container and the system was again closed. Both C and tan δ were then measured at 1 kHz at different intervals. Appropriate leads were taken out from the container for measurements.

Fig. VI-18 shows the variations of C with time for a film thickness d = 3200 A°. It is seen that C and tan δ increase immediately after the transfer and remained practically the same even after a long time of exposure, thus suggesting that equilibrium was attained within a short period. Tan δ also increased with humidity. This was true for different humidity conditions also. This behaviour was similar to the adsorption studies of CaF_2 films by Weaver (1962).

Fig. VI-19 shows the variations of C and tan δ with relative humidity for a film thickness d = 3200 A°.

It is interesting to note that C increases with the
increase of relative humidity. It may be mentioned here
that both C and tan δ almost regained the original values
in a short time when these capacitors were kept back in
vacuuo.

The above results suggest that CaF_2 capacitors can
be used as indicators or sensing elements for humidity,
for which many applications can be envisaged.

f) Dissimilar electrode effect

The studies of CaF_2 capacitors with dissimilar
electrode systems such as $Al/CaF_2/Cu$ or $Al/CaF_2/Au$, showed
some interesting results. It was found that these capacitors
when kept in vacuuo and connected directly to a microvolt-
meter, no emf was observed. However, when the capacitors
were exposed to air a voltage of the order of 150-300 mV
was immediately developed across the capacitor with copper
or gold as positive. When the capacitor was put back in
vacuuo, the voltage measured across the electrodes decreased
and ultimately became zero. When the capacitors were
placed in higher moisture conditions, the voltage measured
was also increased. Further no emf developed when the
capacitors were kept in dry air. It is to be mentioned
that the voltage developed across the electrodes were
independent of the CaF_2 film thickness. Similar effects
were observed irrespective of Cu or Au being top or bottom
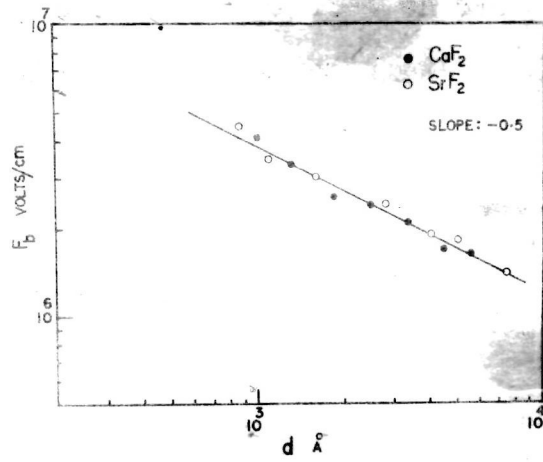
Fig. VI-20
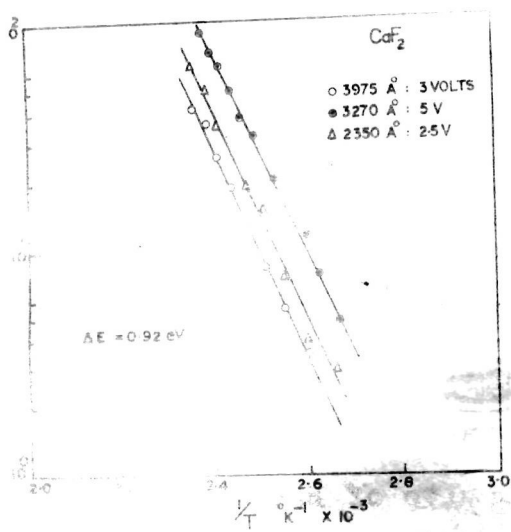
Fig. VI-21
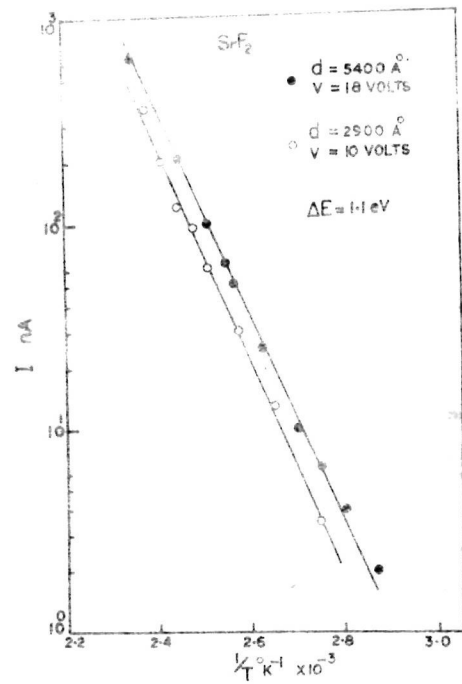
Fig. VI-22

electrodes. However no such emf was developed for similar electrode systems such as $Al/CaF_2/Al$.

These results, namely, the development of an emf across two dissimilar electrodes with CaF_2 film as medium when exposed to humid atmosphere suggest the formation of a galvanic cell in the capacitor system.

g) <u>Breakdown voltage</u>

The dc breakdown voltage of CaF_2 and SrF_2 film capacitors were measured in air by increasing the applied voltage across the capacitors and measuring the current. At or near the breakdown point, sparks were observed over the junction of the top electrode which was accompanied by a sudden increase in current. This was taken as the onset of breakdown. Breakdown voltage was higher for higher film thicknesses. In fig. VI-20, breakdown field is plotted against film thickness for CaF_2 and SrF_2 film capacitors. Breakdown field (F_b) was high (10^6 V/cm) and it decreased with increasing film thickness with a negative slope = 0.5, thus obeying the relation $F_b \propto d^{-1/2}$. This is also in agreement with the results of Budenstein et al. (1969) for CaF_2 films.

h) <u>Activation energy</u>

The activation energies were calculated from the dc current variations with temperature at a fixed applied
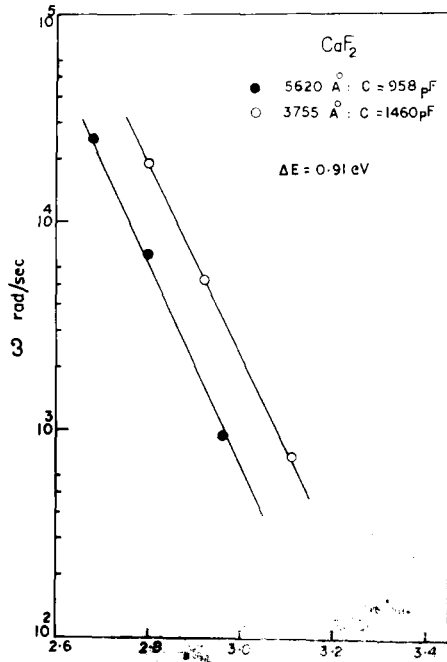
Fig. VI - 23
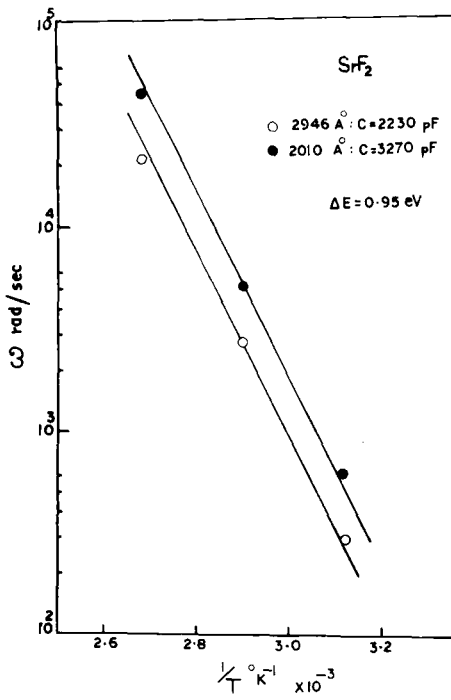
Fig. VI - 24
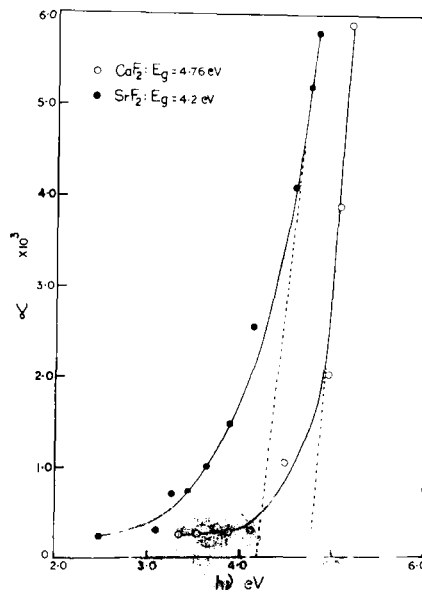
Fig. VI - 25

voltage as in the earlier studies. Fig. VI-21 and VI-22 show the variation of current with 1/T for different film thicknesses at different applied voltages for CaF_2 and SrF_2 films respectively. ΔE estimated from the slopes of these graphs were 0.92 eV and 1.1 eV respectively for CaF_2 and SrF_2, assuming kT in the exponential factor.

ΔE was also calculated from the variations of C with frequency at different temperatures. Figs. VI-23 and VI-24 show a plot of log ω vs 1/T at constant capacitance for different film thicknesses. ΔE estimated from the slopes of the above graph were 0.91 eV and 0.95 eV respectively for CaF_2 and SrF_2 films.

iii) **Optical properties**

The optical properties of CaF_2 and SrF_2 films were studied in the visible and UV regions by the transmittance measurements at normal angle of incidence in a Beckmann DK2 spectrophotometer. The films were deposited at room temperature on quartz. These films were highly transparent in the visible region (T ≃ 99%), but absorption was however observed in the UV region. Absorption coefficient α was calculated as in the case of La_2O_3 films (refer chapter IV) from the transmittance for different film thicknesses. From α, the absorption index (k) was estimated which was negligibly small (< 0.01) in the visible region. In fig. VI-25 α is plotted against photon energy. .It is seen

that α increases sharply for photon energy greater than 4 eV, thus suggesting the onset of the absorption band. The straight line parts of the graphs extrapolated to $\alpha = 0$ yielded the optical band gap (E_g) which was found to be 4.67 eV and 4.2 eV respectively for CaF_2 and SrF_2 films.

The refractive indices of these films were also calculated from the transmittance data neglecting k (refer chapter I). n was found to be 1.25 and 1.2 respectively for CaF_2 and SrF_2 films in the visible region (4000 - 7000 A^o) which were practically independent of wavelength and film thickness in the regions $(d = 2000 - 7000 A^o)$ studied.

D. DISCUSSION

The dielectric properties of CaF_2 and SrF_2 film capacitors were found to be almost similar. Vacuum deposited films of both the compounds were polycrystalline in nature having the cubic structure as those of the bulk materials. However at higher substrate temperature $(200^o C)$, these grew epitaxially on (100) faces of NaCl and a 2-d 100 orientation was observed for SrF_2 films.

The ageing and annealing effects on these films were unlike those of the other films studied in previous chapters. In the present case, there is a considerable

rise in capacitance whereas for others there was a decrease which is generally due to the annealing of defect concentrations as the specimens tend to attain thermodynamic equilibrium. Similar increase in capacitance while ageing was also observed by Weaver (1962) for CaF_2 film capacitors. The capacitance was found to increase by annealing also. The case is not yet clear and does not appear to be due to adsorption of moisture, since the annealing was carried out in vacuo. As annealing not only removes defects, it may also induce some recrystallisation, grain growth etc. which may account for the increase in capacitance by ageing and annealing.

The variations of C, ϵ and tan δ with film thickness for CaF_2 and SrF_2 films were as observed in the case of La_2O_3 films. The dielectric constant (ϵ = 3.65) measured at 1 kHz for CaF_2 films was independent of film thickness and is comparable with the reported value (ϵ = 3.2) by Weaver (1962). The studies on SrF_2 films showed that there was no effect of substrate temperature on the dielectric properties. The variations of C and tan δ with frequency were similar to the previous studies. C was independent of frequency at room temperature and below. The variation of tan δ with frequency showed a flat minima similar to that observed by Rao and Smakula (1966) for CaF_2 and SrF_2 single crystals. But it is

interesting to see that the point at which flat tan δ_{min} starts is shifting towards higher frequency region at higher temperatures.

The variation of C with temperature showed a peculiar feature viz., a step for a particular temperature region in the C vs T curves. This suggests that C was independent of temperature for some temperature range. Simultaneously a peak in tan δ in tan δ vs temperature curve was also observed. The corresponding variations of ϵ and ϵ'' shown in fig. VI-15 also showed a step in ϵ and a peak in ϵ'', the latter is no doubt associated with relaxation effect due to dipole orientation. Similar relaxation has also been reported by Smith (1969) for CaF_2 films and also for other vacuum deposited Niobium and Indium oxide films (Goswami et al. 1974). In the case of SrF_2 films, similar step in C and ϵ and a peak in ϵ'' can also be attributed to a single relaxation effect due to dipole orientation.

Several workers measured the activation energy for bulk as well as films of CaF_2 and there has been some inconsistencies in the results of these workers. Ure (1952) observed 0.52 eV whereas Rao and Smakula (1966) reported a value of 1.4 eV. Smith observed $\Delta E = 0.37$ eV for CaF_2 films. The measurements of ΔE in

the present study for CaF_2 films by two methods led to the same value of about 0.92 eV. The discrepancy between various results reported cannot be easily explained. For SrF_2 films ΔE was found to be about 1.02 eV.

As a result of the step of C with temperature, TCC for CaF_2 and SrF_2 films does not show the general behaviour as observed in previous studies. A TCC minimum which was independent of temperature for a region of temperature was observed for CaF_2 (260-300°K) and SrF_2 (270-300°K) film capacitors. This is an important feature which give practically zero TCC for the two capacitors systems which may have good applications in that operating temperature regions.

During the studies of humidity effect on C and tan δ for CaF_2 films it was found that both of them increased with humidity. The variations depend on the percentage humidity present in the atmosphere. Due to adsorption of moisture the conductivity increases thus giving a high value of C and tan δ. The above observations were similar to the studies of Weaver (1962). The studies of dissimilar electrodes on CaF_2 films are interesting. The observation of an emf across the dissimilar electrodes (Cu and Al or Au and Al) in presence of moisture are almost similar to galvanic effects in electrolytes. This can arise by adsorption of moisture which is likely to ionise CaF_2 to

Ca^+ and F^- ions. Even though the solubility of CaF_2 in water is very low, such ionisation is not unlikely, and it may give rise to the formation of a galvanic cell with two dissimilar electrodes as in the case of any electrolytes.

The breakdown field strength for CaF_2 and SrF_2 films was high of the order of 10^6 V/cm and decreased with increasing film thickness obeying closely the Forlani-Minnaja relation (1964) viz., $F_b \propto d^{-1/2}$. The above results of breakdown are in good agreement with the breakdown studies of Budenstein et al. (1969) and Smith and Budenstein (1969) in the case of several alkaline earth fluorides.

The optical studies show that both CaF_2 and SrF_2 films are highly transparent in the visible region. The optical band gaps are 4.67 eV (CaF_2) and 4.2 eV (SrF_2) and the refractive indices evaluated in the visible region are 1.25 and 1.2 respectively for CaF_2 and SrF_2 films. These refractive indices are lower than the bulk values. Gisin (1969) also observed a lower value of refractive index (n = 1.23) for SrF_2 films. This may be because generally vacuum deposited films have lower densities than the bulk materials and hence lower refractive indices.

The high transmittance of these films are of much interest since they have applications in antireflection coatings. Single and multi-layer antireflection coatings

have various optical applications. At the wavelength
for which the optical thickness of the film is one
quarter wavelength, the beam reflected from the upper
and lower surfaces of the film differ in phase by π
(Heavens, 1955). The reflectance of a quarter-wave
coating is equal to zero if $n_1^2 = n_0 n_2$ where n_1, n_2 and
n_0 are the refractive indices of the film, air and the
substrate respectively. If $n_2 = 1$ and $n_0 = 1.52$ (glass),
then for antireflection, n_1 should be approximately equal
to 1.23. The refractive indices of CaF_2 and SrF_2 films
are approximately satisfying the above requirement for
antireflection coatings. Because of this, these films
showed very high transmittance (about 100%) in the
visible region.

CHAPTER-VII : STUDIES ON NICKEL SULPHIDE FILMS

CHAPTER VII

STUDIES ON NICKEL SULPHIDE FILMS

A. INTRODUCTION

Nickel sulphide (NiS) occurs in two crystalline forms, viz., rhombohedral (millerite) and hexagonal (NiAs structure) forms. The latter has, however, been known for some time to be antiferromagnetic at low temperatures. It has obtained considerable importance since Sparks et al. (1967) reported that a large conductivity change occurred at the magnetic ordering temperature. Hexagonal NiS belongs to a small but interesting class of materials showing an abrupt conductivity transition and hence has become the object of considerable investigations.

Alsen (1925) studied the crystal structure of pyrrhotite, breithauptite, pentlandite, millerite and related compounds. Artificial FeSe, NiS, NiSe, CoS and their mixed crystals have the pyrrhotite structure. The other three compounds belong to the space groups D^4_{6h}, O^5_h and C^5_{3v} respectively. Later on, with the help of Alsen's data, Willems (1927) confirmed that millerite belongs to the space group C^5_3. Ott (1926) reported the lattice parameters of NiS to be a = 9.61 A^o, c = 3.15 A^o and c/a = 0.32,

whereas Jong et al. (1927) reported different values
(a = 3.42 A^O, c = 5.3 A^O). NiS has three phases viz.,
α, β and γ (Levi et al. 1935). Accordingly α - NiS was
identified as millerite (a = 9.61 A^O, c = 3.15 A^O),
β-NiS corresponded to synthetic NiS (a = 3.42 A^O, c = 5.3 A^O)
and γ-NiS was amorphous.

Electrical conductivity of NiS at various pressures
of sulphur vapour was measured by Hauffe et al. (1952).
It was found that in NiS phase below 150 mm Hg, the
conductivity was independent of sulphur pressure whereas
above it, the transition to the NiS_2 phase took place and
the conductivity dropped soon. Measurements of thermoelectric
power showed that NiS was an n-type semiconductor while
NiS_2 was of p-type. Shimonura (1952) measured the specific
resistance and TCR of NiS at various temperatures and
showed that the specific resistance increased almost
linearly with temperature. Delimarskii et al. (1958)
measured the electrical conductivity of NiS at temperatures
from 550°C to 1000°C. In the fused state, the conductivity
was mainly electronic. Sparks et al. (1967, 1968) measured
the electrical resistivity of NiS on a compressed powder
from 77°K to room temperature and a metal to semiconductor
transition was observed at 264 $\pm$ 1^{O}K. But previous neutron
diffraction study showed that a first order antiferromagnetic
transition occurred at 263 $\pm$ 2^{O}K. Two activation energy

values were obtained, viz., $\Delta E = 0.12$ eV between 264-242°K and $\Delta E = 0.01$ eV between 170-77°K.

A crystallographic change in the symmetry of the hexagonal NiS was observed during the metal-semiconductor transition (Trahan et al. 1970). Ohtani et al. (1970) measured the Hall coefficient and electrical resistivity of $Ni_{1-x}S$ (x = 0.005 - 0.015) at 100-200°K and concluded that the material was a p-type semiconductor.

Rustamov et al. (1971) had grown single crystals of nickel chalcogenides (NiS, NiTe and NiSe) and investigated the various properties such as electrical conductivity, thermo e.m.f. and Hall effect of these single crystals at 100-700°K. Measurements showed that all the nickel chalcogenides had n-type conductivity. Near 280°K, a sharp variation of the above parameters was observed due to a reversible phase transition. A metal-insulator transition in NiS_2 was observed by Wilson et al. (1971). Mossbaur effect of ^{57}Fe also confirmed the metal to nonmetal transition in NiS (Coey, 1973). Transport coefficient of NiS in the phase transition region obtained by thermal and electrical conductivity, thermo electric power and Hall coefficient measurements (80-400°K) was reported by Andreev (1972).

The optical absorption measurements on semiconducting NiS_2 were analysed by Kautz et al. (1972) to determine the

energy gap and temperature dependence. Electrical
conductivity measurements showed three regions of
conduction with three activation energies viz., 0.32 eV
above $380^{\circ}K$, 0.068 eV between $380-140^{\circ}K$ and 0.045 eV
below $140^{\circ}K$. Bither et al. (1968) calculated the n and k
of transparent NiS_2 single crystals from reflectance and
transmittance data.

The structure of vacuum deposited thin films of
NiS at different substrate temperatures on NaCl single
crystals, glass and mica was studied by Talele (1974).
Films formed at temperatures less than $100^{\circ}C$ did not
yield any coherent diffraction patterns suggesting the
deposits were either amorphous or had a fine-grained
structure. A new phase of NiS having ZnS structure
$(a = 5.41 A^{\circ})$ was also observed at substrate temperatures
between $150-250^{\circ}C$, which was not reported previously. The
Hall effect studies on thin films of NiS was reported
recently by Goswami et al. (1974).

From the above survey of literature it is clear
that considerable amount of work has been carried out on
the electrical magnetic and structural properties of bulk
NiS. But very little attention has been paid to the
properties of thin films of NiS. From the bulk studies it
is known that the properties of NiS differ depending on the
structure. Since the physical properties of thin films

depend mainly on the structure and the methods of preparation a detailed study has been carried out on the dielectric, electrical and optical properties of vacuum deposited films of NiS.

B. EXPERIMENTAL

The sample used was reagent grade supplied by M/s. BDH Ltd., England. It was found that when NiS was deposited from tungsten or molybdenum boats, in many cases it reacted with the boats perhaps forming an alloy. So NiS was deposited from silica boat which was heated externally by a tungsten filament. The glass substrates were at room temperature and were placed about 10-12 cms away from the source. The bulk powder was pressed into small pellets to avoid spitting while deposition. These were heated slowly in vacuum for about an hour for degassing prior to the deposition. The deposition rate was about 100-150 A^o/min. The capacitors were fabricated using aluminium electrodes in the usual way. Films were deposited on glass substrates for optical measurements. The transmittance in the visible region was measured in a Beckmann DK-2 spectrophotometer and the refluctance in the spectrophotometer designed in our laboratory, the details of which are given in Chapter II. The resistances of the films deposited on glass substrates were measured at different temperatures

in vacuo by a million meg-ohm meter. The breakdown
voltage of these capacitors were measured in air by
applying a dc voltage across the capacitor and measuring
the current.

The structure of the deposited film was analysed
by conventional electron diffraction and that of bulk
powder by X-ray powder pattern method.

C. RESULTS

i) Structure

The bulk NiS was analysed by X-ray diffraction and
found that it had a rhombohedral (millerite) structure in
agreement with the reported values of Ott (1926) with
lattice parameters a = 9.61 A$^\circ$, c = 3.15 A$^\circ$ and c/a = 0.33.
On the other hand, vacuum deposited films were amorphous.

ii) Dielectric properties

a) Ageing and annealing effect

The ageing effect was not similar for all capacitors.
For thicker films C decreased by ageing whereas for some
of the thinner films C increased by ageing. This may be
due to the absorption of moisture as in the case of CaF$_2$
capacitors. However, tan δ in all cases decreased by
ageing and became more or less constant (fig. VII-1). But
finally by annealing in vacuo at about 100°C, both C and tan δ
decreased further and after three or four annealing cycles,
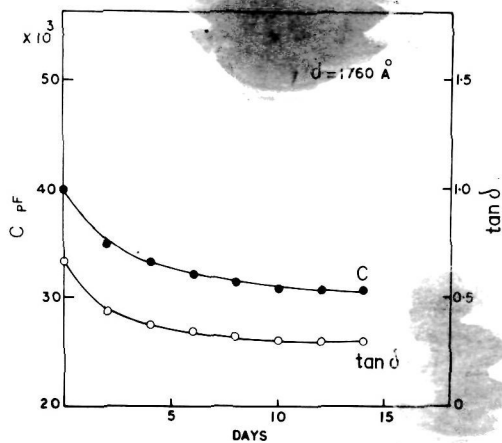
Fig. VII - 1
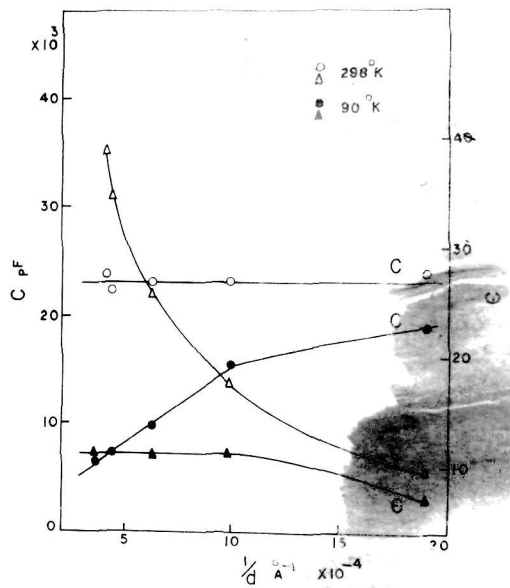
Fig. VII - 2
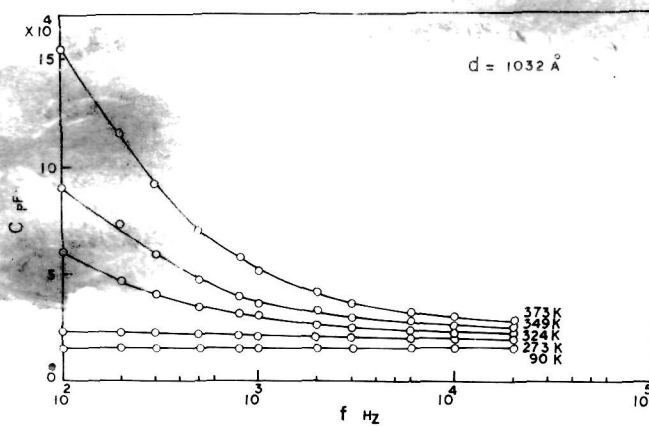
the capacitors were stabilised.

b) Effect of film thickness on C and ε

Fig. VII-2 shows the variations of C and ε with
1/d at 298 and 90°K. It is seen that at room temperature
whilst C remained practically independent for all film
thicknesses (500-2500 A°), ε increased considerably from
about 10 to 39 thus showing its thickness dependence.

The variations of C and ε at about 90°K showed
entirely different features. Here C vs 1/d graph showed
a positive slope thus showing a thickness independent ε
(11.2) for all thicknesses > 1000 A°. But ε is dependent
on film thickness for thinner films (d < 1000 A°), as
observed in the case of Dy_2O_3 films. The temperature
dependent features of these films appear to be associated
with dipolar behaviour which will be discussed later.

c) Frequency and temperature effect on C and tan δ

Fig. VII-3 shows the variation of C with frequency
at different temperatures for a film thickness d = 1032 A°.
It is seen that C is independent of frequency at low
temperatures whereas it decreases continuously with frequency
at higher temperatures. However, at higher frequencies,
C becomes practically independent of frequency. The variation
of C with temperature at different frequencies is shown
in fig. VII-4. It is seen that C increases with increasing
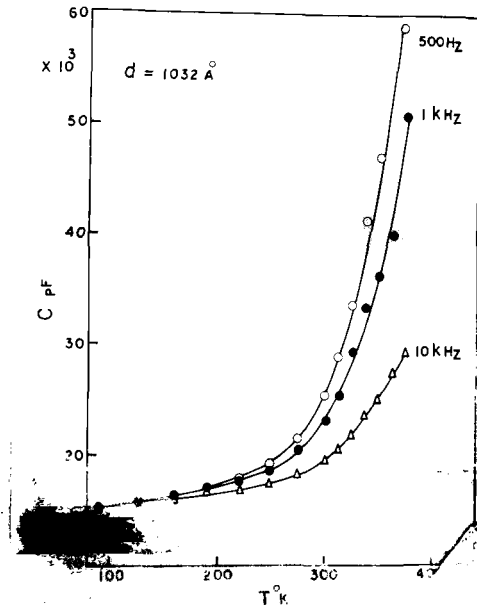
Fig. VII-4
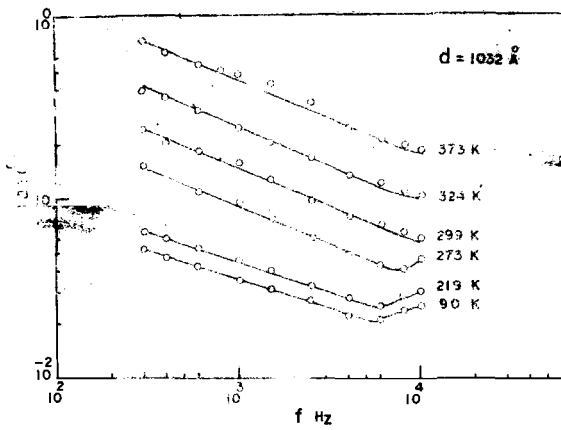
Fig. VII-5
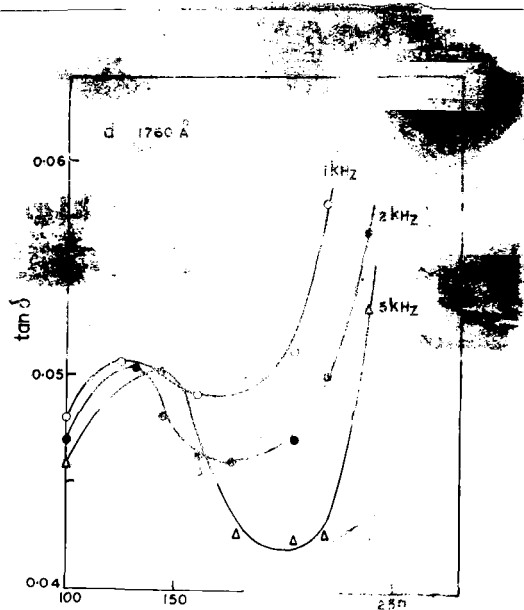
Fig. VII-6

temperature and at higher temperature the frequency curves are more separated and C increases rapidly. But at lower temperature region, the different frequency curves merge together to give a single one.

Fig. VII-5 shows the variation of tan δ with frequency at different temperatures. Tan δ decreased with frequency and again increased thus giving a tan δ_{min}. This is clearly observed in the lower temperature region. The tan δ_{min} shifted towards higher frequency region at higher temperatures and this is similar to that observed in the case of Dy_2O_3 films. However the tan δ_{min} at higher temperature regions could not be observed since they were expected to lie at frequencies greater than 10^4 Hz. It is also seen that tan δ also increases with temperature.

Fig. VII-6 shows the variation of tan δ with temperature for a film thickness d = 1760 A$^{\circ}$. Tan δ increases with temperature and a tan δ_{max} is observed as in the case of CaF_2 capacitors. This shows the relaxation phenomena of NiS capacitors. Further it is interesting to see that these tan δ_{max} shifts to higher temperature region at higher frequencies. It is also possible to calculate an average value of the dipole orientation energy Q using the relation f = fo exp (-Q/kT) (Nadkarni and Simmons, 1970; Simmons et al. 1970) by
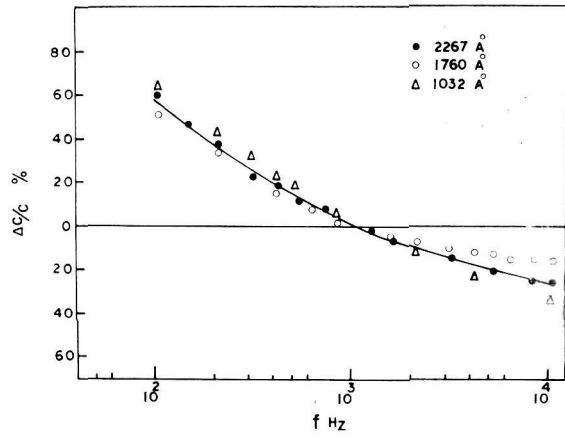
Fig. VII-7
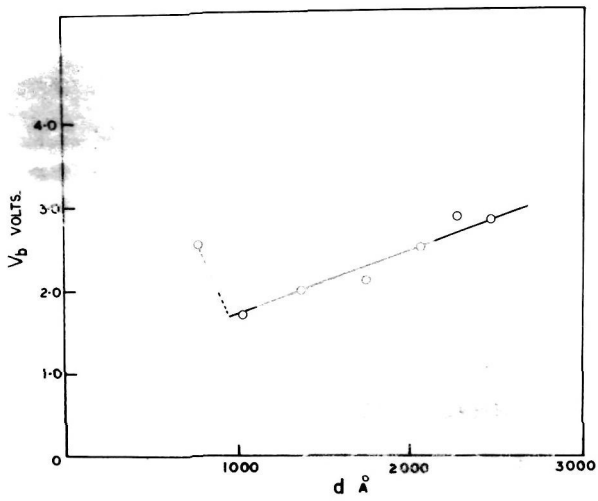
Fig. VII-8
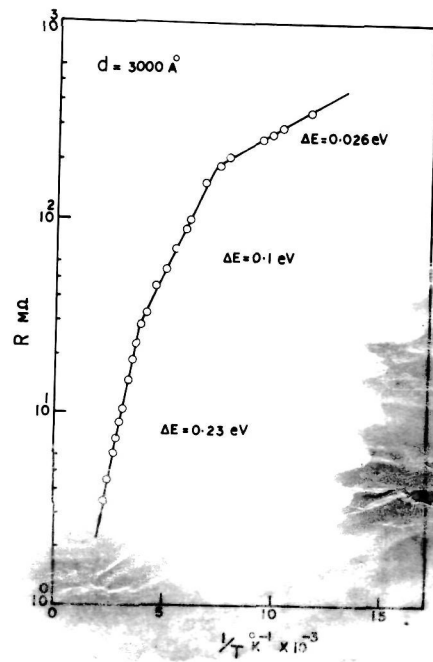
Fig. VII-9

plotting the frequency where maximum occurs. Thus, Q
evaluated for a film thickness of 1760 A^{o} was about
0.28 eV.

d) **TCC and percentage variation of capacitance**

TCC of the capacitors were high and varied from
2000-20000 ppm/^{o}K in the temperature range 100-360°K.
The percentage variation of capacitance ($\Delta C/C$) varied
from +60 to -40 in the frequency range 10^{2}-10^{4} Hz
(fig. VII-7). However, this is much high compared to
those observed in the previous studies. The high TCC and
$\Delta C/C$ show that NiS films were nonstoichiometric.

e) **Breakdown voltage (V_b)**

The breakdown voltage was measured by applying a
dc voltage across the capacitors and measuring the current.
Then I was plotted against V and the straight line parts
of the curves were extrapolated to voltage axis, which was
taken the onset of breakdown voltage. In fig. VII-8, V_b
is plotted against film thickness. It is seen that V_b
increases with d. But in the lower thickness region an
increase in breakdown voltage is observed. This is similar
to that observed by Chopra (1965) in the case of ZnS
capacitors. However, the breakdown field was low of the
order of 10^{5} V/cm.

f) **Activation energy**

The activation energy of NiS film was estimated from the variation of resistance with temperature. The resistance of the NiS films deposited on glass substrates was measured by a million meg ohm meter. Fig. VII-9 shows the typical variation of resistance with $1/T$ for a film thickness d = 3000 A$^\circ$. The activation energy was calculated from the slopes of the graph. It is interesting to see that the graph shows three slopes, suggesting three activation energies, viz.,

     (1) ΔE = 0.0264 eV below 140°K,

     (2) ΔE = 0.1 eV between 140 and 270°K and

     (3) ΔE = 0.23 eV above 270°K.

Further, it was found that the activation energy depends on the thickness of the films as shown in table VII-1. However, the temperature where the slope changes remained the same for all the film thicknesses studied. The above results show that the activation energy increases with the increase of temperature. Further, it was found that the films of lower thickness had higher activation energies throughout the temperature regions.

iii) **Optical properties**

The optical constants of NiS films were calculated in the visible region from the reflectance and transmittance

TABLE VII-1

Film thickness d (A^o)	Activation energy (ΔE)		
	Below 140°K	Between 140 and 270°K	Above 270°K
3600	0.021 eV	0.072 eV	0.15 eV
3000	0.026 eV	0.1 eV	0.23 eV
2700	0.029 eV	0.13 eV	0.24 eV
2600	0.038 eV	0.16 eV	0.26 eV

measurements and the film thicknesses using Hadly curves
(Heavens, 1955). The refractive index was about 2.5 and
the absorption index was high (k = 0.2) compared with
that of the previous studies. The above values are
approximately in agreement with that reported by Bither
et al. (1968) for transparent NiS single crystals.

D. DISCUSSION

The studies on vacuum deposited NiS films showed
that they are non-stoichiometric having many associated
defects including lattice vacancies, interstitials etc.
Studies on the bulk NiS showed that they behave generally
as semiconductors. The electron diffraction studies of
vacuum deposited films of NiS showed that they were either
amorphous or had a fine-grained structure. Compared to
the bulk resistivity of NiS, the vacuum deposited films
showed a higher resistivity. This may be because while
depositing on substrates at room temperature, the sulphur
contents in the film would be increased resulting in a
composition with excess of sulphur. However, the electrical
and dielectric properties of NiS films showed that they
behave more or less like doped insulators, unlike the
semiconducting bulk NiS.

The thickness dependence of C and ϵ of NiS films
at room temperature and at 90°K is similar to those of
MoO_3 (Nadkarni and Simmons, 1970) and In_2O_3 (Goswami and

Goswami, 1974) films. Because of high impurity
concentration, the dielectric layers would show considerable
conductivity even at room temperature and these would
act as shunt resistance or impedence in the ac field.
Hence the capacitance measured would no longer be the
real one and ϵ thus evaluated would not be the characteristic
of the material. However, when cooled to $90^{\circ}K$, the mobile
charge carriers introduced by the impurity would be frozen
and the deposits would have the high resistivity leading
to a constant ϵ as in the previous studies. It is
interesting to see that even at low temperature, ϵ is
independent of film thickness only for $d > 1000 A^{\circ}$.
For thinner films, ϵ is dependent on film thickness. This
thickness dependence caused by voids and discontinuities
can be explained as in the case of Dy_2O_3 films.

It is interesting to mention that similar conclusions
can also be arrived at from the phenomological considerations
of the dielectric behaviour. At extremely low temperatures,
the dipoles cannot contribute much to the dielectric
constant because of the hinderance of their rotation and
hence the contribution would predominantly be due to atomic
and electronic polarisation leading to a constant ϵ. However,
with the increase of temperature and the film thickness,
the contributions for the dipolar orientation would increase
considerably and hence ϵ will also increase.

Despite the amorphous or fine-grained nature of the deposits, the observed constant value of ϵ (for d > 1000 A^o) at low temperature, however, gives some indication regarding the nature of the deposits. At higher temperatures, the effect of doping impurities becomes more predominant. Hence at room temperature region ϵ becomes thickness dependent.

The variation of C with frequency and temperature is as expected. Further, tan δ shows a minima with frequency and the tan δ_{min} shifts towards higher frequency region at higher temperatures. This is similar to that observed in the case of Dy_2O_3 films and can be explained as due to the effect of the electrode resistance in series with the inherent capacitance. The variation of tan δ with temperature is more significant. It shows a tan δ maxima and this maxima shifts towards higher temperature region at higher frequencies. The defects present in the non-stoichiometric films generally give rise to dipoles which will polarise under a suitable ac field. The number of dipoles will also be dependent upon the defect concentration. These dipoles will then show a relaxation effect, i.e., tan δ peak at a suitable ac frequency causing the dipolar orientations. In the present case, however, it appears to be solely due to the dipole orientation and not due to the interfacial polarisation.

as the latter generally occurs at an extremely low
frequency range say 0.01 to 1 Hz (Weaver, 1962; Macfarlane
and Weaver, 1966 and Harrop and Campbell, 1970). The
relaxation frequency is also temperature sensitive.
However, it can be concluded that the dipoles which could
rotate at higher temperatures were frozen at low
temperature and became immobile, thus suppressing the
orientational effects. The TCC and percentage variation
of capacitance are high because of the nonstoichiometric
nature of the films.

The breakdown voltage shows a linear thickness
dependence for film thicknesses greater than 1000 A^o.
Below 1000 A^o, an increase in breakdown voltage was
observed. Such dependence was also observed by Chopra
(1965) and Pakswer et al. (1963). The increased breakdown
voltage at lower thickness is perhaps not significant due
to the large uncertainty in the thickness data in this
region as a result of the island nature of the deposit.

Resistance measurements at different temperatures
show distinct slopes increasing from low temperature
regions to high temperature. The three slopes observed
are (1) below $140^o K$, (2) between $140-270^o K$ and (3) above
$270^o K$. Consequently three activation energies are obtained.
This is similar to the results of Kautz et al. (1972) for

bulk NiS, except the fact that he observed an intermediate activation energy between 140-380°K. Moreover, it is interesting to see that ΔE varies with film thickness in the three regions, having higher values for lower film thicknesses. Thinner films generally have a higher resistivity, mostly due to island structure of the films. Another factor that contributes to the resistivity of films is quantum size effect. When the thickness of film is reduced, the mean free path is also reduced due to closeness of the boundaries. The resistivity is increased because of the energy lost at each collision (Mayer, 1959). Hence the thinner films will have a higher activation energy. The dipole orientation energy (Q = 0.28 eV) calculated was in agreement with that measured by resistance measurements, thus giving a correlation between the ac and dc measurements. These activation energies are also comparable with that reported by Bither et al. (1968) for semiconducting NiS (0.25 eV).

CHAPTER-VIII : SUMMARY AND CONCLUSIONS

CHAPTER VIII

SUMMARY AND CONCLUSIONS

In the above chapters detailed studies have been made on the dielectric, electrical, optical and structural properties of different vacuum deposited films with a view to understand their behaviour so that these could be made use of in different electronic and optical devices. The studies of these properties by independent techniques have also thrown some light on the basic mechanisms involved and an overall picture of the interaction of electromagnetic field with matter. The materials studied were oxides (Dy_2O_3 and La_2O_3), fluorides (LaF_3, CaF_2 and SrF_2) and also a sulphide (NiS). The influence of factors such as ageing, annealing, film thickness, substrate temperature, effects of frequency and temperature on C, ϵ and tan δ and also breakdown field have been studied independently. The dc electrical conduction studies have thrown light on the nature of conduction process in oxide dielectrics. The optical studies showed that all these films with the exception of NiS were highly transparent in the visible region. Further, the transmittance studies in the UV region have given an idea of the optical bandgap of some of these dielectrics.

Dielectric films as deposited are unstable and hence require ageing and annealing. This is generally accompanied by a reduction of C and tan δ. It was also observed that the presence of defects such as voids, discontinuities, impurities etc. considerably affected the dielectric and electrical properties of these films. By ageing and annealing most of the defects could be reduced. It was also found that whilst the oxide films were practically unaffected by moisture, the fluoride films were much sensitive to it.

From the general behaviours studied, the oxide dielectrics (Dy_2O_3 and La_2O_3) can be categorised together. The fluoride materials show similar behaviour in most cases whereas NiS falls in a different class. In the following, their properties are discussed accordingly.

The rare earth oxides of Dy and La have similar properties. Both the films were amorphous when studied by electron diffraction and electron microscopy techniques. Also these films had defects which could be removed by ageing and annealing, thus showing a considerable decrease in C and tan δ during the above studies. These films had a thickness independent dielectric constant (for d > 1000 A^o) showing that they were stoichiometric in nature. Both C and tan δ decreased with frequency. But for Dy_2O_3 films tan δ showed a sharp minima whereas tan δ for La_2O_3 films

had a flat one. But in both cases C and tan δ increased with temperature. The TCC of these films were comparable with the accepted values in all practical purposes. The percentage variations of capacitance ($\Delta C/C$) were much smaller ($< \pm$ 1%) for these films. Also they had high dielectric field strength ($F_b = 10^6$ V/cm) and it decreased with increasing film thickness following the Forlani-Minnaja relation (1964) namely $F_b \propto d^{-1/2}$.

The dc electrical conduction in Dy_2O_3 and La_2O_3 films was not reported previously. These studies proved some important features on the conduction mechanism in these two films. Generally space-charge limited conduction is not expected in amorphous films. But from the present investigations on I-V characteristics, it is observed that the conduction in these films are space-charge limited. Conduction in Dy_2O_3 films followed the relation $I \propto V^2/d^3$ modified by shallow traps whereas in La_2O_3 films it obeyed $I \propto V^{1+1}/d^{21+1}$ (where 1 = 3) showing an exponential trap distribution. The activation energy measured would give an idea of the trap depth. An important result is the agreement of activation energies evaluated from the dielectric and electrical measurements, which in fact links the dielectric and electrical measurements.

The capacitors with fluoride materials (LaF_3, CaF_2 and SrF_2) as dielectric showed similar behaviour. It is

interesting to note that all the three materials had
crystalline structure corresponding to their bulk materials
even when deposited on substrates at room temperature.
CaF_2 film capacitors showed an increase in capacitance
during ageing. Both CaF_2 and SrF_2 capacitors showed an
increase in C while annealing and stabilised after a few
annealing cycles. However, in all cases tan δ decreased
during ageing and annealing. Further, C decreased with
frequency and increased with temperature. CaF_2 and SrF_2
showed a peculiar behaviour in the variation of C with
temperature, viz., a step in the C vs T graph. Due to
this the TCC became practically zero for a particular region
of temperature. Tan δ decreased with frequency showing a
flat minima. CaF_2 and SrF_2 films showed tan δ_{max} with
temperature due to dipolar relaxation. The percentage
variation of capacitance ($\Delta C/C$) was very small for CaF_2
and SrF_2 films whereas it was about 4% for LaF_3 films.
The breakdown field of LaF_3 films was low (10^5 V/cm)
compared to that of CaF_2 and SrF_2 films (10^6 V/cm) and the
variation of breakdown field with film thickness followed
the Forlani-Minnaja relation.

The I-V characteristics studies showed that LaF_3
films exhibit an unusual polarisation, much greater than
that present in normal ionic crystals. The activation
energies obtained from the capacitance and current-temperature

measurements agreed well in all cases. An interesting
feature is that when two dissimilar electrodes were used
for CaF_2 film capacitors, an emf was observed suggesting
the formation of a galvanic type cell. Further, C and tan δ
of CaF_2 films were sensitive to moisture, which may be used
to measure the percentage humidity.

The optical transmittance measurements showed that
the absorption for LaF_3 is in the far UV region. However,
CaF_3 and SrF_2 had absorption in the UV region and the
bandgaps estimated are 4.67 eV and 4.2 eV respectively for
CaF_2 and SrF_2 films. LaF_3 showed interference in the
visible region. The refractive indices evaluated are
1.6, 1.25 and 1.2 respectively for LaF_3, CaF_2 and SrF_2 films.
The low refractive indices and high transmittance of CaF_2
and SrF_2 films show their application in multilayer
antireflection coatings. Further in all the above cases
the absorption index was negligibly small.

The behaviour of NiS films were different from the
oxide and fluoride films. NiS films were amorphous in
nature. Effect of film thickness on C and ε showed that
these films were nonstoichiometric. At room temperature,
C was independent of frequency, whereas ε was thickness
dependent. But when cooled to low temperature ($90^{o}K$),
C varied linearly with temperature (for d > 1000 A^{o}) and
ε was independent of film thickness. These behaviours were

similar to the nonstoichiometric films like doped MoO_3
(Simmons et al. 1970) and In_2O_3 films (Goswami et al.1974).
The variations of C and tan δ with frequency were as
usual. Tan δ showed a sharp minima which shifted to
higher frequencies at higher temperatures. A tan $δ_{max}$
was also observed in the tan δ vs T curves which is due
to relaxation effect. The percentage variations of
capacitance and TCC were much greater for NiS films
than the other films studied.

The resistance measurements with temperature showed
that there were three slopes suggesting three activation
energies. Further, ΔE increased with temperature and also
with increasing film thicknesses. The optical studies
showed that n (2.5) and k (0.2) are much higher for
NiS films.

A comprehensive data for the different dielectric,
optical and other parameters are given in table VIII-1
at the end of this chapter.

The present investigations show that the various
physical properties of thin films are in some cases
different from their bulk properties. The properties of
thin films are mainly dependent on their deposition
conditions, thickness and other factors. These arises
from the numerous defects present in evaporated films.

Also these studies gave a coherent picture of the
dielectric, electrical and optical properties of thin
films. Present studies not only peep into their basic
properties, but also suggests that they have many
applications both in electronic and optical devices.

TABLE VIII-1

Material	Nature	ϵ (1 kHz)	$\tan \delta$ (1 kHz)	TCC (ppm/°K) (100-400°K)	$\Delta C/C$ (10^2-10^5 Hz)	F_b (V/cm)	n (7000A°-4000A°)	k	E_g
Dy_2O_3	Amorphous	6.7	0.007	200 to 800	± 1%	10^6	1.85	0	--
La_2O_3	Amorphous or fine-grained	11.0	0.007	300 to 3000	± 1%	10^6	1.80 to 1.89	0.03	4.6 eV
* LaF_3	Crystalline trigonal	4.7 x	0.01	100 to 6000	+3 to -1%	10^5	1.60	0	--
* CaF_2	Crystalline cubic	3.65	0.004	200 to 900	± 0.5%	10^6	1.25	0.01	4.67 e]
* SrF_2	Crystalline cubic	4.45	0.004	200 to 900	± 0.5%	10^6	1.20	0.01	4.2 eV
* NiS	Amorphous	10.39 x	0.2	2000 to 20000	+60 to -40%	10^5	2.5	0.2	--

*   Relaxation effect

x   Thickness dependent

ACKNOWLEDGEMENTS

(R. RAMESH VARMA)

REFERENCES

REFERENCES

1. Abeles, F. (1950) J. Phys. Radium, 11, 310.

2. Agrawal, M.D. (1974) Physica, 72, 397.

3. Alsen, N. (1925) Geol. For. Forh., 47, 19.

4. Andeen, C., Fontanella, J. and Schuele, D. (1971)
    J. Appl. Phys., 42, 2216.

5. Andreev, A.A. (1972) Sov. Phys. Solid State, 14, 706.

6. Argall, F. and Jonscher, A.K. (1968) Thin Solid Films,
    2, 185.

7. Arkel, A.E. Van. (1924) Physica, 4, 286.

8. Axelrod, N.N. (1968) "Optical Properties of Dielectric
    Films", The Electrochem. Soc. Inc., N.Y.

9. Barsis, E. and Tayler, A. (1966) J.Chem. Phys., 45, 1154.

10. Batsanova, L.R. and Grigoreva, G.N. (1962)
    Izv. Sibirst. Old. Akad. Nauk. SSSR., 2, 115.

11. Batsanov, S.S., Grigoreva, G.N. and Sokolova, N.P.
    (1962) Zh. Strukt. Khim., 3, 339.

12. Baun, W.L. and Mcdevitt, N.I. (1963)
    J. Am. Ceram. Soc., 46, 294.

13. Berman, L.V. and Zhukov, A.G. Optika i Spektroskopiya,
    19, 783.

14. Bither, T.A., Bouchard, R.J., Cloud, W.H., Donhue, P.C.
    and Siemons, W.J. (1968) Inorg. Chem., 7, 2208.

15. Bogoroditskii, N.P., Pasynkov, V.V., Rifat, R.B. and
    Volokobinskii, Yu. M. (1965) Dokl. Akad. Nauk SSSR.,
    160, 578.

16. Bondarenko, B.V. and Tzarer, B.M. (1959) Radiotekh. i.
    Electron., 4, 1059.

17.   Bondarenko, B.V., Ermakov, S.V. and Tsarev, B.M.
       (1964) Vapr. Teorii i Primeneniya Redkozem. Metal.,
       Akad. Nauk. SSSR., 92-101.

18.   Bourg, A. and Talbot, D. (1964) C.R. Acad. Sci.,
       259, 4608.

19.   Bourg, A. and Bourg, M. (1965) Compt. Rend.,
       260, 1138.

20.   Bourg, A., Barbaronx, N. and Bourg, M. (1965)
       Opt. Acta., 12, 151.

21.   Bragg, W.L. (1914) Proc. Roy. Soc., A-89, 468.

22.   Budenstein, P.P., Hayes, P.J., Smith, J.L. and
       Smith, W.L. (1969) J. Vac. Sci. Tech., 6, 289.

23.   Bujor, M. and Vook, R.W. (1969) J. Appl. Phys.,
       40, 5373.

24.   Buschbaum, K.M. and Schnering, H.G. (1965)
       Z. Anorg. Allgem. Chem., 340, 232.

25.   Caffyn, J.E., Goodfellow, T.L., Olymbios, E.M.
       and Perrin, D.J. (1967) Phys. Stat. Sol., 22, 549.

26.   Callen, H.B. (1949) Phys. Rev., 76, 1394.

27.   Campbell, D.S. (1970) in "Hand book of Thin Film
       Technology", Ed. Maissel, L.I. and Glang, R.,
       McGraw Hill Book Co., New York.

28.   Chen, J.H. and McDonough, M.S. (1969) Phys. Rev.,
       185, 453.

29.   Chernobrovkin, D.I. and Bakhtinov, V.V. (1971)
       Dielektriki., 1, 134.

30.   Chernobrovkin, D.I., Bakhtinov, V.V. and Sakharov,
       Yu.G. (1971) Prib. Tekh. Eksp., 3, 159.

31.   Chernobrovkin, D.I. and Sakharov, Yu.G. (1971)
       U.S.S.R. 322, 796 (Cl. H 01g).

32.   Chopra, K.L. (1965) J. Appl. Phys. 36, 184.

33.   Chopra, K.L. (1965) J. Appl. Phys., 36, 656.

34. Chopra, K.L. (1969) "Thin Film Phenomena", McGraw-Hill Book Co,,N.Y.

35. Claveric, J., Compet, G., Perigord, M., Portier, J. and Ravez, J. (1974) Mater. Res., 9, 585.

36. Coey, J.M.D. (1973) Solid State Commun., 13, 43.

37. Collins, R.A., Bowman, G. and Sutherland, R.R. (1971) J. Phys. D., 4, L49.

38. Day, J. and Calis, M. (1954) Fr. 1,061,050.

39. Delimarskii, Yu.K. and Velikanov. (1958) Zhur. Zeorg. Khim., 3, 1075.

40. Denham, P., Field, G.R., Morse, P.L. and Wilkinson, G.R. (1970) Proc. Roy. Soc., Ser. A, 317, 55.

41. Derbeneva, S.S. and Batsanov, S.S. (1967) Dokl. Akad. Nauk. SSSR., 175, 1662.

42. Fielder, W.L. (1967) NASA Tech. Note, TND-3816, p.20.

43. Fielder, W.L. (1969) NASA Tech. Note, NASA TN D-5505.

44. Fisher, J.C. and Giaever, I. (1961) J. Appl. Phys., 32, 172.

45. Foex, M., Traverse, J.P. and Coutures, J.P. (1965) Bul. Soc. Franc. Mineral. Crist., 88, 341.

46. Forlani, F. and Minnaja, N. (1964) Phys. Stat. Sol., 4, 311.

47. Frohlich, H. (1937) Proc. Roy. Soc., A160, 230.

48. Frohlich, H. (1958) "Theory of Dielectrics", Oxford Univ. Press, Fair Lawn, N.J.

49. Gaffee, D.I. (1962) Proc. IEE., 109B, 336.

50. Goldsmith, J.A. and Ross, S.D. (1967) Spectrochim. Acta, Part A 23, 1909.

51. Gosh, K. and Gosh, B. (1938) Ind. J. Phys., 12, 259.

52. Goswami, A. and Goswami, A.P. (1973) Thin Solid Films, 16, 175.

53. Goswami, A. and Goswami, A.P. (1974) Thin Solid Films, 20, S3.

54. Goswami, A. and Goswami, A.P. (1974) Ind. J. Pur. Appl. Phys., 12, 26.

55. Goswami, A. and Goswami, A.P. (1974) International Crystallography Conference, Melbourne, Australia, 194.

56. Goswami, A. and Ojha, S.M. (1974) International Crystallography Conference, Melbourne, Australia, 187.

57. Goswami, A. and Varma, R.R. (1974) Thin Solid Films, 22, S2.

58. Gundlach, K.H. (1964) Phys. Stat. Sol., 4, 527.

59. Hacskaylo, M. (1968) U.S. 3,387,999 (Cl.117-201).

60. Hadley, L.N. (1955) cited by Heavens, O.S., "Optical Properties of Thin Solid Films", Butterworths Scientific Publications, London.

61. Hare, W. (1963) Phys. Stat. Sol., 3, K 446.

62. Harrop, P.J. and Campbell, D.S. (1968) Thin Solid Films, 2, 273.

63. Harrop, P.J. and Wanklyn, J.N. (1964) J. Electrochem. Soc., 111, 1133.

64. Harrop, P.J., Wood, G.C. and Pearson, C. (1968) Thin Solid Films, 2, 457.

65. Hass, G., Ramsey, J.B. and Thun, R., (1959) J. Opt. Soc. Am., 49, 116.

66. Hauffe, K. and Flindt, H.G. (1952) Z. Physik. Chem., 200, 199.

67. Heavens, O.S. (1955) "Optical Properties of Thin Solid Films", Butterworths Scientific Publications, London.

68. Heikes, R.R. and Johnson, W.D. (1957) J. Chem. Phys., 26, 582.

69. Hickmott, T.W. (1966) J. Appl. Phys., 37, 4380.

70. Hirosa, H. and Wada, Y. (1964) Japan. J. Appl.
     Phys., 3, 179.

71. Holland, L. (1956) "Vaccum Deposition of Thin Films",
     Chapman and H 11 Ltd., London.

72. Ioffe, A.F. and Regel, A.R. (1960)
     Progr. Semicond., 4, (1960).

73. Jacobs, G. (1957) J. Chem. Phys., 27, 1441.

74. Jaffe, H. (1952) Phys. Rev., 35, 354.

75. Janker, G.H., Oosterhout, G.W. Van and Santen,
     J.H. Van.(1958) U.S. 2,862,891.

76. Johnson, H.B., Tolar, N.J., Miller, G.R. and
     Cutler, I.B. (1966) J.Am. Ceram. Soc., 49, 458.

77. Jong, W.F. de and Willems, H.W.V. (1927)
     Physica, 7, 74; (1927)
     Z. anorg. allgem. chem., 160, 185; (1927) ibid, 161, 311.

78. Jonscher, A.K. (1969) J.Electrochem. Soc., 116, 217C.

79. Jonscher, A.K. and Walley, P.A. (1969)
     J. Vac. Sci. Tech., 6, 662.

80. Kadzhoyan, R.A. and Egiyan, K.A. (1968)
     Izv. Akad. Nauk. Arm. SSR, Fiz., 3, 348.

81. Kagaku, N.K.K. (1965) Brit. 1010038, Cl. C.23C.

82. Kautz, R.L., Dresselhaus, M.S., Adler, D. and
     Linz, A. (1972) Phys. Rev. B, 6, 2078.

83. Kittel, C. (1966) "Introduction to Solid State
     Physics", Asia Publishing House, Bombay.

84. Klein, N. and Gafni, H. (1966) IEEE Trans.
     Electron. Devices, ED13, 281.

85. Klein, N. and Levanon, N. (1967) J.Appl. Phys.,
     38, 3721.

86. Koch, F.A. and Vook, R.W. (1973)
     J. Appl. Phys., 44, 2475.

87. Lampert, M.A. (1956) Phys. Rev., 103, 1648,

88. Lampert, M.A. (1964) Rept. Progr. Phys., 27, 329.

89. Lapluye, G., Morinet, G. and Palla, P. (1960) Compt. rend., 250, 305.

90. LaRoy, B.C., Lilly, A.C. and Tiller, C.O. (1973) J. Electrochem. Soc., 120, 1668.

91. Laufer, A.H., Pirog, J.H. and McNesby, J.R. (1965) J. Opt. Soc. Am., 55, 64.

92. Laurila, E.A. (1950) Phys. Rev., 77, 405.

93. Levi, G.R. and Baroni, A. (1935) Z. Krist., 92, 210.

94. Lewowski, T., Sendecki, S. and Sujak, B. (1965) Acta Phys. Polon., 28, 343.

95. Lilly, A.C., LaRoy, B.C. and Tiller, C.O. (1973) J. Electrochem. Soc., 120, 1673.

96. Lowndes, R.P. (1969) J. Phys. C, 2, 1595.

97. MacChesney, J.B., Gallagher, P.K. and Marcello, F.V. di. (1963) J.Am. Ceram. Soc., 46, 197.

98. MacFarlane, J.C. and Weaver, C. (1966) Phil. Mag., 13, 671.

99. Maddocks, F.S. and Thun, R.E. (1962) J. Electrochem. Soc., 109, 99.

100. Maissel, L.I. and Glang, R. (1970) "Handbook of Thin Film Technology", McGraw-Hill Book Co., N.Y.

101. Manfredi, M. and Paracchini, C. (1974) Phys. Stat. Sol., (a) 21, 427.

102. Mann, H.T. (1966) in Basic Problems in Thin Film Physics. Ed. Niedermayer, R. and Mayer, H. Vandenhoek and Ruprecht, Gottingen, p.691.

103. Mansman, M. (1964) Z. Anorg. Allgem. Chem., 331, 98.

104. Marzullo, S. and Bunting, E.N. (1958) J. Am. Ceram. Soc., 41, 49.

105.   Mathews, J.W. (1959) Phil. Mag., 4, 1017.

106.   Mayer, H. (1959) "Structure and Properties of
        Thin Films", Wiley, New York, p.225.

107.   McLean, D.A. (1961) J. Electrochem. Soc., 108, 48.

108.   Mirowski, B., Rapior, A., Szczurek, I. and
        Wierzbicki, Z. (1970) Proc. Int. Conf. Phys.
        Chem. Semicond. Heterojunctions Layer Struct.,
        4, 171.

109.   Mordovin, O.A., Timofeeva, N.I. and Drozdova,
        N.I. (1967) Izv. Akad. Nauk. SSSR. Neorg.
        Mater., 3, 187.

110.   Moss, T.S. (1959) "Optical Properties of
        Semiconductors", Butterworths Scientific
        Publications, London.

111.   Mott, N.F. and Gurney, R.W. (1948)
        "Electronic Process in Ionic Crystals",
        2d ed., chap. V. Oxford Univ. Press, Fair Lawn, N.J.

112.   Nadkarni, G.S. and Simmons, J.G. (1970)
        J. Appl. Phys., 41, 545.

113.   O'Dwyer, J.J. (1967) Phys. Chem. Solids, 28, 1137.

114.   Oftedal, I. (1929) Z. Physik. Chem., B5, 272.

115.   Ohtani, T., Kosuge, K. and Kachi, S. (1970)
        J. Phys. Soc. Japan, 28, 1588.

116.   Ott, H. (1926) Z. Krist., 63, 222.

117.   Pakswer, S. and Pratinidhi, K. (1963)
        J. Appl. Phys. 34, 711.

118.   Pashley, D.W. (1959) Phil. Mag., 4, 316, 324.

119.   Pashley, D.W., Stowell, M.J., Jacobs, M.H.
        and Law, T.J. (1964) Phil. Mag., 5, 127.

120.   Pauling, L. (1929) Z. Krist., 69, 415.

121.   Philips, V.A. (1960) Phil. Mag., 5, 571.

122. Podgorsak, E.B. (1973) Phys. Rev. B, 8, 3405.

123. Queyroux, F. (1965) Comptes. Rend., 261, 4430.

124. Rao, G.V.S. and Rao, C.N.R. (1970)
      Appl. Spectrosc., 24, 436.

125. Rao, G.V.S., Ramda, S., Mehrotra, P.N. and
      Rao, C.N.R. (1970) J. Solid State Chem. 2, 377.

126. Rao, K.V. and Smakula, A. (1966)
      J. Appl. Phys., 37, 319.

127. Reichelt, K. and Rey, M. (1973)
      J. Vac. Sci. Tech. 10, 1153.

128. Robin-Kandare, S. and Robin, J. (1966)
      Compt. Rend. Ser.A, B.262, 1211.

129. Rose, A. (1955) Phys. Rev., 97, 1538.

130. Rudenko, V.S. and Boganov, A.G. (1970)
      Izv. Akad. Nauk. SSSR, Neorg. Mater., 6, 2158.

131. Rudolph, J. (1959) Z. Naturforsch., 14a, 727.

132. Rustamov, A.G., Kerimov, I.G., Valiev, L.M. and
      Babaev, S. Kh. (1971) Izv. Akad. Nauk. SSSR.
      Neorg. Mater., 7, 1123.

133. Seager, C.H. (1971) Phys. Rev. B, 3, 3479.

134. Seetharaman, S. and Abraham, K.P. (1973)
      J. Scient. Ind. Res., 32, 641.

135. Seitz, F. (1949) Phys. Rev., 76, 1376.

136. Sher, A., Solomon, R., Lee, K. and Muller, M.
      (1966) Phys. Rev., 144, 593.

137. Shigeru Waku and Mamoru, U. (1968)
      Denki Tsushin Kenkyusho Kenkyu Jitsuyoka Hokoku.,
      16, 975.

138. Shimonura, K. (1952) J. Sci.
      Hiroshima Univ. Ser., A-16, 319.

139. Shockley, W. and Read, W.T. (1950)
      Phys. Rev., 78, 275.

140.   Shottky, W. (1914) Z. Physik., 15, 872.

141.   Siddal, G. (1959-60) Vacuum, 9, 274.

142.   Simmons, J.G., Nadkarni, G.S. and Lancaster, M.C.
        (1970) J. Appl. Phys., 41, 538.

143.   Simmons, J.G. (1964) J. Appl. Phys., 35, 2472.

144.   Simmons, J.G. (1970) Hand book of Thin Film
        Technology, ed. by Maissel, L.I. and Glang, R.
        McGraw-Hill Book Co., N.Y., 14-32.

145.   Smakula, A. (1950) Phys. Rev., 77, 408.

146.   Smith, J.L. (1969) Thin Solid Films, 3, R9.

147,   Smith, J.L. and Budenstein, P.P. (1969)
        J. Appl. Phys., 40, 3491.

148.   Smoes, S., Drowart, J. and Verhaegen, G. (1965)
        J. Chem. Phys., 43, 732.

149.   Smyth, C.P. (1955) "Dielectric Behaviour and
        Structure", McGraw-Hill Book Co., Inc., N.Y.

150.   Socha, A.J. (1960) U.S. 2,176,574.

151.   Solomon, R., Sher, A. and Muller, M.W. (1964)
        Bull. Am. Phys., Soc., 9, 742.

152.   Solomon, R., Sher, A. and Muller, M.W. (1966)
        J. Appl. Phys., 37, 3427.

153.   Sparks, J.T. and Komoto, T. (1967)
        Rev. Mod. Phys., 40, 752.

154.   Sparks, J.T. and Komoto, T. (1968)
        J. Appl. Phys., 39, 715.

155.   Staritzky, E. (1956) Anal. Chem., 28, 2023, 2024.

156.   Staritzky, E. and Asprey, B. (1957)
        Anal. Chem., 29, 856.

157.   Stephan, G., Nisar, M. and Roth, A. (1972)
        C.R. Acad. Sci. Ser., B-274, 807.

158. Stuart, M. (1967) Phys. Stat. Sol., 23, 595.

159. Sutter, P.H. and Nowick, A.S. (1963)
J. Appl. Phys., 34, 734.

160. Sutton, P.M. (1964) J.Am. Ceram. Soc., 47, 188.

161. Swanson and Fuyat. (1953) NBS Circular, 539, Vol.III.

162. Swanson, H.E., Gilfrich, N.T. and Cook, M.I.
(1957) NBS Circular, No.539, 7, 21.

163. Swanson, H.E., Gilfrich, N.T. and Ugrinic. (1955)
NBS Circular, No. 539, Vol.V, 67.

164. Swanson, H.E. and Tatge, (1951)
J. Research NBS, 46, 318.

165. Talele, G.D. (1974) Ph.D. Thesis, Univ. of Poona.

166. Tare, V.B. and Schmalzried, H. (1964)
Z. Phys. Chem. Frankfurt., 43, 30.

1671 Templeton, D.H. and Dauben, C.H. (1954)
J. Am. Chem. Soc., 76, 5237.

168. Thun, R.E. and Maddocks, F.S. (1966)
U.S., 3271192.

169. Tiller, C.O., Lilly, A.C. and LaRoy, B.C. (1973)
Phys. Rev., B-8, 4787.

170. Tolansky, S. (1948) "Multiple-beam Interferometry".
Oxford Univ. Press, London.

171. Trahan, J., Goodrich, R.G. and Watkins, S.F.
(1970) Phys. Rev. B. 3, 2859.

172. Trombe, F. and Foex, M. (1951)
Compt. rend., 233, 254.

173. Tsutsumi, T. and Matsuo, T. (1970)
Fr. Demande. 2,023,215 (Cl.H 011).

174. Ure, R.W. (1957) J. Chem. Phys., 26, 1363.

175. Von Hippel, A. and Alger, R.S. (1949)

176.   Vook, R.W. and Bujor, M. (1970)
        J. Vac. Sci. Tech., 7, 115.

177.   Vratny, F. (1959) "Thin Film Dielectrics",
        The Electrochem. Soc. Inc., N.Y.

178.   Weaver, C. (1962) Advan. Phys., 11, 83.

179.   White, W.B. (1967) Appl. Spectrosc., 21, 167.

180.   Willems, H.W.V. (1927) Physica, 7, 203.

181.   Wilson, J.A. and Pitt, G.D. (1971)
        Phil. Mag., 23, 1297.

182.   Winkler, G. (1969) Oesterr. Akad. Wiss., Math, -
        Naturwiss. Kl., Sitzungsber., Abt. 2, 177.

183.   Yoshioka, T., Sato, H., Suda, N. and Kisagata, Y.
        (1970) Ger. Offen. 2003596.

184.   Young, L. (1961) "Anodic Oxide Films".
        Academic Press. Inc., N.Y.

185.   Zachariasen, W. (1926) Z. Physik. Chem., 23, 134.

186.   Zalkin, A., Tempelton, D.H. and Hopkins, T.E.
        (1966) Inorg. Chem., 5, 1466.